UNIVERSIDADE FEDERAL DE PERNAMBUCO

CENTRO DE CIÊNCIAS BIOLÓGICAS

PROGRAMA DE PÓS-GRADUAÇÃO EM CIÊNCIAS BIOLÓGICAS

ANDRÉ LUIZ DE SOUZA BARROS

AVALIAÇÃO DO USO DE “SEMENTES” DE OURO E ULTRASSOM NO TRATAMENTO DO CÂNCER POR HIPERTERMIA

Recife

2015

ANDRÉ LUIZ DE SOUZA BARROS

AVALIAÇÃO DO USO DE SEMENTES DE OURO E ULTRASSOM NO TRATAMENTO DO CÂNCER POR HIPERTERMIA

Tese apresentada ao Programa de Pós-Graduação em Ciências Biológicas da Universidade Federal de Pernambuco, como pré-requisito para obtenção do título de Doutor em Ciências Biológicas, Área de concentração – Biologia Química para a Saúde.

ORIENTADORA: Profª. Drª. Teresinha Gonçalves da Silva

CO-ORIENTADORA: Profª. Drª. Silene Carneiro do Nascimento

Recife

2015

Barros, André Luiz de Souza
Avaliação do uso de "sementes" de ouro e ultrassom no tratamento do câncer por hipertermia/ André Luiz de Souza Barros– Recife: O Autor, 2015.

109 folhas : il., fig., tab.
Orientadora: Teresinha Gonçalves da Silva
Coorientadora: Silene Carneiro do Nascimento
Tese (doutorado) – Universidade Federal de Pernambuco.
Centro de Ciências Biológicas. Ciências Biológicas/ Biologia Química para Saúde, 2015.
Inclui referência e apêndices

1. Cancer- quimioterapia 2. Ultrassom 3. I. Silva, Teresinha Gonçalves da (orientadora) II. Nascimento, Silene Carneiro do (coorientadora) III. Título

615.58 CDD (22.ed.) UFPE/CCB-2016-058

" AVALIAÇÃO DO USO DE SEMENTES DE OURO E ULTRASSOM NO TRATAMENTO DO CÂNCER POR HIPERTERMIA"

Tese apresentada ao programa de Pós Graduação em Ciências Biológicas da Universidade Federal de Pernambuco, como requisito final exigido para a obtenção do título de Doutor em Ciências Biológicas, área de concentração: Biologia Química para a Saúde.

Data de Aprovação: 25/ 02/2015

COMISSÃO EXAMINADORA

Profª. Drª. Teresinha Gonçalves da Silva - (Orientador/UFPE)

Profª. Drª. Adriana Fontes - (UFPE)

Profª. Drª. Maria Tereza dos Santos Correia - (UFPE)

Prof. Dr. Severino Alves Junior - (UFPE)

Profª. Drª. Jaciana dos Santos Aguiar - (UFPE)

Aos meus pais, José Barros (in memorian) e Eliane Souza, por estarem sempre presentes na minha vida.

AGRADECIMENTOS

A Profª. Drª. Teresinha Gonçalves da Silva por ter me acolhido, orientado e incentivado, contribuindo para minha formação pessoal e profissional. Além de tudo pela grandiosa amizade.

Ao me pai, José Barros (*in memorian*), por todo o apoio, valores e ensinamentos durante toda a minha vida.

A minha mãe, Eliane Maria de Souza Barros, por estar sempre ao meu lado me amparando e dando incentivo.

A Jeyce Andrade, pelo apoio e carinho incondicional.

A toda minha família pelo apoio contínuo.

Ao Dr. Carlos Austerlitz, por toda contribuição e amizade.

Ao Dr. Ioannis Gkigkitzis pelas contribuições matemáticas e computacionais

A Drª. Christina Peixoto, pela grandiosa ajuda na preparação das lâminas de microscopia óptica e processamento do material para microscopia eletrônica.

A técnica e amiga, Maria do Desterro Rodrigues Pela ajuda nos experimentos *in vitro.*

A Drª. Jaciana Aguiar, pela grande ajuda na parte experimental desse trabalho, sempre com alegria e paciência.

A todos os alunos e amigos do LBPF pela ajuda direta e indireta.

Aos amigos Nestor, Vitor, Leandro, David e Wendell por todo companheirismo.

A amiga Maria Suzete Mendonça pelos ensinamentos e apoio sempre.

A coordenação da pós-graduação em Ciências Biológicas.

A Adenilda Eugênia, por todo suporte.

Ao apoio financeiro da CNPq.

MUITO OBRIGADO!

“O objetivo não é ver aquilo que ninguém viu, mas pensar o que ninguém pensou sobre aquilo que todo mundo vê.”

Arthur Schopenhauer

RESUMO

O câncer é tratado, atualmente, como uma epidemia global e apesar dessa grande expressividade epidemiológica a base terapêutica utilizada no combate ao câncer limita-se a quimioterapia, a radioterapia e a cirurgia. Esses tratamentos apresentam uma série de limitações e efeitos adversos. Hipertermia é uma proposta de tratamento de câncer onde as células do tumor são afetadas pela elevação da temperatura local de acordo com a temperatura e o tempo de exposição à fonte de calor. O objetivo desse trabalho foi testar os efeitos da hipertermia obtidos através de uma técnica baseada no uso do ultrassom para irradiar sementes de ouro inseridas no interior de tumores sólidos. Neste sentido, o presente trabalho avaliou a eficácia desta técnica em modelos computacionais, *in vitro* e pré-clínicos. Para definir a forma geométrica e a difusão de calor da semente de ouro, foi utilizado um código computacional com base na equação de difusão de calor. A partir dos parâmetros definidos teoricamente foi elaborada uma técnica cirúrgica para confirmação pré-clínica e foram realizadas terapias conjuntas usando doxorrubicina. Os resultados das simulações computacionais mostraram que as sementes com 0,8x10mm e 1x 10mm, irradiadas durante 600s com frequência 1,5 MHz produziram uma taxa de geração de calor igual a 6×10^6 W/m^3. No modelo de tratamento por dose única os animais foram irradiados durante 30 min com a frequência de 1MHz e as temperaturas foram avaliadas nas regiões centrais e periféricas do tumor. Os resultados obtidos no tratamento por dose única mostraram que o aumento na temperatura foi capaz de produzir necrose coagulativa em 81,9 ±7,2% da área total do tumor. No tratamento por três doses, os animais foram irradiados durante 15min com intervalos de 5 dias. Os resultados apresentados pelos animais tratados com três doses mostraram taxa de inibição tumoral igual a 84.7%. A associação do pré-tratamento com sementes de ouro irradiadas com ultrassom e doxorrubicina reduziu a IC_{50} desse fármaco em cerca de 50% em cultura de células e apresentou 87% de inibição tumoral contra o carcinoma de Ehrlich. Podemos concluir, a partir dos nossos resultados, que a hipertermia produzida pela irradiação de sementes de ouro com ultrassom é um método eficaz na destruição de tumores sólidos e pode ser usado como um eficiente adjuvante na quimioterapia.

Palavras-chave: Câncer; Hipertermia; Sementes de ouro; Ultrassom; Doxorrubicina

ABSTRACT

Cancer is currently a global epidemic and despite this, the main therapeutics modalities are limited to chemotherapy, radiotherapy and surgery. Hyperthermia is a proposal for treatment of cancer where tumor cells are affected by the increase of the local temperature according to time of exposure to the heat source and temperature range used. The aim of this study was evaluate the effects of hyperthermia obtained through a technique based on the use of ultrasound to irradiate gold seeds inserted into solid tumors. The present study evaluated the efficacy of this technique in computer models, in vitro and preclinical. To define the geometric shape and the heat diffusion of gold seed, we used a computational code based on the heat diffusion equation. From the theoretically defined parameters, a surgical technique was designed to preclinical confirmation and joint therapies using doxorubicin. Results from computer simulations show that seeds with 0,8x10mm and 1x10mm irradiated for 600s on 1,5MHz frequency produced heat generation rate of 6×10^6 W/m^3. In single-dose model treatment, animals were irradiated with 1 MHz for 30 min and temperature was evaluated in the central and peripheral regions of the tumor. In this treatment, increase in temperature was able to produce coagulative necrosis of 81.9 ± 7.2% of the total area of the tumor. In a three dose treatment, animals were irradiated for 15 minutes every five days. The results showed tumor inhibition rate was equal to 84.7%. The combination of pre-treatment with gold seeds irradiated with ultrasound and doxorubicin decreased the IC50 of the drug in about 50% in cells cultures and showed 87% tumor inhibition against Ehrlich carcinoma. In conclusion, the hyperthermia produced by gold seeds exposed to ultrasound is effective method for the destruction of solid tumors and can be used as an efficient adjuvant in cancer chemotherapy.

Keywords: Cancer; Hyperthermia; Gold seeds; Ultrasound; Doxorubicin

LISTA DE FIGURAS

LISTA DE ABREVIATURAS E SIGLAS

Bax – Antagonista do Bcl-2 (indutora de apoptose ou pro-apoptótica)

Bcl-2 – célula B de Linfoma-2 = proteína inibidora de apoptose (morte celular programada)

cAMP – Monofosfato de adenosina cíclico

CDK – Cinase dependente de ciclinas

CDKI – Inibidor de CDK

cDNA – Ácido desoxirribonucléico complementar

CEUA-UFPE – Comitê de ética no uso de animais da Universidade Federal de Pernambuco

IC_{50} – Concentração que produz 50 % de inibição no crescimento celular

C-myc – Proteína similar ao oncogene viral de Mielocitomatose (V-myc) = Proto-oncogene que atua como fator de transcrição de outros genes.

CO_2 – Dióxido de Carbono

COBEA – Colégio Brasileiro de Experimentação Animal

COX-2 – Ciclooxigenase-2

DMEM – Meio de cultivo celular Dulbecco´s Modified Eagle´s

DMSO – Dimetilsulfóxido

DNA – Ácido desoxirribonucleico

DOX- Doxorrubicina

E2F – Fator ativador da transcrição em eucariontes maiores 2

EDTA – Ácido etilenodiamino tetra-acético

EFA – Ácidos graxos essenciais, ou seja, que devem ser obtidos da dieta

EGF – Fator de crescimento epidermal

EGFR – Receptor do EGF

FDA – “Food and Drug Administration”

GR- Gold rod

GMR- Gold macro rod

GR+U- gold rod irradiado com ultrassom

GR+U+DOX- gold Rod irradiado com ultrassom combinado com doxorrubicina

HEP-2 – carcinoma epidermóide de laringe

HIF – Fator induzido por hipóxia

HT-1080 – Fibrosarcoma humano

HTB5 – Carcinoma de células transicionais de bexiga humana

HTB9 – Carcinoma de bexiga humana

ICLAS – Conselho de Laboratório de Animais Experimentais

iHDAC – inibidores das histonas deacetilase

IKK – Cinase do IκB

INCA – Instituto Nacional do Câncer

K562 – Eritroleucemia

kDa – kilodalton (unidade de medida do peso molecular de proteínas)

MAPK – Cinases de proteínas ativadas por mitógenos

MCF-7 – adenocarcinoma de mama

MEC – Matriz extracelular

MMPs – Metaloproteases da matriz

MTT – ([brometo de (3-(4,5-dimetiltiazol-2-yl)-2,5-difenil tetrazólio])

NCI-H292 – Carcinoma mucoepidermóide de pulmão

NF-κB – Fator nuclear de transcrição-kapaB

OMS – Organização Mundial de Saúde

P21 – Proteína de 21kDa inibidora de CDK (CDKI) da família Cip/Kip

P27 – Proteína de 27kDa inibidora de CDK (CDKI) da família Cip/Kip

P50 ou NF-kB1 – Proteína de 50kDa que se liga ao p65 formando o heterodímero do NF-kB

P53 – proteína de 53kDa ou proteína tumoral 53, conhecida como supressora tumoral

PBS – Solução tampão fosfato

Raf – Proteína efetora da via do Ras

Rho – Subfamília de proteínas GTPases da família Ras, que incluem, entre outras, Rac1 e RhoA.

RNA – Ácido ribonucléico

RNAm – Ácido ribonucléico mensageiro

ROS – Espécies reactivas de oxigênio

RPM – Rotações por minuto

TNF – Factor de necrose tumoral

VEGF – Fator de crescimento do endotélio vascular

.

,

SUMÁRIO

Capítulo I

1. INTRODUÇÃO

O Câncer é caracterizado pelo surgimento de células anormais que crescem além de seus limites usuais e que podem invadir partes adjacentes do corpo e se espalhar para outros órgãos. A distribuição dos casos de câncer no mundo enquadra essa doença atualmente como uma epidemia global, cerca de 10 milhões de pessoas são diagnosticadas por ano e projeções indicam que esse número seja de 15 milhões até 2020 (BOYLE; LEVIN, 2008).

Dentre os métodos terapêuticos convencionais para combater o câncer, a quimioterapia, a radioterapia e a cirurgia, representam a base terapêutica de atuação. Esses tratamentos apresentam uma série de limitações e inconvenientes como, por exemplo, a longa duração, possuírem inúmeros efeitos adversos e principalmente, serem caros. O número de casos da doença aliado ao conjunto de limitações das terapias existentes atualmente tem impulsionado uma corrida pelo desenvolvimento de técnicas e estratégias terapêuticas cada vez mais eficazes. Neste sentido a hipertermia e a termoablação são apontadas, dentre muitas técnicas de tratamento, como promissoras no combate ao câncer.

A hipertermia é o tratamento clínico para doenças malignas, no qual os tecidos tumorais são aquecidos por agentes externos a temperaturas de no mínimo 40-41°C e mantidas por um longo período de tempo. A hipertermia é normalmente administrada em conjunto com outras modalidades terapêuticas, formando uma estratégia terapêutica multimodal. A eficiência terapêutica da hipertermia depende de uma resposta diferenciada ao calor para o tecido tumoral em relação ao tecido sadio (BARONZIO, 2014).

O calor provoca alguns efeitos intracelulares letais decorrentes do rompimento da membrana plasmática e mitocôndrias, aglomeração da cromatina nuclear e tumefação celular. É importante salientar que estes efeitos dependem do tempo de exposição e da temperatura utilizada. O tratamento dos tumores torna-se mais efetivo a temperaturas de 40°C ou superiores. A vascularização primitiva dos tumores contribui para essa efetividade reduzindo a capacidade de dissipação do calor. Também está comprovado que a exposição ao calor causa danos de conformação às proteínas celulares, reduzindo bastante a capacidade fisiológica de funcionamento. A hipertermia acentuada causa uma toxicidade térmica imediata,

pois se as temperaturas teciduais forem elevadas acima de um limiar de 56°C durante pelo menos 1 segundo, levarão a irreversível morte celular através de necrose coagulativa (BARONZIO, 2014; KNORR et al., 2014).

Diversos estudos relatam que elevar a temperatura local do tecido, ou induzir um processo de hipertermia, induz um aumento do fluxo sanguíneo tumoral, assim como modifica a permeabilidade da parede vascular. Essas características constituem um interessante adjuvante na tentativa de melhorar a distribuição e penetração dos fármacos anticancer no tecido alvo. A alteração do fluxo sanguíneo aumenta a oxigenação local e a concentração de nutrientes em regiões inicialmente deficitárias, que tipicamente apresentam limitações no acúmulo destes elementos. O aumento da permeabilidade vascular, por sua vez, aumenta o extravasamento de moléculas, como os medicamentos, para o ambiente intersticial tumoral. De fato, existem diversos estudos que demonstram a sinergia positiva entre aquecimento local (hipertermia) e quimioterapia. No entanto, os efeitos benéficos da hipertermia podem ir além da conhecida modulação das condições fisiológicas locais, pois o calor interfere diretamente no ambiente celular, promovendo danos tanto em proteínas e complexos proteicos, quanto nos agentes reparadores de DNA, o que pode ajudar a aumentar a citotoxicidade dos agentes terapêuticos (ISSELS et al., 2010; OWUSU; ABERN; INMAN, 2013).

O aumento da temperatura no tumor tem sido obtido por meio de várias técnicas como, por exemplo, a utilização de fluidos magnéticos (JORDAN et al., 1999), emissão de microondas (DUBOIS, 1996), nanopartículas magnéticas (JOHANNSEN et al., 2005), nanoesferas de ouro (TERENTYUK et al., 2009; O'NEAL et al., 2004), nanobastões de ouro (HUANG; REGE; HEYS, 2010), nanoshells (STERN et al., 2007), laser intersticial (MA; GAO; ZHANG, 2003), radiofrequência (DUBOIS, 1996), ultra-som (EBBINI et al., 1988) e ultrassom focalizado de alta intensidade (UCHIDA et al., 2002).

Levando em consideração todas as informações relacionadas à hipertermia e conhecendo as propriedades físicas do ultrassom, elaboramos uma técnica baseada no uso do ultrassom para irradiar sementes de ouro inseridas no interior de tumores sólidos. Neste sentido, o presente trabalho avaliou em modelos computacionais e pré-clínicos a eficácia desta técnica.

2. OBJETIVOS

2.1. Geral

Avaliar a eficácia e viabilidade do uso de sementes de ouro e ultrassom no tratamento do câncer por hipertermia.

2.1. Específicos

- Avaliar a transferência de calor das sementes de ouro irradiadas com ultrassom através de cálculos analíticos;

- Avaliar a transferência de calor das sementes de ouro irradiadas com ultrassom através de modelos computacionais;

- Determinar a forma geométrica das sementes de ouro para inserção nos tumores;

- Avaliar os efeitos hipertérmicos induzidos por sementes de ouro irradiadas com ultrassom em cultura de células;

- Elaborar a técnica cirúrgica para inserção das sementes de ouro no tumor;

- Avaliar o os efeitos antitumorais da hipertermia produzida pelo aquecimento das sementes de ouro irradiadas com ultrassom no modelo de Carcinoma de Ehrlich;

- Avaliar os efeitos da hipertermia induzida pela combinação de sementes de ouro e ultrassom associados à quimioterapia convencional em cultura de células;

- Avaliar os efeitos da hipertermia induzida pela combinação de sementes de ouro e ultrassom associados à quimioterapia convencional no modelo de Carcinoma de Ehrlich;

3. REVISÃO BIBLIOGRÁFICA

3.1. O Câncer

Câncer é o termo empregado a um conjunto de doenças que se familiarizam por apresentar uma desorganização genética que acarreta o descontrole celular. Os mecanismos de autossuficiência aos fatores de crescimento, evasão a apoptose, angiogênese e invasão tecidual são as principais características apresentadas pelas células malignas(HANAHAN; WEINBERG, 2011) . A formação e progressão do câncer conhecido como carcinogênese é um processo complexo que se desenvolve em três principais etapas: iniciação, promoção e progressão(SANTELLA et al., 2005).

A iniciação é causada por alterações genéticas irreversíveis predispondo células normais susceptíveis à evolução maligna e imortalidade, sendo considerado um processo aditivo (COUSSENS; WERB, 2010). A iniciação também pode começar por mutações espontâneas, como por exemplo, erro na replicação do DNA, embora seja menos comum (COHEN; ARNOLD, 2011). A promoção ocorre através de agentes que aumentam a proliferação celular nos tecidos sensíveis, isso contribui para o aumento das alterações genéticas e interfere no controle do crescimento celular (MARTÍN DE CIVETTA; CIVETTA, 2011). A progressão é um processo irreversível caracterizado pela instabilidade genética, aceleração no crescimento, invasão, metástase e mudanças nas características bioquímicas e morfológicas das células (ABEL; DIGIOVANNI, 2011).

Por ser a segunda causa de morte no mundo, perdendo apenas para as doenças cardiovasculares, e ter uma etiologia bem complexa, o câncer tem estimulado vários pesquisadores ao redor do mundo, na tentativa de se buscar tratamentos mais efetivos e que causem menos efeitos adversos, entretanto, poucas novidades são usadas na terapêutica convencional(MARAMALDI; DUNGAN; POORVU, 2008).

O tratamento do câncer tem como principais metas a cura, o prolongamento da sobrevida e a melhoria da qualidade de vida. Dentre as principais formas de tratamento estão à cirurgia, a radioterapia, a quimioterapia e a terapia gênica. A cirurgia e a radioterapia são apropriadas para tratamento da doença localizada e regional e pode curar nos estágios iniciais do câncer, mais em geral possuem um

papel limitado em cânceres mais avançados. Além disso, as células cancerígenas ainda apresentam alta resistência a diversas formas de tratamento tornando cada vez mais difícil a luta contra o câncer (VON MINCKWITZ; MARTIN, 2012).

3.2. Ultrassom

O ultrassom é gerado por transdutores que convertem a energia elétrica em mecânica e vice-versa. Esta transdução decorre do efeito piezo-elétrico que consiste na deformação das dimensões físicas de certos materiais como, por exemplo, o quartzo e a turmalina quando submetido a um campo elétrico. Zonas de compressão alternam-se com zonas de rarefação. Densidades de partículas decrescem para o mínimo na rarefação entre zonas adjacentes de compressão. Ocorrem vibrações mecânicas e ondas ultrassônicas são geradas (LAWRENCE, 2007; SHRIKI, 2014).

O feixe do ultrassom forma um campo acústico, o qual é dividido em campo próximo (Zona de Fresnel) e campo distante (Zona de Fraunhofer). O primeiro é a região mais próxima da face do transdutor, distingue-se pela não uniformidade na distribuição de intensidade do feixe. O campo distante é a região mais afastada da face do transdutor e a variação de intensidade do feixe é mais uniforme. A região focal do feixe (Zn), determinada pela posição do último máximo axial de pressão é o limite entre os dois campos. Essa é a região de maior concentração de energia ultrassônica do feixe (ARTHURS, 2011; SHRIKI, 2014), também denominada de foco natural. Há dois tipos de ondas: longitudinal e transversal. Na onda longitudinal, as partículas vibram ao longo da mesma direção da propagação. Na onda transversal, a vibração ocorre na direção perpendicular à propagação. As ondas transversais se propagam apenas em sólidos. Para fins de terapia por ultrassom, o osso, devido a sua densidade, é o único tecido biológico onde as ondas transversais, também denominadas de ondas de cisalhamento ou ondas de pressão tem um papel importante. (KINSLER et al., 1999).

As ondas apresentam certas características físicas, que auxiliam nas descrições das mesmas (figura 1): A amplitude refere-se à magnitude da vibração da onda, o termo pode ser aplicado ao deslocamento de partícula ou à pressão do meio; A frequência é definida como o número de ciclos de uma onda que ocorre por segundo, expressa em Hertz (Hz); O Comprimento de onda é a medida de um ciclo completo que vai de um pico de onda ao pico precedente ou seguinte; Velocidade de

propagação é a velocidade com que a onda se propaga no meio; Densidade é definida como massa sobre volume; compressibilidade determina a diminuição do volume fracionário quando a pressão é aplicada no material (LAWRENCE, 2007; LIEU, 2010; SHRIKI, 2014).

Figura 1- Características físicas das ondas.

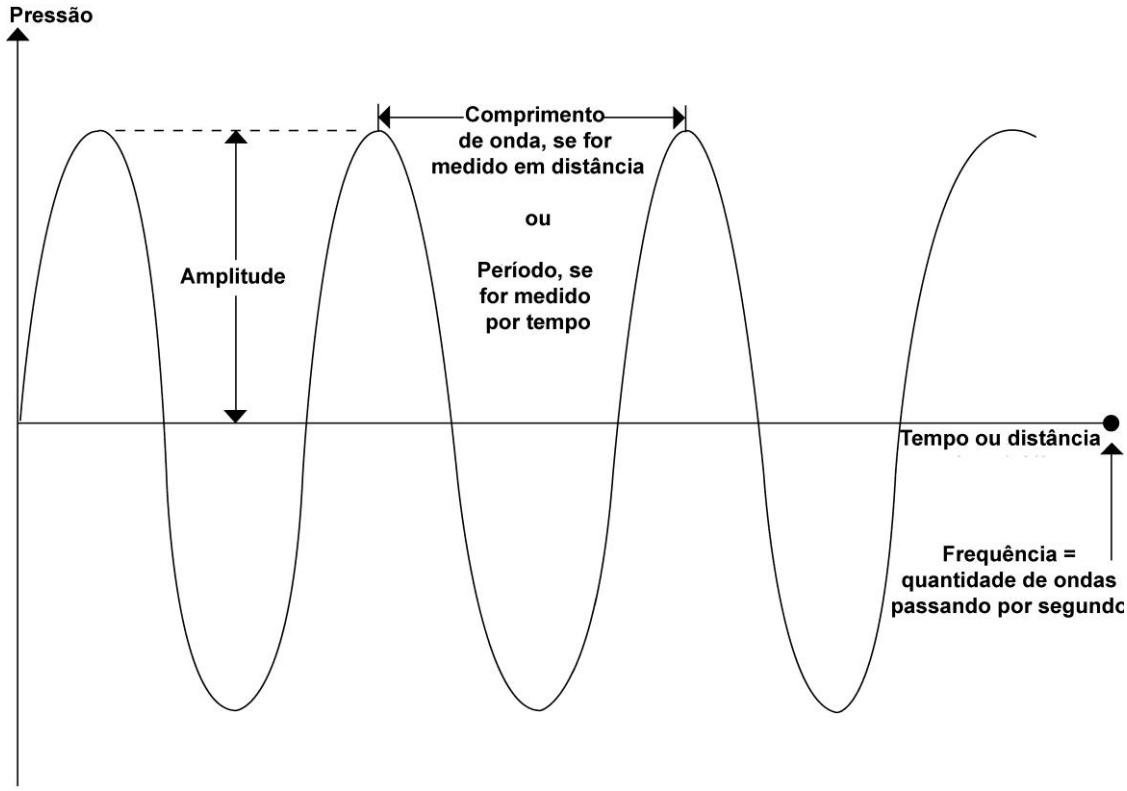

Fonte: Adaptado de Lieu, 2010

3.3. Interações do Ultrassom nos Tecidos Biológicos

A propagação da onda ultrassônica nos tecidos vivos depende do tipo de tecido e das características físicas da onda. Durante a propagação, há perda de energia por absorção. No limite entre dois tecidos, o ultrassom é parcialmente refletido e a outra parte da energia é transmitida, podendo ser refratada e espalhada (MIELE, 2006).

A impedância acústica de um meio está relacionada com a resistência à passagem do som. Também pode ser definida (para ondas planas) como o produto da densidade pela velocidade de propagação do respectivo meio (Equação 1).

$$Z = \rho c \qquad \textbf{Eq. (1)}$$

onde *Z* é impedância acústica (ou ultrassônica) ($kg.m^{-2}.s^{-1}$), ρ é a densidade ($kg.m^{-3}$) e *c* é a velocidade (ms^{-1}).

Entre a camada de pele e o transdutor, normalmente, coloca-se uma camada de gel para melhorar o acoplamento e permitir uma melhor transmissão ultrassônica. Minimiza-se, assim a reflexão oriunda da interface ar/tecido (LAWRENCE, 2007).

A reflexão consiste na alteração da direção da propagação do feixe. O ângulo refletor é igual ao ângulo incidente. Estes ângulos são definidos em relação ao eixo perpendicular a superfície. Quando a onda ultrassônica passa por uma interface entre dois meios, parte do feixe é transmitida através da interface e parte refletida. A diferença de impedância, entre os meios, é responsável pela parte refletida do feixe ultrassônico. Deste modo, o feixe ao atravessar uma interface com a mesma impedância acústica, não sofre reflexão, pois toda onda é transmitida para o segundo meio. Se há uma grande diferença de impedância acústica, como no caso entre osso e tecidos moles, a magnitude da onda refletida será alta (LIEU, 2010; MIELE, 2006). A reflexão tem grande importância no diagnóstico, pois promove a identificação dos contornos das estruturas biológicas na imagem.

Absorção é o processo pelo qual a energia acústica é transformada em outras formas de energia, primariamente calor. Este processo dissipa a energia sonora, ao contrário de todas as outras interações, como a reflexão, refração, espalhamento e divergência, que diminuem a intensidade, por alterar a direção do feixe. A absorção do feixe é dependente da frequência do mesmo, da viscosidade e do tempo de relaxação do meio (FISH, 1990; HEDRICK et al., 1995).

O aquecimento tecidual decorrente da aplicação de ultrassom nos tecidos é influenciado por diversos fatores, sendo a perfusão sanguínea, o principal deles. A equação biotérmica (Equação 2) relaciona a temperatura do meio decorrente do aquecimento pelo ultrassom com a densidade do meio, com o calor específico, com a condutividade térmica, com a perfusão sanguínea e com a potencia acústica (DUCK et al., 1997).

$$\rho_t Cp \frac{\partial T}{\partial t} = \nabla . (k \nabla T) + \rho_b Cp_b \omega_b (T - T_a) + Q(\vec{r}) \qquad \textbf{Eq. (2)}$$

Onde, T é a temperatura no tempo t e no ponto (x,y,z), ρ é a densidade do meio, Cp é o calor específico do meio, k a condutividade do meio, ω_b é a razão de perfusão sanguínea, ρ_b é a densidade do sangue, Cp_b é o calor específico do sangue, T_a a temperatura do sangue arterial e $Q(x,y,z)$ a potência acústica depositada por unidade de volume. O primeiro termo do lado direito da equação é relacionado ao processo de difusão, o segundo termo descreve as influências dos vasos sanguíneos presentes no local de estudo. O terceiro termo descreve o campo térmico originado pela absorção da onda ultra-sônica (CORTELA; PEREIRA; NEGREIRA, 2004).

3.4. O uso da hipertermia no tratamento do câncer

A humanidade tem explorado o calor para propósitos terapêuticos desde os tempos antigos. Existem inúmeros relatos históricos sobre o uso da cauterização contra tumores e varias doenças não malignas na cultura egípcia e oriental. A importância do uso terapêutico do calor na civilização grega é refletida no precedente aforismo atribuído a Hipócrates (460-357 a.C.), ele recomendou cauterização com aço incandescente para pequenos tumores e muitas outras doenças (HORSMAN; OVERGAARD, 2007). As aplicações da cauterização usando metais aquecidos ou lentes remanesceram populares entre a comunidade científica até a metade do século XIX, quando métodos mais sofisticados para elevação da temperatura local de tecidos tornaram-se disponíveis (GILDER, 1987).

Em 1866, a cura de um paciente com sarcoma, após um ataque de erisipela que induziu febre sugeriu a possibilidade do calor ser seletivamente letal a células neoplásicas (BUSCH, 1866). Esse relato impulsionou o uso de toxinas bacterianas para produção de hipertermia, através da febre, em pacientes com câncer (COLEY, 1910; STARNES, 1992; DAMSTRA et al., 2008). No começo do século XX, o maior desenvolvimento ocorreu com o advento de ondas curtas (ou radio frequência), que permitiu o aquecimento não invasivo tanto local como profundo (GILDER, 1987). Em 1927, o uso de radiofrequência para geração de calor demonstrou que temperaturas entre 44-45ºC são letais em tumores de ratos (JONHSON, 1940).

No final da década de 60 a aplicação de sangue quente por perfusão local demonstrou ser capaz de provocar aquecimento em tumores humanos o estudo mostrou que o calor sozinho pode permitir a total regressão de melanomas e sarcomas e aumentar a sobrevivência de pacientes (CAVALIERE; GIOGATTO; GIOVANELLA, 1967). Outro estudo indicou que o calor e uma droga anticâncer (Melphalan) não somente é capaz de curar o tumor principal, mas também reduzir a incidência de metástase desses tumores (STEHLIN, 1969). Os trabalhos desses dois grupos levaram a uma nova onda de interesse na pesquisa em hipertermia ao longo dos anos.

3.5. Efeitos biológicos induzidos pela hipertermia.

Os diversos efeitos do aquecimento podem estar associados a impactos diretos ou indiretos no funcionamento celular, estes podem induzir condições de apoptose, ou mesmo alterar o sistema de reparação e/ou mutação. Estudos de sobrevivência de células in vitro mostraram que o efeito citotóxico do calor é fortemente dependente do valor de temperatura e do tempo de exposição. Curvas de sobrevivência em função do tempo e da temperatura indicam a presença de um comportamento de dois estados no processo de desestabilização celular. Um estado com alta citotoxicidade (Temp >43°C), e um estado de temperaturas moderadas (Temp <43°C) em que as células são resistentes a uma exposição contínua ao calor.

Matar células depende da duração do aquecimento e da alta temperatura atingida durante uma particular sessão de tratamento (figura 2). Quanto maior a temperatura e mais longa a duração no tumor, mais forte o efeito letal e menor termotolerância. As proteínas são os alvos predominantes na hipertermia, à desnaturação intracelular de proteínas desestabilizam membranas celulares, citoesqueletos, enzimas, tradução de sinais, sínteses macromoleculares e o núcleo celular (HILDEBRANDT et al., 2002; VAN DER ZEE, 2002). Esse conjunto de alterações pode levar a morte celular por necrose ou apoptose (figura 3) (ROTI ROTI, 2008).

Em tecidos normais, é sabido que o calor induz uma rápida resposta do aumento do fluxo sanguíneo, que é acompanhando pela dilatação dos vasos e um aumento da permeabilidade da parede vascular (SONG, 1984). No caso de tecidos tumorais, sabe-se que as alterações no fluxo sanguíneo, induzidas pelo calor, são

consideravelmente distintas dos tecidos sadios. Achados anteriores indicam que o aumento do fluxo sanguíneo na região tumoral responde a um fator de aproximadamente 2 vezes quando aquecido por uma hora a 43,5 °C, enquanto o fluxo sanguíneo em tecidos sadios sofre um aumento muito superior (CHO et al., 2010).

Figura 2- Comportamento dos efeitos celulares e moleculares em função da Temperatura.

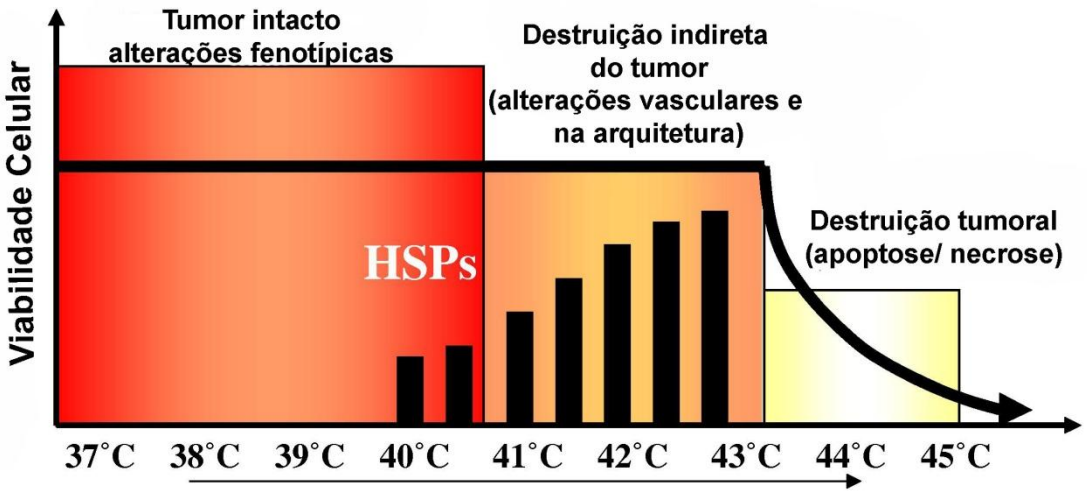

Fonte: Adaptado de Issels, 2008.

Em resumo, existem diversos relatos que evidenciaram que a resposta da rede vascular tumoral ao calor é consideravelmente inferior ao comportamento do tecido sadio. O efetivo uso clínico da hipertermia depende da manipulação cuidadosa destes princípios biológicos. A vascularização tumoral é menos eeficaz em trocar calor, e mais propícia a ser danificada quando tratada com hipertermia.

Em certas circunstâncias, a hipertermia parece estimular o sistema imune, como, por exemplo, inibindo o crescimento tumoral por um desarranjo das paredes celulares. Já em outras situações a elevação da temperatura inibe a ação imune, devido à indução de danos específicos principalmente nos macrófagos. Ainda em relação ao processo de modulação imunológica, temperaturas menores que 40°C, promovem um aumento de células NK ativadas por linfocina ou LAK, em função a exposição a IFN-gama, porém estes efeitos são reversos em temperaturas acima de 42°C (HILDEBRANDT et al., 2002; ZHANG et al., 2008).

Figura 3- Esquematização dos efeitos celulares induzidos por hipertermia.

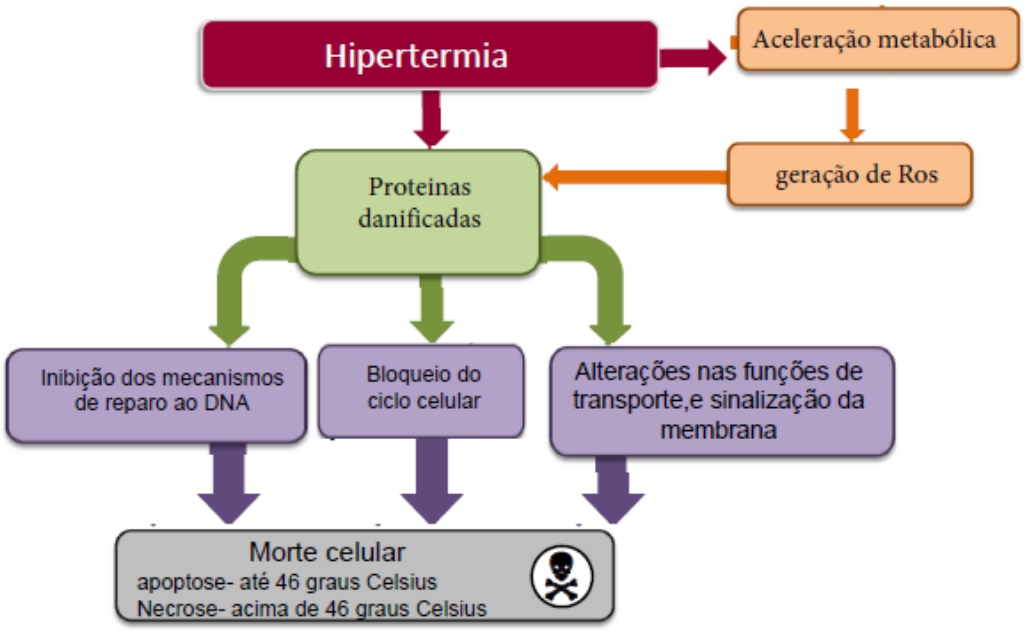

Fonte: Adaptado de (BETTAIEB; WRZAL; AVERILL-BATES, 2013)

3.6. Hipertermia associada à radioterapia e agentes quimioterápicos

O uso combinado da radiação e hipertermia no tratamento do câncer baseia-se, principalmente, no aumento da oxigenação no tumor. Células em condições de hipóxia são aproximadamente três vezes mais radioresistentes quando comparadas com células em condições normais de oxigenação e, em tumores sólidos humanos as condições de baixa oxigenação reduz a sensibilidade do tumor à radiação ionizante, através de mecanismos indiretos que incluem mudanças proteômicas e genômicas. A hipertermia moderada pode alterar esta limitação, pois a alteração do fluxo sanguíneo e aumento da permeabilidade dos vasos, aumenta diretamente a concentração de oxigênio no tecido (GONZALEZ GONZALEZ et al., 1986; VAN DER ZEE, 2002; ZAGAR et al., 2010a, 2010b).

A combinação de calor com agentes quimioterápicos pode produzir um efeito cooperativo, que deve depender do agente específico. Em geral, a citotoxicidade de drogas demonstra um aumento na inibição do crescimento celular (*in vitro*) em condições de temperaturas elevadas. Existem extensivas revisões avaliando os

efeitos positivos da combinação da hipertermia e quimioterapia publicados na literatura (COLOMBO et al., 2003; ISSELS et al., 2010; KULSHRESTHA et al., 2012; OWUSU; ABERN; INMAN, 2013; TSCHOEP-LECHNER et al., 2013).

Figura 4- Esquematização dos principais efeitos da hipertermia usada como adjuvante.

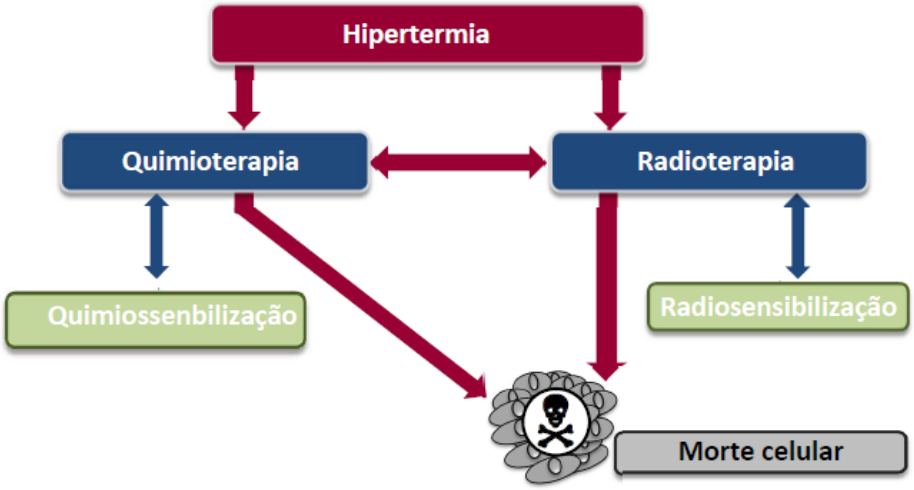

Fonte: Adaptado de (BETTAIEB; WRZAL; AVERILL-BATES, 2013)

REFERÊNCIAS

ABEL, E. L.; DIGIOVANNI, J. Multistage carcinogenesis. **Current Cancer Research**, v. 6, p. 27–51, 2011.

ARTHURS, G. The Physics of Ultrasound. In: **AAGBI Core Topics in Anaesthesia**. [s.l: s.n.]. p. 1–16.

BARONZIO, G. A Brief Overview of Hyperthermia in Cancer Treatment. **Journal of Integrative Oncology**, v. 03, n. 01, p. 1–10, 2014.

BETTAIEB, A.; WRZAL, P.; AVERILL-BATES, D. Hyperthermia: Cancer Treatment and Beyond. **Cancer Treatment - Conventional and Innovative Approaches**, p. 28, 2013.

BOYLE, P.; LEVIN, B. World cancer report 2008. 2008.

CAVALIERE, R.; GIOGATTO, B.; GIOVANELLA, B. Selective heat sensitivity of cancer cells. **Cancer**, 1967.

CHO, C.-H. et al. Tumour perfusion assessment during regional hyperthermia treatment: comparison of temperature probe measurement with H(2)(15)O-PET perfusion. **International journal of hyperthermia : the official journal of European Society for Hyperthermic Oncology, North American Hyperthermia Group**, v. 26, p. 404–411, 2010.

COHEN, S. M.; ARNOLD, L. L. Chemical carcinogenesis. **Toxicological sciences : an official journal of the Society of Toxicology**, v. 120 Suppl 1, p. S76–S92, 2011.

COLEY, W. B. The Treatment of Inoperable Sarcoma by Bacterial Toxins (the Mixed Toxins of the Streptococcus erysipelas and the Bacillus prodigiosus). **Proceedings of the Royal Society of Medicine**, v. 3, p. 1–48, 1910.

COLOMBO, R. et al. Combination of intravesical chemotherapy and hyperthermia for the treatment of superficial bladder cancer: preliminary clinical experience. **Critical reviews in oncology/hematology**, v. 47, p. 127–139, 2003.

CORTELA, G. A.; PEREIRA, W. C. A.; NEGREIRA, C. A. Simulación del campo térmico generado por transductores ultrasónicos circulares. **IFMBE Proceedings**, v. 5, p. 1619–1622, 2004.

COUSSENS, L. M.; WERB, Z. Inflammation and cancer. **Nature**, v. 420, p. 860–7, 2010.

DAMSTRA, R. J. et al. Erysipelas as a sign of subclinical primary lymphoedema: A prospective quantitative scintigraphic study of 40 patients with unilateral erysipelas of the leg. **British Journal of Dermatology**, v. 158, p. 1210–1215, 2008.

DUBOIS, L. Temperature control and thermal dosimetry by microwave radiometry in hyperthermia. **IEEE Transactions on Microwave Theory and Techniques**, v. 44, p. 1755–1761, 1996.

EBBINI, E. S. et al. Cylindrical-section ultrasound phased-array applicator for hyperthermia cancer therapy. **IEEE Transactions on Ultrasonics, Ferroelectrics, and Frequency Control**, v. 35, p. 561–572, 1988.

GILDER, S. S. B. Hyperthermia in cancer therapy. **South African Medical Journal**, v. 72, p. 589, 1987.

GONZALEZ GONZALEZ, D. et al. Combined treatment with radiation and hyperthermia in metastatic malignant melanoma. **Radiother Oncol**, v. 6, p. 105–113, 1986.

HANAHAN, D.; WEINBERG, R. A. **Hallmarks of cancer: The next generationCell**, 2011.

HILDEBRANDT, B. et al. **The cellular and molecular basis of hyperthermiaCritical Reviews in Oncology/Hematology**, 2002.

HORSMAN, M. R.; OVERGAARD, J. Hyperthermia: a potent enhancer of radiotherapy. **Clinical oncology (Royal College of Radiologists (Great Britain))**, v. 19, n. 6, p. 418–26, ago. 2007.

HUANG, H. C.; REGE, K.; HEYS, J. J. Spatiotemporal temperature distribution and cancer cell death in response to extracellular hyperthermia induced by gold nanorods. **ACS Nano**, v. 4, p. 2892–2900, 2010.

ISSELS, R. D. Hyperthermia adds to chemotherapy. **European Journal of Cancer**, v. 44, p. 2546–2554, 2008.

ISSELS, R. D. et al. Neo-adjuvant chemotherapy alone or with regional hyperthermia for localised high-risk soft-tissue sarcoma: A randomised phase 3 multicentre study. **The Lancet Oncology**, v. 11, p. 561–570, 2010.

JOHANNSEN, M. et al. **Clinical hyperthermia of prostate cancer using magnetic nanoparticles: presentation of a new interstitial technique.International journal of hyperthermia : the official journal of European Society for Hyperthermic Oncology, North American Hyperthermia Group**, 2005.

JORDAN, A. et al. **Magnetic fluid hyperthermia (MFH): Cancer treatment with AC magnetic field induced excitation of biocompatible superparamagnetic nanoparticlesJournal of Magnetism and Magnetic Materials**, 1999.

KINSLER, L. E. et al. **Fundamentals of acoustics**. [s.l: s.n.]. v. 1p. 560

KNORR, C. et al. Hyperthermic isolated limb perfusion (HILP) in malignant melanoma. Experience with 101 patients. **European Journal of Surgical Oncology**, v. 32, n. 2, p. 224–227, 29 nov. 2014.

LAWRENCE, J. P. Physics and instrumentation of ultrasound. **Critical care medicine**, v. 35, p. S314–S322, 2007.

LIEU, D. Ultrasound physics and instrumentation for pathologists. **Archives of pathology & laboratory medicine**, p. 1541–1556, 2010.

MA, N.; GAO, X.; ZHANG, X. X. Two-layer simulation model of laser-induced interstitial thermo-therapy. **Lasers in Medical Science**, v. 18, p. 184–189, 2003.

MARAMALDI, P.; DUNGAN, S.; POORVU, N. L. Cancer treatments. **Journal of gerontological social work**, v. 50 Suppl 1, p. 45–77, 2008.

MARTÍN DE CIVETTA, M. T.; CIVETTA, J. D. [Carcinogenesis]. **Salud pública de México**, v. 53, p. 405–14, 2011.

MIELE, F. R. **VOLUME I U ltrasound P hysics & i nstrumentation**. [s.l: s.n.]. v. I

OWUSU, R. A.; ABERN, M. R.; INMAN, B. A. **Hyperthermia as adjunct to intravesical chemotherapy for bladder cancerBioMed Research International**, 2013.

ROTI ROTI, J. L. Cellular responses to hyperthermia (40-46 degrees C): cell killing and molecular events. **International journal of hyperthermia : the official journal of European Society for Hyperthermic Oncology, North American Hyperthermia Group**, v. 24, p. 3–15, 2008.

SANTELLA, R. M. et al. **DNA adducts, DNA repair genotype/phenotype and cancer risk**Mutation Research - Fundamental and Molecular Mechanisms of Mutagenesis. **Anais**...2005

SHRIKI, J. **Ultrasound physicsCritical Care Clinics**, 2014.

SONG, C. W. Effect of local hyperthermia on blood flow and microenvironment: A review. **Cancer Research**, v. 44, 1984.

STARNES, C. O. Coley's toxins in perspective. **Nature**, v. 357, p. 11–12, 1992.

STEHLIN, J. S. Hyperthermic perfusion with chemotherapy for cancers of the extremities. **Surgery, gynecology & obstetrics**, v. 129, p. 305–308, 1969.

STERN, J. M. et al. Efficacy of laser-activated gold nanoshells in ablating prostate cancer cells in vitro. **Journal of endourology / Endourological Society**, v. 21, p. 939–943, 2007.

TERENTYUK, G. S. et al. Laser-induced tissue hyperthermia mediated by gold nanoparticles: toward cancer phototherapy. **Journal of Biomedical Optics**, v. 14, n. 2, p. 21016–21019, 2009.

TSCHOEP-LECHNER, K. E. et al. Gemcitabine and cisplatin combined with regional hyperthermia as second-line treatment in patients with gemcitabine-refractory

advanced pancreatic cancer. **International journal of hyperthermia : the official journal of European Society for Hyperthermic Oncology, North American Hyperthermia Group**, v. 29, p. 8–16, 2013.

UCHIDA, T. et al. Transrectal high-intensity focused ultrasound for treatment of patients with stage T1b-2n0m0 localized prostate cancer: A preliminary report. **Urology**, v. 59, p. 394–398, 2002.

VAN DER ZEE, J. **Heating the patient: A promising approach?Annals of Oncology**, 2002.

VON MINCKWITZ, G.; MARTIN, M. Neoadjuvant treatments for triple-negative breast cancer (TNBC). **Annals of Oncology**, v. 23, 2012.

ZAGAR, T. M. et al. Hyperthermia combined with radiation therapy for superficial breast cancer and chest wall recurrence: a review of the randomised data. **International journal of hyperthermia : the official journal of European Society for Hyperthermic Oncology, North American Hyperthermia Group**, v. 26, p. 612–617, 2010a.

ZAGAR, T. M. et al. Hyperthermia for locally advanced breast cancer. **Int.J.Hyperthermia**, v. 26, p. 612–617, 2010b.

ZHANG, H. G. et al. **Hyperthermia on immune regulation: A temperature's storyCancer Letters**, 2008.

Capítulo II

4 ARTIGO CIENTÍFICO I

The Effect of the Shape and Size of Gold Seeds Irradiated with Ultrasound on the Bio-Heat Transfer in Tissue

Artigo aceito pelo periódico: Advances in Experimental Medicine and Biology

Author's Proof

The Effect of the Shape and Size of Gold Seeds Irradiated with Ultrasound on the Bio-Heat Transfer in Tissue

I. Gkigkitzis, C. Austerlitz, I. Haranas, A. Barros, T. Gonçalves and D. Campos

Abstract The aim of this report is to propose a new methodology to treat prostate cancer with macro-rod-shaped gold seeds irradiated with ultrasound and develop a new computational method for temperature and thermal dose control of hyperthermia therapy induced by the proposed procedure. A computer code representation, based on the bio-heat diffusion equation, was developed to calculate the heat deposition and temperature elevation patterns in a gold rod and in the tissue surrounding it as a result of different therapy durations and ultrasound power simulations. The numerical results computed provide quantitative information on the interaction between high-energy ultrasound, gold seeds and biological tissues and can replicate the pattern observed in experimental studies. The effect of differences in shapes and sizes of gold rod targets irradiated with ultrasound is calculated and the heat enhancement and the bio-heat transfer in tissue are analyzed.

8.1 Introduction

Available methods to kill cancer cells may involve X-rays [36], γ-rays [7], beta rays [34], neutrons [38], high-energy electrons [15], protons [40], light and photosensitizers [24], light and gold nanoparticles, surgery, cryosurgery [16], chemicals [39], and hyperthermia [44] and thermoablation [17]. Hyperthermia is heating of certain organs or tissues to temperatures between 41 and 48 °C as a treatment of cancer.

I. Gkigkitzis
Department of Mathematics and Physics, East Carolina University, Greenville, NC, USA
e-mail: gkigkitzisi@ecu.edu

C. Austerlitz • D. Campos
Clinica Diana Campos, Recife, PE, Brazil

A. Barros, • T. Gonçalves
Bioassays Laboratory for Pharmaceutical Research, Antibiotics Department, Biological Sciences Center, Federal University of Pernambuco, Recife, Brazil

I. Haranas (✉)
Department of Mathematics, East Carolina University, Greenville, NC, USA
e-mail: yiannis.haranas@gmail.com

© Springer International Publishing Switzerland 2015
P. Vlamos, A. Alexiou (eds.), *GeNeDis 2014*, Advances in Experimental Medicine and Biology 820, DOI 10.1007/978-3-319-09012-2_8

Uncorrected Proof

Author's Proof

Thermoablation is the attempt to heat tissues to temperatures above 47 °C (up to 56 °C). Thermoablation is characterized by acute necrosis, coagulation, or carbonization of the tissue. In clinical hyperthermia, thermoablation is mostly undesired [33]. Many institutions have used a target dose 42–43 °C for 60 min at some point within the tumor volume [6]. However, the goal of hyperthermia is to raise the entire tumor volume to 43 °C or above [6]. In ultrasound surgery the cancerous tissue can be destroyed by rising the temperature to cytotoxic level. The desired temperature in tumor is often 50–60 °C. Although lower temperatures could also be used, the use of high temperatures can reduce the treatment time significantly.

Hyperthermia cancer treatment has proven to be an effective method in cancer treatment compare to surgery, chemotherapy and radiation. Hyperthermia has been used on the treatment of many types of cancer, including sarcoma, melanoma, and cancers of the head and neck, brain, lung, esophagus, breast, bladder, rectum, liver, appendix, cervix, peritoneal lining, and prostate [10, 12, 32, 48]. Hyperthermia may include local, regional, and whole-body hyperthermia [3, 10, 48]. In local hyperthermia, heat is applied to a tumor by using external applicators positioned around or near the appropriate region, and energy focused on the tumor to raise its temperature; intraluminal or endocavitary probes placed inside the cavity and inserted into the tumor to deliver energy and heat the area directly [13]; and interstitial probes or needles [4, 5, 13] inserted into the tumor. In this case, the heat source is inserted into the probe. Radiofrequency ablation (RFA) is a type of interstitial hyperthermia that uses radio waves to heat and kill cancer cells. In regional hyperthermia, external applicators may be positioned around the body cavity or organ to be treated, and microwave or radiofrequency energy is focused on the area to raise its temperature. Whole-body hyperthermia is used to treat metastatic cancer that has spread throughout the body.

Hyperthermia in cancer treatment has been achieved by magnetic fluid [23], interstitial microwave probe [13, 14, 41], long frosted contact probe [29], magnetic nanoparticles [22], near-infrared-absorbing nanoparticles [28], gold nanospheres [45], gold nanorods [19], gold iron oxide [30], gold nanoshells [43], gold-coated brass [35], double-doped magnetic silica nanospheres [31], plasmonic photothermal [20], nonradioactive ferromagnetic seed [18] interstitial microwave antenna [26], interstitial laser [8], radiofrequency [41], ultrasound [9], diffuse focus ultrasound [25], focused ultrasound [46], and laser [42].

All such methods described so far make use of needles, probes, nanoparticles, optical fibers, and ferromagnetic alloys plated with gold. However, there is no find in the consulted literature about the use of macro gold rods irradiated with ultrasound to treat cancer tumor. Also, there is no find about hypothermia of normal tissue or organ near the lesion treated with hyperthermia.

This work has the objective to investigate a method and an analytical formalism to provide the optimization of the amount of pure solid gold rods implanted in prostate in terms of heat propagation when it is being irradiated with ultrasound, by measurements and/or analytical calculation, while avoiding hyperthermia of the urethra. The use of ultrasound is largely an effort to reduce the use of chemotherapy and radiotherapy for treating cancer. Chemotherapy is considered to impose

Uncorrected Proof

Author's Proof

difficulties because drugs often produce harmful side effects. And radiotherapy is also problematic because X-rays travel through normal tissue to arrive at the tumor site and it is known that the X-rays sometimes damage normal tissue. Ultrasound has the ability to noninvasively concentrate energy into a controllable volume deep in tissue [47].

8.2 Material and Methods

The insufficiency of the response of single nanospheres to energy sources for the production of controllable hyperthermia and the need to use ensembles of nanoparticles to augment the contribution have been theoretically demonstrated [11, 19]. Heating of surrounding matrix becomes possible if particle size is large enough (in the presence of an amplified electric field enhancement). Gold seeds are the "hot" spots where the heating intensity is greatly enhanced. In this study, the attempt is to initiate a theoretical computational analysis for the optimization of spatiotemporal temperature distribution due to hyperthermia induced by gold seeds, macro-rods and macrospheres, heated through ultrasound, over a square matrix domain. Heat conduction is described by partial differential heat diffusion equations. These macroscopic equations are no longer applicable in scales where the temperature fields are not considered continuous (length scale comparable to or smaller than the mean free path of the material) [19, 21]. However, the equations are applicable and describe the heat diffusion at larger scales, such as mm scale.

Modeling ultrasound heating of a single macro-rod surrounded by a water medium is a first step towards understanding the thermal processes of macro-rod heating in relation to possible imaging parameters. Ultrasound directed to a dissipative medium leads to energy transfer, partial absorption, and conversion to heat. At the power level considered in this study (less than 1 W/cm^2), heating contributions due to direct linear and nonlinear absorption of ultrasonic pressure by water or tissue will be neglected. Phenomenological models for ultrasound wave amplitude attenuation account for wave amplitude loss due to various mechanisms (absorption, scattering, mode conversion) as ultrasound travels through materials. The higher the frequency, the more energy is consumed in the increase of molecular motion, and the less energy for the sound beam to propagate. However, since therapeutic ultrasound has a frequency range of 0.7 and 5.0 MHz and we are interested in tissue penetration of a few centimeters (prostate cancer), for simplicity, attenuation is described by a constant (attenuation coefficient) in the power rate equation. These effects will be considered in detail in future studies.

A temperature distribution model for either a fluid or tissue containing a heating source (gold Nano spheres heated by a laser beam) based on the Pennes' bio-heat equation was introduced in [11] and we adjust this model to our domain:

Uncorrected Proof

Author's Proof

$$\rho\, C_{\mathrm{p}}\, \frac{\partial T}{\partial t} = \nabla(k \nabla \mathrm{T}) + Q + Q_{\mathrm{Vh}} + W \tag{8.1}$$

where t is time, T is the temperature, C_{p} is the heat capacity, k is the thermal conductivity, ρ is the density, Q is the heat source, Q_{Vh} is the viscous heating, and W is the work pressure. The last two terms can be set equal to 0 for simplicity. The metabolic heat generation is considered negligible. Since the heat conductivity of gold is high, temperature gradients across the rod are weak so that temperature inside it should remain essentially constant. An initial temperature, $T_{\mathrm{I}} = T$ is assigned on the entire domain and the appropriate boundary condition for the tissue inward heat flux q_0 is

$$q_0 = -\vec{n}\, \nabla(k\, \nabla T) = h\, (T_{\mathrm{EXT}} - T) \tag{8.2}$$

The heat transfer coefficient h enters the equation, as unit power per Kelvin and unit area (SI unit: $\mathrm{W/m^2K^1}$). The exterior temperature of the cooling fluid is T_{EXT}. The heat transfer problem is solved with appropriate boundary conditions knowing that healthy tissues (urethra) surrounding the infected region should be preserved and its temperature should be maintained constant. The value of h depends on the geometry and the ambient thermal conditions. Since metabolic heat generation is negligible in this model, Q is determined by the absorbed ultrasound energy in the tissue given by [2]

$$Q = a\, \frac{|P|^2}{\rho\, c} \tag{8.4}$$

where c is the speed of sound in the medium, a is the attenuation coefficient and P is the acoustic pressure which is the time harmonic ultrasound field solution of the Helmholtz equation in an inhomogeneous medium [2]:

$$\nabla\left(\frac{1}{\rho}\nabla P\right) - \frac{1}{\rho\, c^2}\, \frac{\partial^2 P}{\partial t^2} = 0 \tag{8.5}$$

where k, the wave number, is given by $k = (\rho\, c)^{-1/2}$. It has been generally accepted that it is an extremely challenging task to solve the Helmholtz equation even numerically, in particular, for the high-frequency cases and for arbitrary domains and boundary conditions. For ultrasound solution waves, the acoustic pressure is related to quantities and properties such as the underlying wave velocity, the characteristic acoustic "impedance," the particle velocity (particles of the medium that are set into oscillation by the frequency associated with the wave) and organ characteristic scatter signature due to its structure (scattered echoes originating from relatively small, weakly reflective, irregularly shaped objects such as blood cells) and the variable compressibility of the domain. The lack and/or uncertainties of measurements practically constrain the identifiability of these parameters and we

Uncorrected Proof

Author's Proof

choose a simple pattern oriented thermal modeling of the bio-heat transfer equation where we sample over different values of the gold rod heat source values Q because it gives good agreement with the main features of the experimental data as described later in this section. Results on the applications of ultrasound have been published by other authors for 600, 300, 60, and 10 s into the heating procedure [21] and simulations have been obtained for 180–300 s (Kadah 2009). The COMSOL Multiphysics program ([49] Royal Institute of Technology in Stockholm, Sweden) is used to compute the temperature spatial distribution at the nodes of a 2-D finite element mesh. The heat source Q (unit power per unit volume) describes heat generation within the domain.

Comparisons between experimental measurements and the heat transfer-predicted values are available in the literature [19] for models of hyperthermia induced by gold nanoparticle dispersions in different laser energy levels (0.008, 0.016, and 0.032 W/mm^3) with good agreement in most cases, and the same scale of ultrasound energy levels is used for the simulations but results for higher and lower energies are analyzed. All constants and material properties used in the solution of the bio-heat diffusion can be found in the "built-in" databases of predefined materials for COMSOL Modules.

In the figures (Figs. 8.1a, b, 8.2a, b, 8.3a, b, 8.4a, b, 8.5a, b, 8.6a, b, 8.7a, b, 8.8a, b, and 8.9a–d) the corresponding simulations can be found for different sizes and shapes of gold seeds. One side of the domain corresponds to a cooling boundary (Fig. 8.10).

8.3 Results and Discussion

A theoretical computational analysis for the determination of the pattern of the spatiotemporal temperature distribution due to hyperthermia induced by gold seeds (macro-rods and macro-spheres) heated through ultrasound has been carried out. A 2-D simulation of the ultrasound induced hyperthermia in the tissue is demonstrated. The temperature distributions resulting from the heating of gold seeds are calculated using the bio-heat equation. For ultrasound generated heat at the gold seed of rates 10^5–10^6 W/m^3 plots of temperature raise against time and against radial and axial coordinate, have shown that the endpoint temperature depends on the gold target size. The bio-heat transfer partial differential equation has been simulated over a square domain, with a side boundary condition to describe the cooling of the urethra that leads to minimal side effect of ultrasound-gold seed heating of the surrounded healthy tissue. Different irradiation times up to 1,000 s have been monitored, and the dimensions of the domain and the seed can vary according to the desired design. Relative deviations have now been studied in detail as in the case of 1 mm $\times$ 10 mm gold rod (with the experiment). When the heat of the gold seeds was raised to appropriate temperatures, the bio-heat transfer in tissue in the parallel axis of the rods to reach 43 °C was found to be in the order of 0.5–1 cm for the 1 mm $\times$ 10 mm rod . In the case of the

Uncorrected Proof

Author's Proof

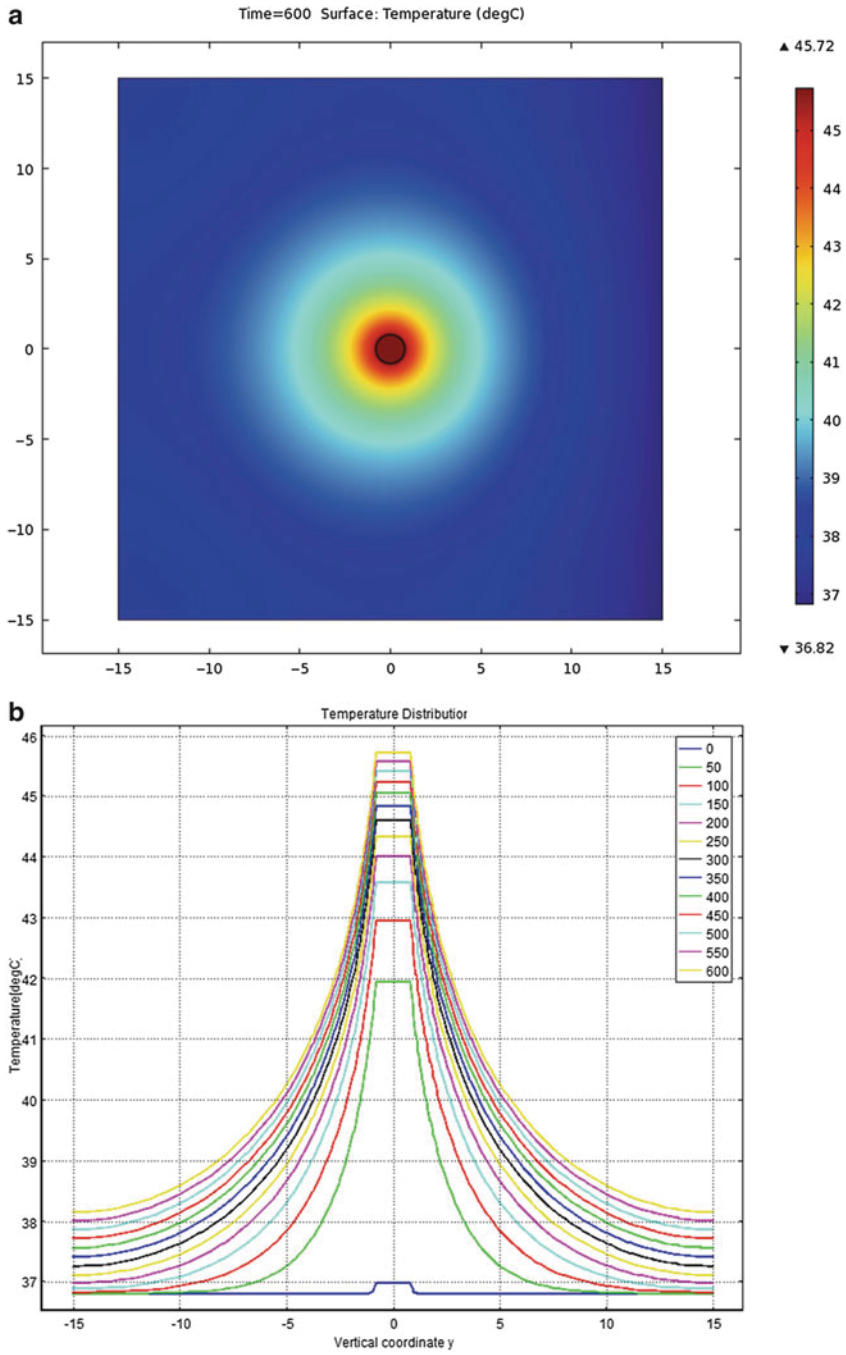

Fig. 8.1 (**a** and **b**) Contour plot and temperature distribution plot of the temperature field of the temperature field in the target area at volumetric heat generation rate 6×10^6 W/m^3 and a run time of 600 s, for gold sphere of radius 0.8 mm in a 30 mml $\times$ 30 mm square domain AU4

Author's Proof

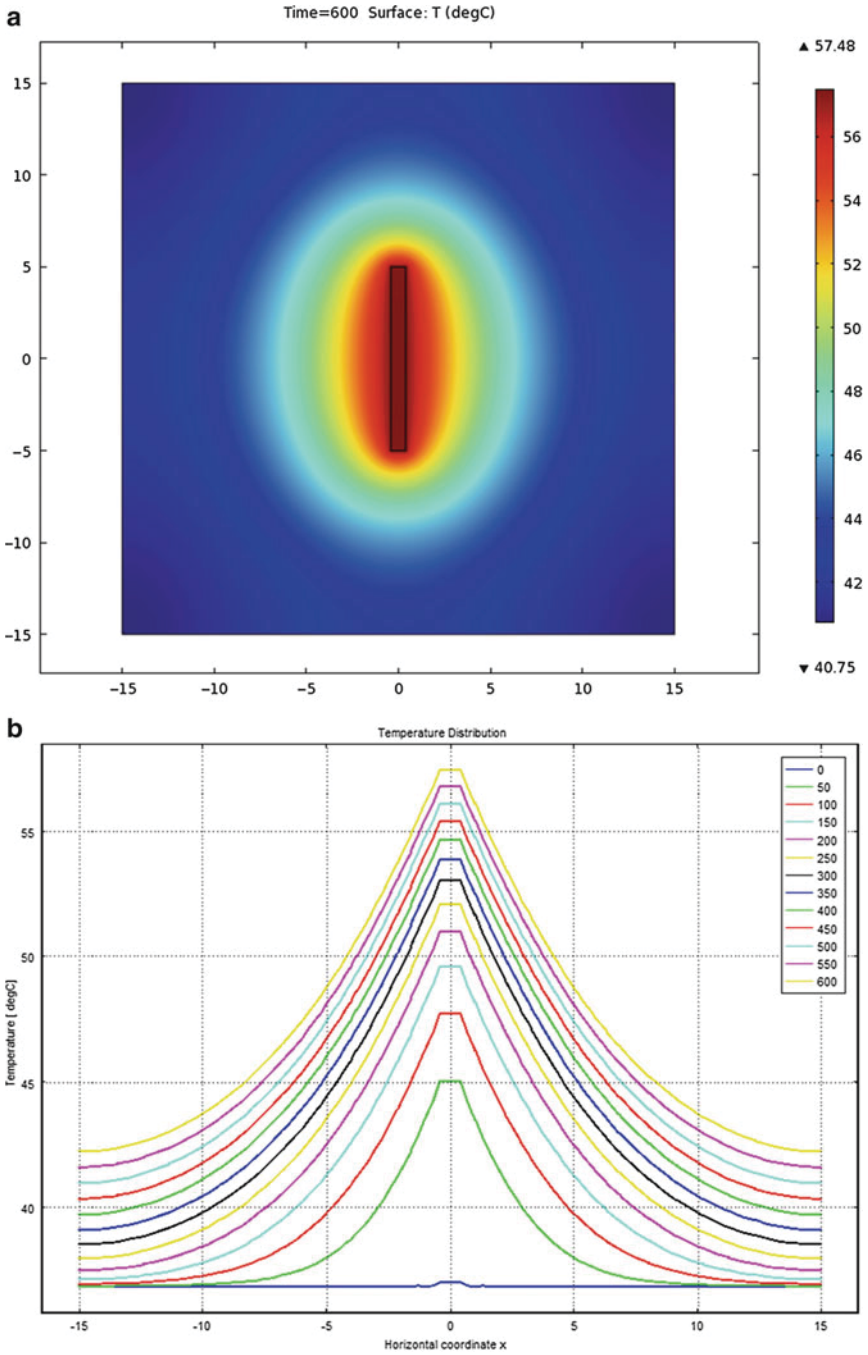

Fig. 8.2 (**a** and **b**) Contour plot and temperature distribution plot of the temperature field of the temperature field in the target area at volumetric heat generation rate 6×10^6 W/m^3 and a run time of 600 s, for gold rod of 0.8 mm × 10 mm in a 30 mml × 30 mm square domain

Author's Proof

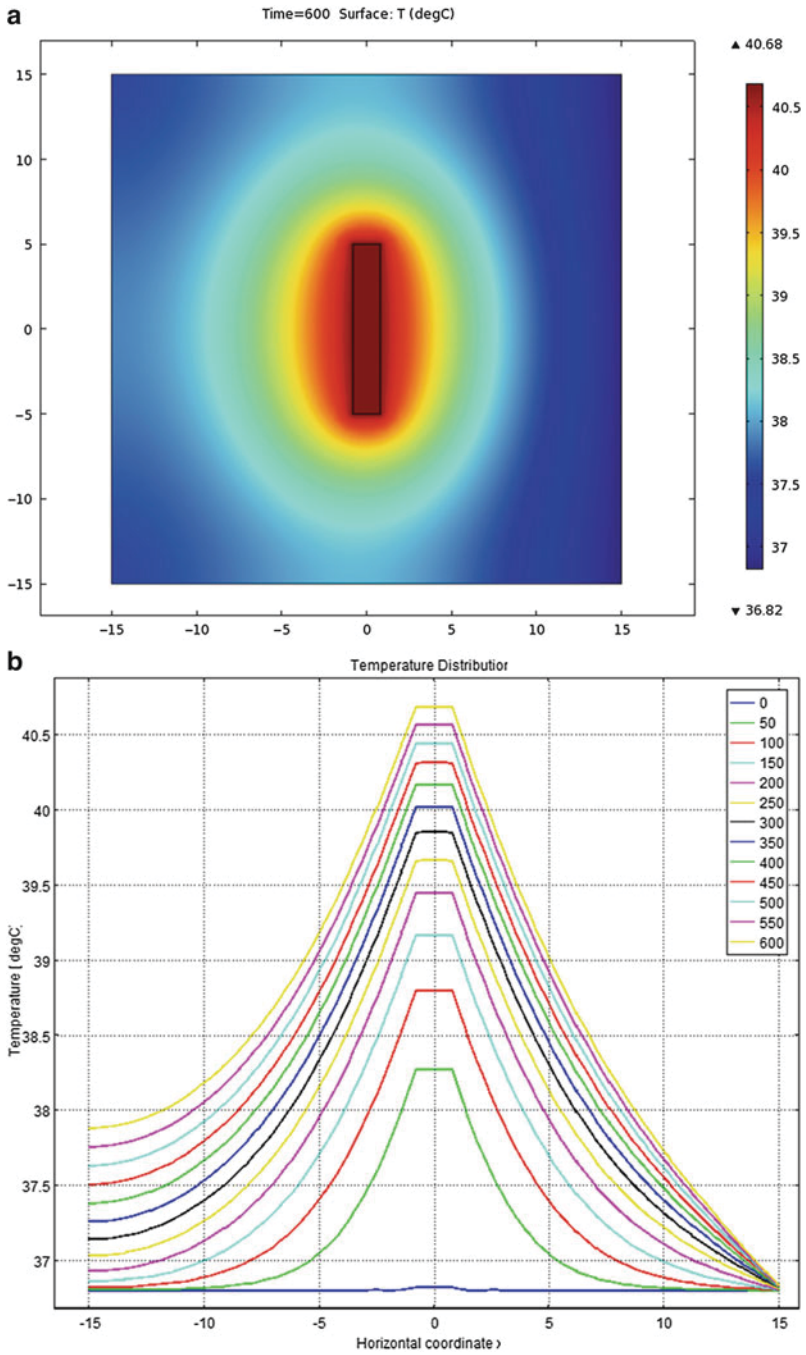

Fig. 8.3 (**a** and **b**) Contour plot and temperature distribution plot of the temperature field of the temperature field in the target area at volumetric heat generation rate 6×10^5 W/m^3 and a run time of 600 s, for gold rod of 1.6 mm × 10 mm in a 30 mml × 30 mm square domain

Author's Proof

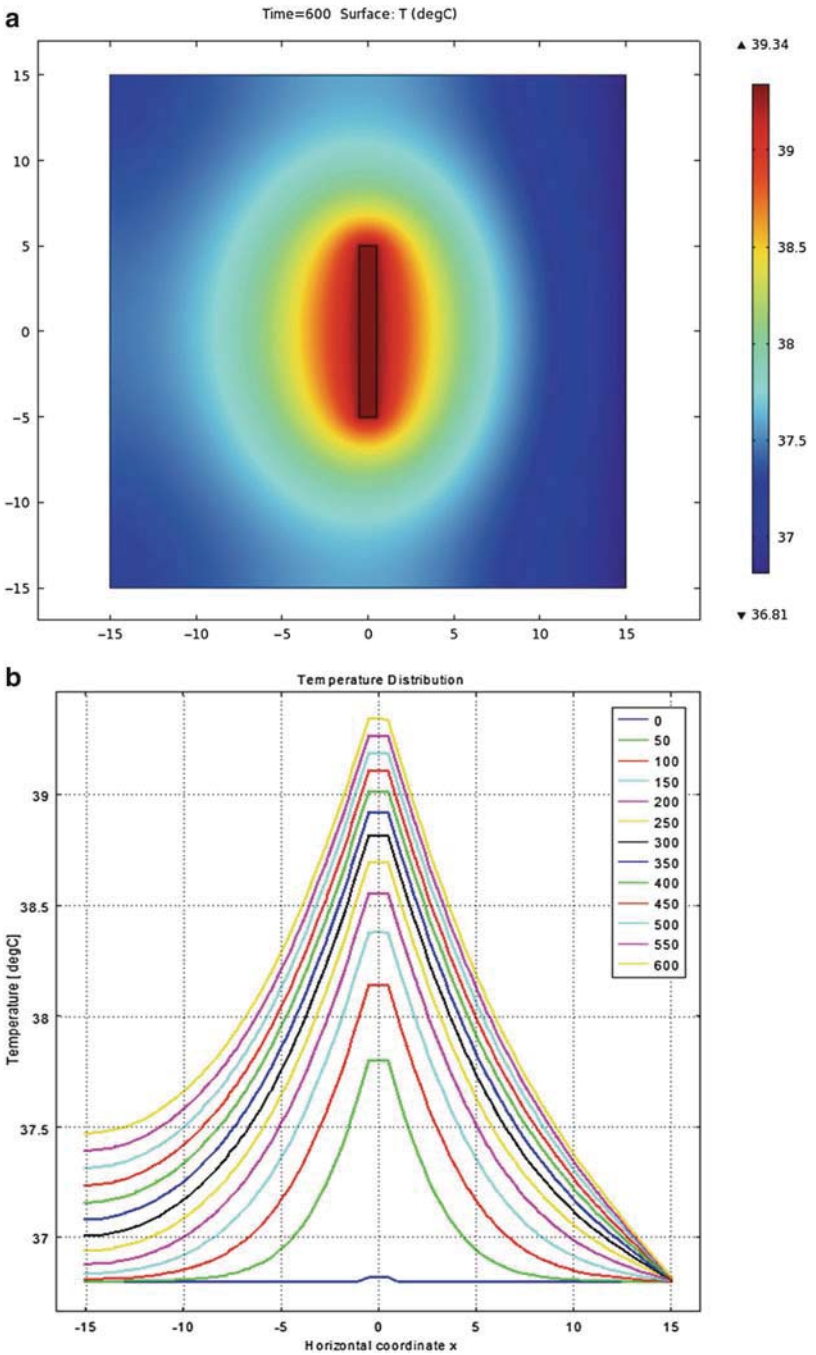

Fig. 8.4 (**a** and **b**) Contour plot and temperature distribution plot of the temperature field of the temperature field in the target area at volumetric heat generation rate 6×10^5 W/m^3 and a run time of 600 s, for gold rod of 1.0 mm × 10 mm in a 30 mml × 30 mm square domain

Author's Proof

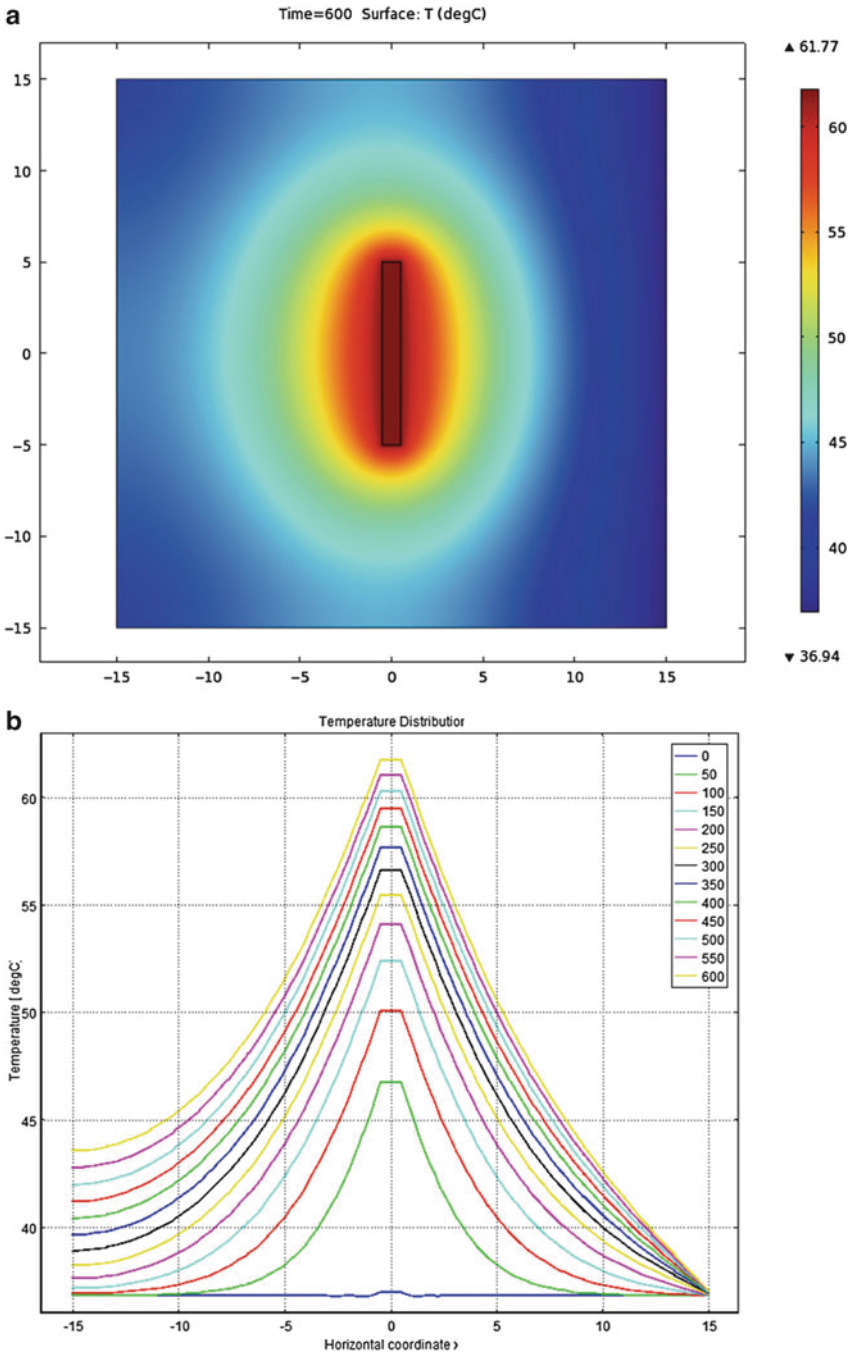

Fig. 8.5 (**a** and **b**) Contour plot and temperature distribution plot of the temperature field of the temperature field in the target area at volumetric heat generation rate $Q = 6 \times 10^6 \mathrm{W/m}^3$ and a run time of 600 s, for gold rod of 1.0 mm × 10 mm in a 30 mm × 30 mm square domain

Author's Proof

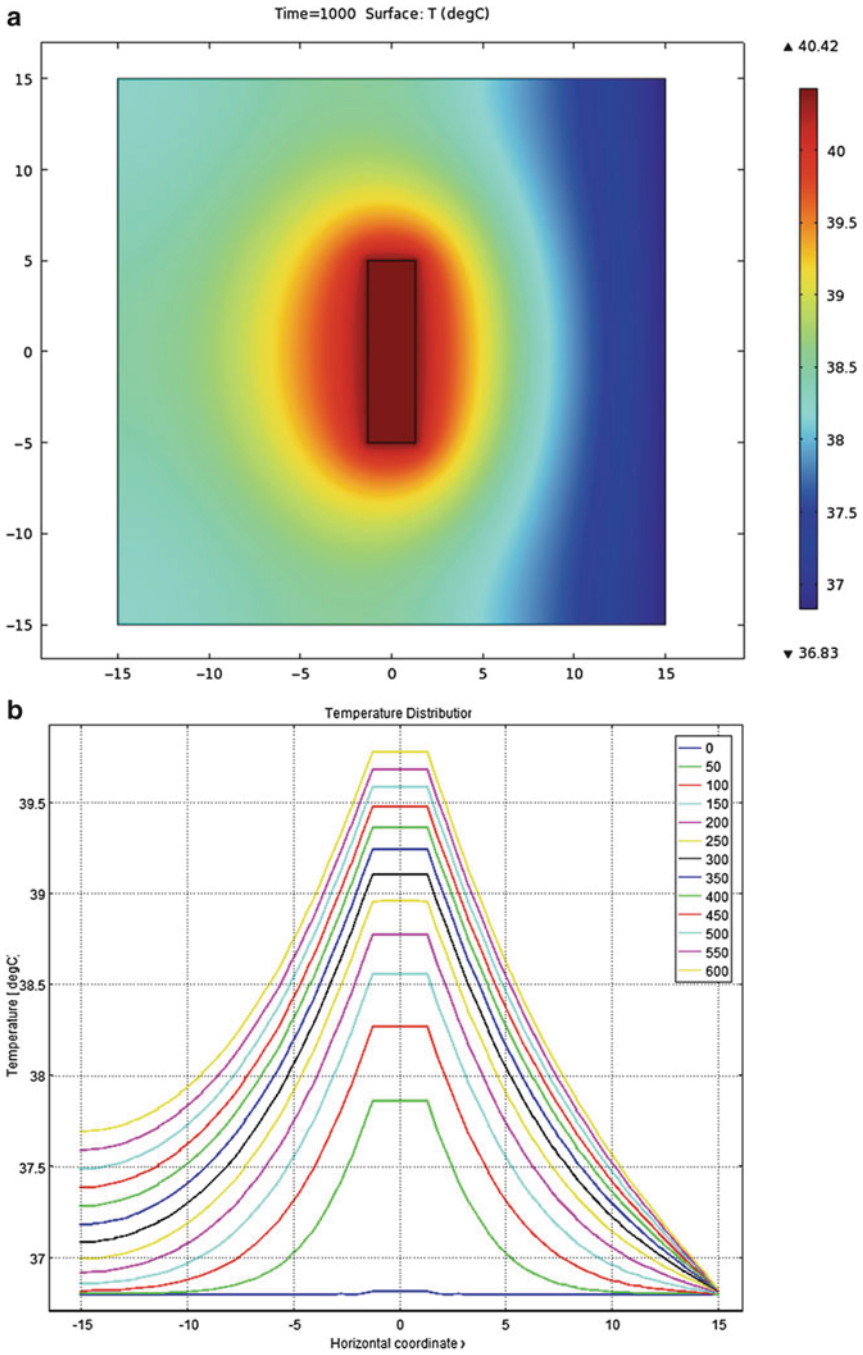

Fig. 8.6 (**a** and **b**) Contour plot and temperature distribution plot of the temperature field of the temperature field in the target area at volumetric heat generation rate $Q = 3 \times 10^5 \mathrm{W/m}^3$ and a run time of 1,000 s, for gold rod of 2.6 mm × 10 mm in a 30 mm × 30 mm square domain

Author's Proof

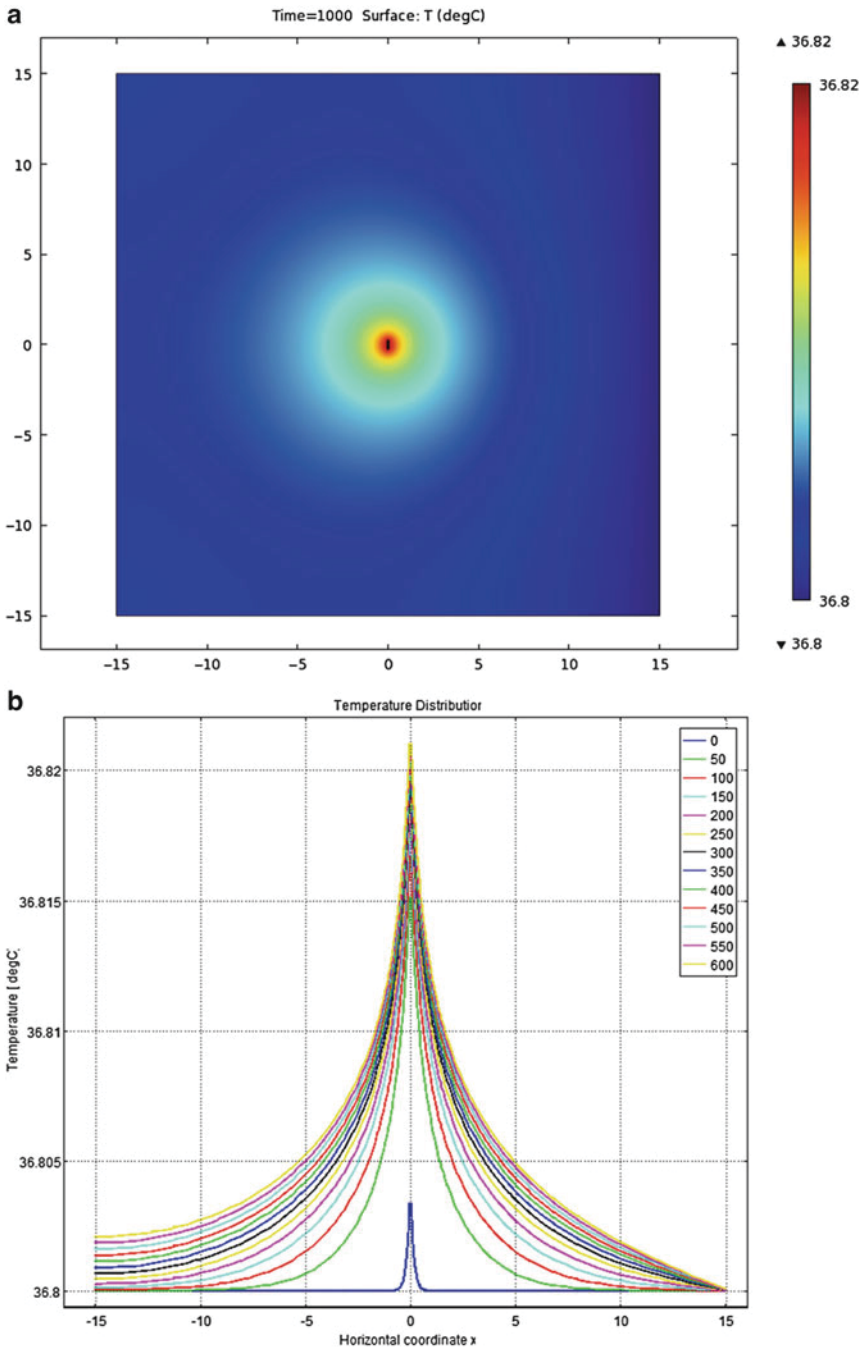

Fig. 8.7 (**a** and **b**) Contour plot and temperature distribution plot of the temperature field of the temperature field in the target area at volumetric heat generation rate $Q = 6 \times 10^5 \text{W/m}^3$ and a run time of 1,000 s, for gold rod of 6 μm × 50 μm in a 30 mm × 30 mm square domain

Author's Proof

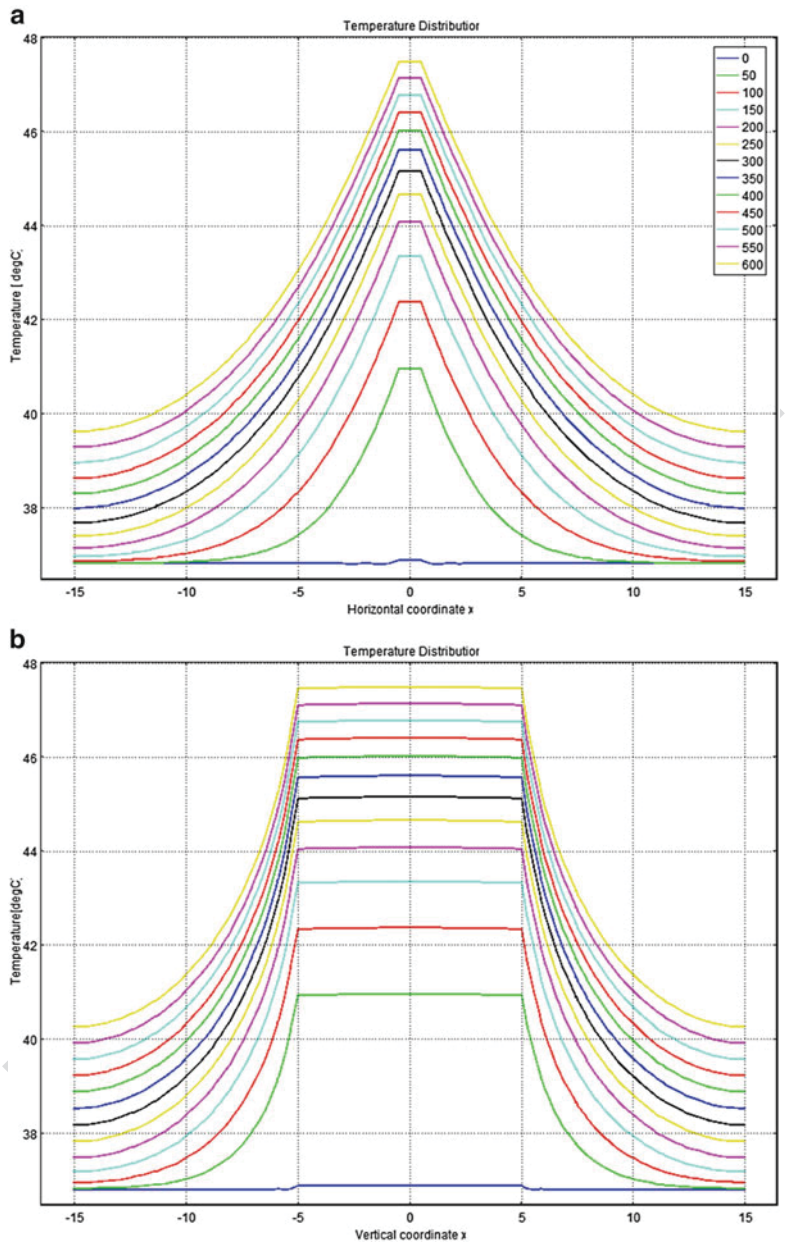

Fig. 8.8 (**a** and **b**) Temperature distribution plot of the temperature field of the temperature field in the target area at volumetric heat generation rate $Q = 2.4 \times 10^6 \mathrm{W/m}^3$ and a run time of 600 s, for gold rod of 1 mm × 10 mm in a 30 mm × 30 mm square domain

Author's Proof

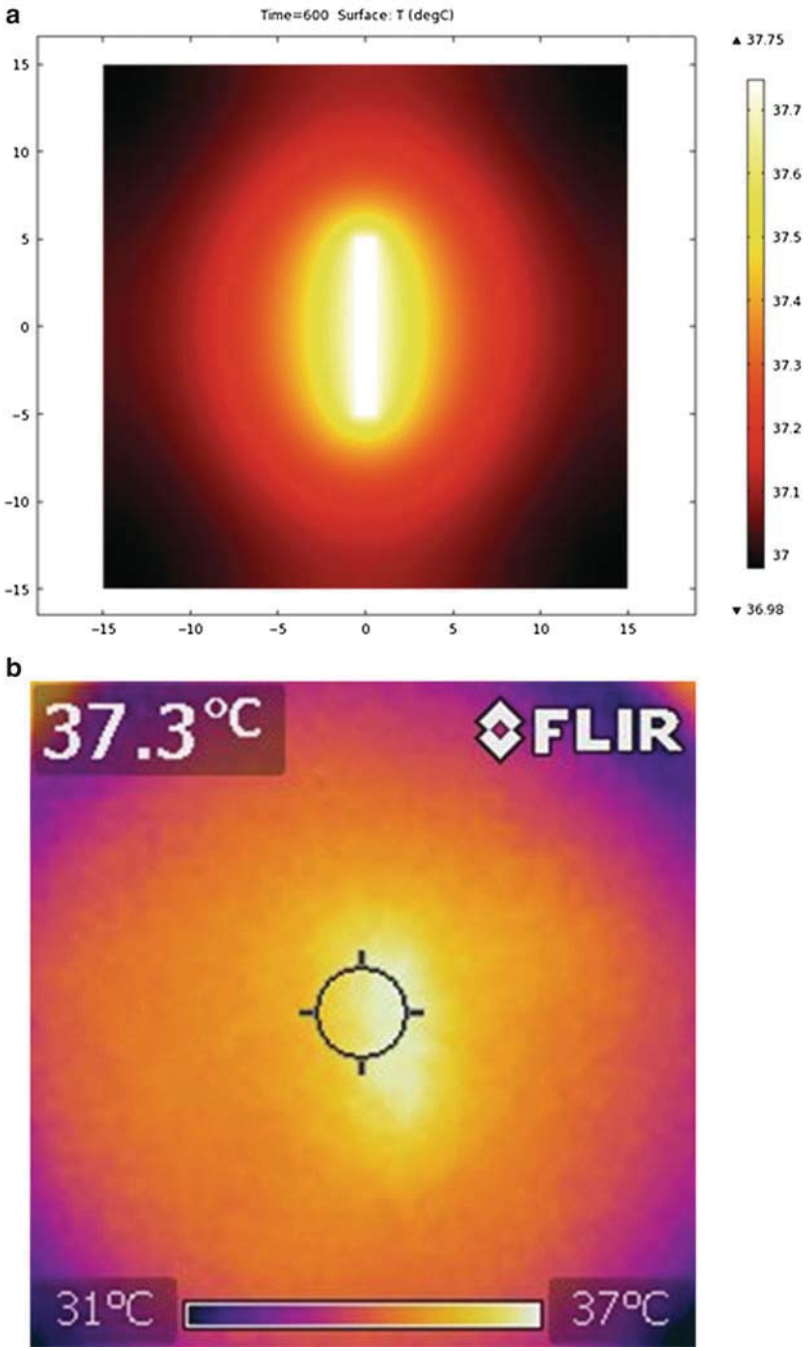

Fig. 8.9 (**a**–**d**) Contour plot and temperature distribution plot of the temperature field of the temperature field in the target area at volumetric heat generation rate $Q = 2.2 \times 10^5$ W/m^3 and a run time of 1,000 s, for gold rod of 1 mm × 10 mm in a 30 mm × 30 mm square domain. No boundary condition for this graph. Comparison of theoretical results (*left column*) vs. experimental results (*right column*) (communicated by Austerlitz, experiment with gold rod inserted in chicken breast and irradiated with ultrasonic energy of the given heat generation rate and run time)

Author's Proof

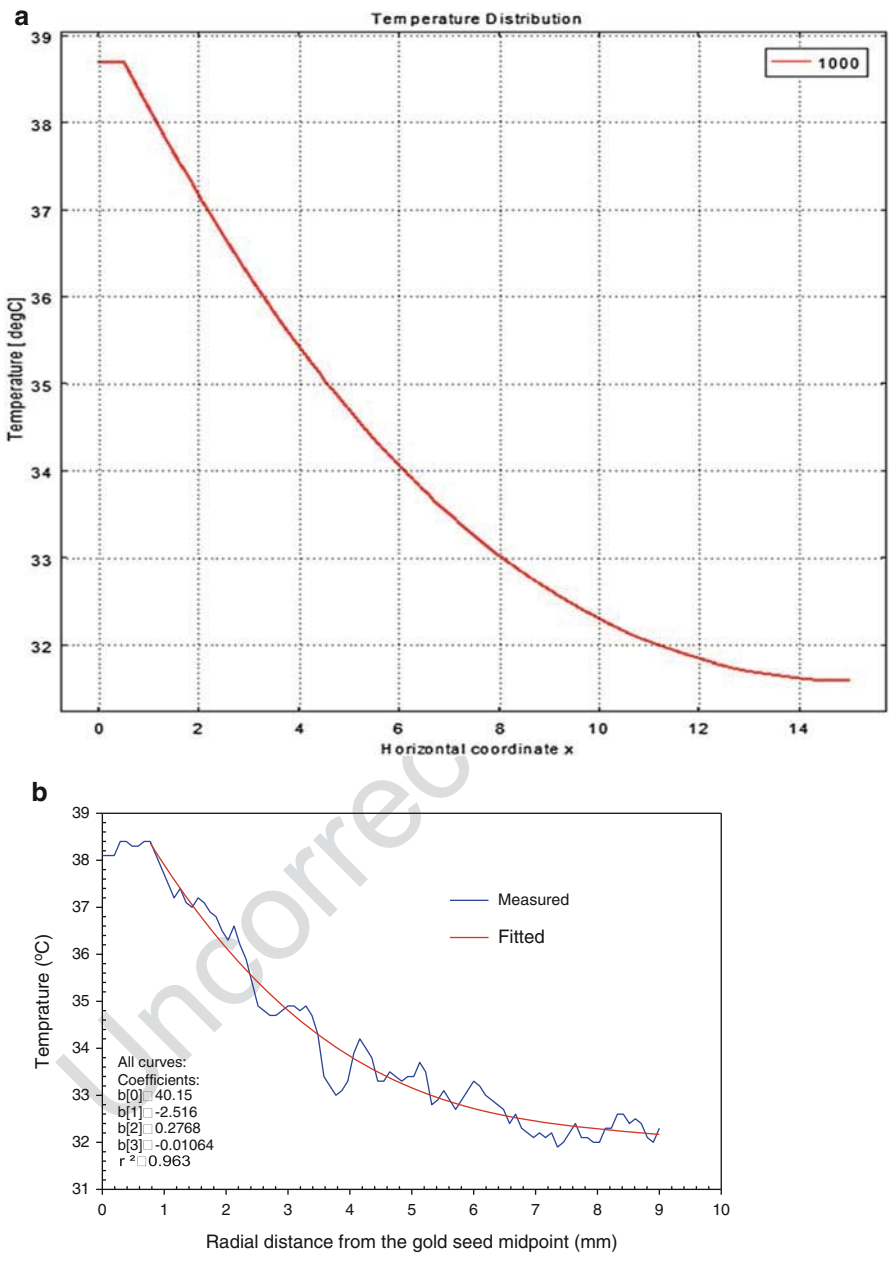

Uncorrected

Fig. 8.9 (continued)

Author's Proof

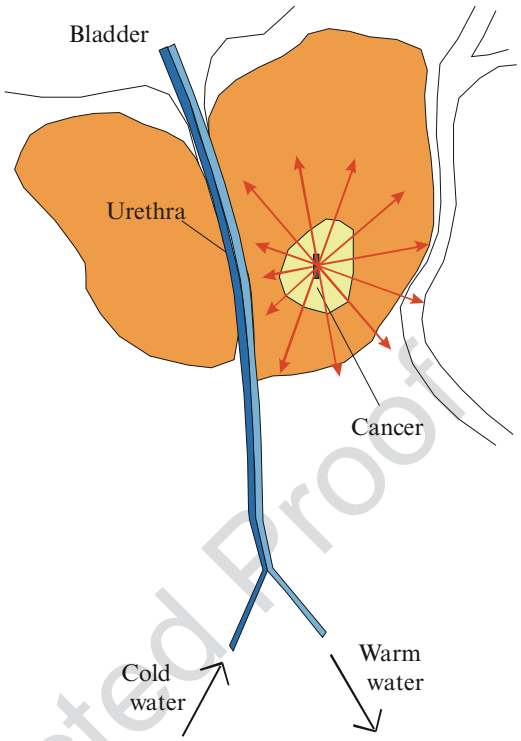

Fig. 8.10 One side of the domain corresponds to a cooling boundary

orthogonal axis, the radial distances to reach this same temperature were more than 10 mm, respectively. Within 10 %, the radial temperature distribution in tissue emanating from the 1 mm $\times$ 10 mm rod, agrees with predicted experimental data (personal communication, Austerlitz). As expected, the radial temperature distribution for the 0.8 mm diameter sphere was less than that observed for the parallel axis of the 0.8 mm diameter but with 10 mm height rod. The simulations indicate that the methodology of ultrasound heated gold seeds may have therapeutic powers similar to radioactive substances. With the use of gold seed gun and needles of appropriate lengths and curvatures, uniform distributions of seeds can be obtained throughout the area of an implant, the seeds being small causing minimal trauma, and little disturbance to the patient. This procedure can be repeated rather easily and gold seeds are reusable. Furthermore, sound energy is non ionizing radiation and therefore its use does not impose the hazards, such as cancer production, attributed to ionizing radiation. Ultrasound kinetic energy when absorbed by tissues can also be converted into heat.

Currently, we study the use of other possible (gold-coated) materials: aluminum, copper, granite, high-strength alloy steel, iron, lead zirconate titanate, silicon, silica glass, structural steel, titanium beta-21S, and tungsten. Relative comparison will be made versus the case of nanoparticles (in preparation). The

Uncorrected Proof

Author's Proof

use of ultrasonic vibrations in heat-treating metals and alloys is based on the transmission of elastic vibrations to the parts either through the surrounding medium (water, oil, emulsion, molten metal, or salt) or by firm contact with the wave guide [1a]. It has been shown that in austenite, the influence of elastic vibrations and the absorption of part of the energy of elastic vibrations leads to a certain increase in the temperature of samples. As was shown in [1], samples may heat up greatly under the influence of ultrasonic vibrations [1a]. In [1] the possibility of any influence of elastic ultrasonic vibrations on diffusion, ionic mobility, viscosity, or thermal diffusion was denied. The mechanism of the action of ultrasonic vibrations probably consists of changes in the conditions of evaporation on the surfaces of the parts being treated. The use of ultrasonic vibrations is especially effective for parts made of steels with low hardenability. The passage of ultrasonic vibrations through a solid body is accompanied by a series of effects such as intense heating of the samples to the melting temperature, the appearance of traces of residual deformation, and accumulations of structural fatigue and even fatigue destruction. Application of high-power 20 kHz ultrasound resulted in temperature increases of the order of 200 °C occurring 20–30 s after initiation of insonation in resonant specimens of fine-grained polycrystalline brass, copper, and steel [27]. Typically, the nanoparticles have a size of the order of a few tens of nanometers, because as mentioned above the particle has to be small for the SPR effect. If the radiation pulse width is short enough, heating is limited to the vicinity of the nanoparticle. Thus generally a large number of nanoparticles would be needed to effectively heat an entire cell, for example, the size of which can be of the order of microns to tens of microns. Complementary use of sub-micron silicon carbide (SiC) particles as photothermal agents for the heating of bacteria by pulsed mid-infrared (MIR) radiation [37]. If a material is a good conductor of heat then the heat will move quickly. Metals are widely used for heat transfer purposes because they have properties which allow for propagation (movement in a line) of heat while being able to withstand the temperature extremes sometimes associated with heating. Conduction is when the heat moves through an object or from one object to another because the two objects are in contact with one another. It is the only mode of heat travel throughout solids. The ability to transfer heat within an object is called thermal conductivity "*k*" (measured in W/m K). It varies for different materials. Gold, silver, and copper have high thermal conductivity.

The spatial temperature distribution in a multi-tissue arrangement is computed at three different frequencies and simulation times (Table 2). Figure 8.1b shows a contour plot of the temperature distribution in the skin, breast and tumor tissues at 0.75 MHz at the end of 180 s. The maximum temperature (hot spot) occurred in the tumor and decreased when moving farther in other tissues. Increasing the time allowed for ultrasound therapy up to 300 s raised the temperature observed in the tumor and the surrounding tissues (Fig. 8.1a). The temperature distribution, employing a therapeutic transducer at a higher frequency of 1.5 MHz, at the end

Uncorrected Proof

Author's Proof

of 180- and 300-s ultrasound therapy is shown in Figs. 8.2a and 8.3a. The highest temperature observed in the tumor was 45.5°e which is suitable for destroying cancerous cells without a noticeable damage to the surrounding tissues. Simulation results using a transducer at a frequency of 2.75 MHz and at the end of 180 and 300 s, respectively is illustrated in Figs. 8.3a and 8.4a. It is observed that the temperature predicted in the tumor is about 51.04 °C. The surrounding area near the tumor has been affected by higher temperatures compared to previous simulation results at lower frequencies. Increasing the time allowed for ultrasound raised the temperature of the tumor as well as the surrounding tissues. This rise in the temperature of the surrounding healthy tissue leads to their destruction, which is a drawback of the therapeutic process. In addition, the temperature distribution is observed to be more localized, thus indicating better transducer focusing capabilities at higher frequencies. Numerical computations and analytical calculations of temperatures in various tissues are summarized in Table II. A good agreement was only observed at a frequency of 1.5 MHz.

First, we validated our model by simulating the heating of spherical particles and comparing the results with the lattice expansion measurements of Austerlitz (work in progress). Numerical simulations are compared with analytical results. An elevation in the temperature (hot spot) of the skin tissue was observed in all computations. Thus, a bolus of degassed water of temperature 10 °C is used as a cooling system in farther simulations. It acts as a heat sink, so as to avoid any pain or burning of the skin. In order to calculate the temperature field in the multi-tissue system, the uniform pressure of ranges from 0.045 to 0.0354 MPa is assumed to be applied on the surface of the breast tissue at the time from 180 to 300 s, so the spatial temperature profiles are very similar for both solutions. The numerical results show that employing a transducer at a frequency of 1.5 MHz is the most suitable for a successful ultrasound therapy. At this frequency, the highest temperature observed in the tumor was 45.5 °C which is favorable for destroying cancerous cells without a noticeable damage to the surrounding tissues. On the other hand, analytical results show that the highest temperature predicted in the tumor was 47.77 °C. The two solutions are considered in good agreement. The difference between the two solutions is minimized when a lower thermal conductivity value (e.g., k less than 0.5 W/m °C) for the tumor in the FEM computations is used. The discrepancy between the numerical and analytical results is more noticeable at the two other frequencies. This is caused by the fact that heat conduction is ignored in the analytical method. As the frequency of simulation increases, the ultrasound intensities increases and the specific absorption rate increases. Thus, the heat generation in tissues is increased, and the surrounding area near the tumor has been affected by higher temperatures, but the temperature distribution is more localized, as shown in Figs. 8.3a and 8.4a.

Uncorrected Proof

Author's Proof

Conclusion

Computer modeling has been used to determine the likely temperature distribution of a given treatment and to plan the future of hyperthermia treatments. So, the goal of computer simulation is extremely useful in providing a firm scientific basis for the future of clinical investigation of focused ultrasound.

In this report, we propose a methodology that has the goal of sustaining hypothermia in the urethra and treat prostate cancer with macro-rod-shaped gold and ultrasound. Experimental studies that monitor the interaction of therapeutic ultrasound with heat-conducting material such as gold seeds in biological tissues can be a demanding research task. Numerical modeling of bio-heat transfer resulting from gold seed irradiation and seed size effect comparison can be very important and useful in non-invasive cancer therapy. A model-based analysis of these interactions and the corresponding temperature distribution was carried out, for time and irradiation rate found in current literature. Therapy design can be integrated into a predictive treatment planning model for prostate cancer ultrasound hyperthermia-hypothermia therapy by specifying the most appropriate ultrasound and gold seed parameters based on desired levels of temperature distribution both on tumor and healthy tissue. Utilization of this optimization model will enable a physician to evaluate tumor hyperthermia treatment and to better design a patient-specific therapy to achieve maximum destruction of the tumor and injury minimization of healthy tissue by controlling size, shape, and location of gold seeds implanted in tissue, and ultrasound parameters. In order to fully make use of numerical modeling results for the application of ultrasound on tissue containing seeds, and generation of hyperthermia to cancer control, physiological factors such as pH, oxygen consumption, nutrients, and blood flow of both tumor and normal host tissue should be measured in vivo and the analysis of these factors needs to be documented not only at normal temperatures but also under hyper thermic conditions to further elucidate the proper conditions for a selective destruction of tumor tissue with normal tissue sparing. Heating tissues using ultrasound decreases the viscosity of fluid elements, increases metabolic rate, increases blood flow which assists in the reduction of swelling, and stimulates the immune system. All these factors might play a significant role in the final outcome.

The experimental study of the interaction of therapeutic ultrasound with biological tissues and the monitoring of the temperature distribution is a very expensive and difficult task. Thus, numerical modeling of ultrasound hyperthermia treatment at different simulation frequencies and therapy durations is a very important therapeutic demand. A model-based analysis of the interaction of ultrasound intensity with breast tissue including a tumor was carried out in an effort to predict the path of the sound waves and the temperature

(continued)

Author's Proof

(continued)

field in the regions of interest. Numerical and analytical calculations of temperature in various tissues were in good agreement at a certain frequency of 1.5 MHz. The computed results form a foundation for a better understanding of the interaction of ultrasound with biological tissues. More complex and extensive analytical methods including all aspects of heat conduction and wave attenuation should be considered in the future.

References

1. Balalaev GA (1965) Zashchita stroitel'nykh konstruktsiĭ i khimicheskikh apparatov ot korrozii AU9
2. Bhatia AB (1985) Ultrasonic absorption: an introduction to the theory of sound absorption and dispersion in gases, liquids, and solids. Dover Publications, New York
3. Chang E, Alexander HR, Libutti SK, Hurst R, Zhai S, Figg WD, Bartlett DL (2001) Laparoscopic continuous hyperthermic peritoneal perfusion1. Journal of the American College of Surgeons 193:225–229
4. Chang I (2003) Finite element analysis of hepatic radiofrequency ablation probes using temperature-dependent electrical conductivity. Biomedical Engineering Online 2:12
5. Cosman ER, Rittman W (2002) Ablation treatment of bone metastases. US Patent 6,478,793
6. Coughlin CT (1992) Prospects for interstitial hyperthermia. Interstitial Hyperthermia: Physics, Biology and Clinical Aspects 3:1
7. Critz FA, Tarlton RS, Holladay DA (1995) Prostate specific antigen-monitored combination radiotherapy for patients with prostate cancer. I-125 implant followed by external-beam radiation. Cancer 75:2383–2391
8. Dowlatshahi K (1993) Apparatus for interstitial laser therapy having an improved temperature sensor for tissue being treated. Google Patents
9. Ebbini ES, Umemura SI, Ibbini M, Cain CA (1988) A cylindrical-section ultrasound phased-array applicator for hyperthermia cancer therapy. IEEE Transactions on Ultrasonics, Ferroelectrics and Frequency Control 35:561–572
10. English P, All S Hyperthermia in cancer treatment. AU10
11. Fasla B, Benmouna R, Benmouna M (2010) Modeling of tumor's tissue heating by nanoparticles. Journal of Applied Physics 108:124703
12. Fenn AJ (2007) Breast cancer treatment by focused microwave thermotherapy. Jones & Bartlett Learning, Burlington, MA
13. Fessenden P, Lee ER, Samulski TV (1984) Direct temperature measurement. Cancer Research 44:4799s
14. Fetter RW, Gadsby PD, Kabachinski JL (1989). Microwave hyperthermia probe. US Patent 4,841,988
15. Frischbier HJ, Thomsen K (1971) Treatment of cancer of the vulva with high energy electrons. AU11 Am J Obstet Gynecol 111(3):431–5
16. Gage AA (1992) Cryosurgery in the treatment of cancer. Surgery, Gynecology & Obstetrics 174:73
17. Hafeli U (1997) Scientific and clinical applications of magnetic carriers. Springer, New York
18. Haider SA, Cetas TC, Wait JR, Chen JS (1991) Power absorption in ferromagnetic implants from radiofrequency magnetic fields and the problem of optimization. IEEE Transactions on Microwave Theory and Techniques 39:1817–1827

Uncorrected Proof

Author's Proof

19. Huang HC, Rege K, Heys JJ (2010) Spatiotemporal temperature distribution and cancer cell death in response to extracellular hyperthermia induced by gold nanorods. ACS nano 4:2892–2900
20. Huang X, Jain PK, El-Sayed IH, El-Sayed MA (2008) Plasmonic photothermal therapy (PPTT) using gold nanoparticles. Lasers in Medical Science 23:217–228
21. Hynynen K, Watmough DJ, Mallard JR (1983) Local hyperthermia induced by focused and overlapping ultrasonic fields—an in vivo demonstration. Ultrasound in Medicine and Biology 9:621–627
22. Johannsen M, Gneveckow U, Eckelt L, Feussner A, Waldöfner N, Scholz R, Deger S, Wust P, Loening SA, Jordan A (2005) Clinical hyperthermia of prostate cancer using magnetic nanoparticles: presentation of a new interstitial technique. International Journal of Hyperthermia 21:637–647
23. Jordan A, Scholz R, Wust P, Fähling H (1999) Magnetic fluid hyperthermia (MFH): cancer treatment with AC magnetic field induced excitation of biocompatible superparamagnetic nanoparticles. Journal of Magnetism and Magnetic Materials 201:413–419
24. Kennedy JC, Pottier RH, Pross DC (1990) Photodynamic therapy with endogenous protoporphyrin: IX: basic principles and present clinical experience. Journal of Photochemistry and Photobiology B: Biology 6:143–148
25. Lele PP (1990) Diffuse focus ultrasound hyperthermia system. Google Patents
26. Lyons BE, Britt RH, Strohbehn JW (1984) Localized hyperthermia in the treatment of malignant brain tumors using an interstitial microwave antenna array. IEEE Trans Biomed Eng 31(1):53–62
27. Mignogna RB, Green RE, Duke JC, Henneke EG, Reifsnider KL (1981) Thermographic investigation of high-power ultrasonic heating in materials. Ultrasonics 19:159
28. O'neal DP, Hirsch LR, Halas NJ, Payne JD, West JL (2004) Photo-thermal tumor ablation in mice using near infrared-absorbing nanoparticles. Cancer Letters 209:171–176
29. Panjehpour M, Overholt BF, Milligan AJ, Swaggerty MW, Wilkinson JE, Klebanow ER (1990) Nd: YAG laser-induced interstitial hyperthermia using a long frosted contact probe. Lasers in Surgery and Medicine 10:16–24
30. Park DW, Kim KS (2011) Seed-mediated synthesis of iron oxide and gold/iron oxide nanoparticles. Journal of Nanoscience and Nanotechnology 11:7214–7217
31. Park SE, Lee JW, Haam SJ, Lee SW (2009) Fabrication of double-doped magnetic silica nanospheres and deposition of thin gold layer. Bull Korean Chem Soc 30:869
32. Perez CA, Brady LW (1987) Principles and practice of radiation oncology AU12
33. Ramanujan RV, Lao LL Magnetic particles for hyperthermia treatment of cancer.
34. Regueiro CA, Valcarcel FJ, Romero J, De La Torre A (2002) Treatment of conjunctival lymphomas by beta-ray brachytherapy using a strontium-90-yttrium-90 applicator. Clinical Oncology 14:459–463
35. Roberts DW (1992) Interstitial hyperthermia in brain: the clinical experience. Interstitial Hyperthermia: Physics, Biology and Clinical Aspects 3:231
36. Romestaing P, Lehingue Y, Carrie C, Coquard R, Montbarbon X, Ardiet JM, Mamelle N, Gerard JP (1997) Role of a 10-Gy boost in the conservative treatment of early breast cancer: results of a randomized clinical trial in Lyon, France. Journal of Clinical Oncology 15:963
37. Rosenberg M, Petrie TA (2012) Theoretical study on the possible use of SiC microparticles as photothermal agents for the heating of bacteria. Nanotechnology 23:055103
38. Russell KJ, Caplan RJ, Laramore GE, Burnison CM, Maor MH, Taylor ME, Zink S, Davis LW, Griffin TW (1994) Photon versus fast neutron external beam radiotherapy in the treatment of locally advanced prostate cancer: results of a randomized prospective trial. International Journal of Radiation Oncology Biology Physics 28:47–54
39. Schiller JH, Harrington D, Belani CP, Langer C, Sandler A, Krook J, Zhu J, Johnson DH (2002) Comparison of four chemotherapy regimens for advanced non-small-cell lung cancer. New England Journal of Medicine 346:92–98

Uncorrected Proof

Author's Proof

40. Slater JD, Rossi CJ, Yonemoto LT, Bush DA, Jabola BR, Levy RP, Grove RI, Preston W, Slater JM (2004) Proton therapy for prostate cancer: the initial Loma Linda University experience. International Journal of Radiation Oncology Biology Physics 59:348–352
41. Stauffer PR, Sneed PK, Suen SA, Satoh T, Matsumoto K, Fike JR, PHILLIPS TL (1989) Comparative thermal dosimetry of interstitial microwave and radiofrequency-LCF hyperthermia. International Journal of Hyperthermia 5:307–318
42. Steger AC, Lees WR, Walmsley K, Bown SG (1989) Interstitial laser hyperthermia: a new approach to local destruction of tumours. British Medical Journal 299:362
43. Stern JM, Stanfield J, Lotan Y, Park S, Hsieh JT, Cadeddu JA (2007) Efficacy of laser-activated gold nanoshells in ablating prostate cancer cells in vitro. Journal of Endourology 21:939–943
44. Stromberg J, Martinez A, Gonzalez J, Edmundson G, Ohanian N, Vicini F, Hollander J, Gustafson G, Spencer W, Yan D (1995) Ultrasound-guided high dose rate conformal brachytherapy boost in prostate cancer: treatment description and preliminary results of a phase I/II clinical trial. International Journal of Radiation Oncology, Biology, Physics 33:161
45. Terentyuk GS, Maslyakova GN, Suleymanova LV, Khlebtsov NG, Khlebtsov BN, Akchurin GG, Maksimova IL, Tuchin VV (2009) Laser-induced tissue hyperthermia mediated by gold nanoparticles: toward cancer phototherapy. Journal of Biomedical Optics 14:021016
46. Uchida T, Sanghvi NT, Gardner TA, Koch MO, Ishii D, Minei S, Satoh T, Hyodo T, Irie A, Baba S (2002) Transrectal high-intensity focused ultrasound for treatment of patients with stage T1b-2n0m0 localized prostate cancer: a preliminary report. Urology 59:394–398
47. Wu J, Nyborg WLM (2006) Emerging therapeutic ultrasound. World Scientific, Hackensack, NJ
48. Wust P, Hildebrandt B, Sreenivasa G, Rau B, Gellermann J, Riess H, Felix R, Schlag PM (2002) Hyperthermia in combined treatment of cancer. The Lancet Oncology 3:487–497
49. COMSOL Multiphysics®. © 1997–2008 COMSOL AB

Uncorrected Proof

5 ARTIGO CIENTÍFICO II

Preclinical Validation of the Located Hyperthermia Using Gold Macro-Rods and Ultrasound as an Effective Treatment for Solid Tumors

Artigo será submetido ao periódico: Journal of Cancer

Preclinical Validation of the Located Hyperthermia Using Gold Macro-Rods and Ultrasound as an Effective Treatment for Solid Tumors

Andre L. S. Barros[1], Carlos Austerlitz[2], Ioannis Gkigkitzis[3], Diana Campos[4] , Jeyce K. F. de Andrade[1], Teresinha G. Silva[1]*, Silene C. Nascimento[1], Ioannis Haranas[5]

[1] Bioassays Laboratory for Pharmaceutical Research, Antibiotics Department, Biological Sciences Center, Federal University of Pernambuco, Recife, Brazil.
[2] Department of Computer Science, Southern Illinois University, USA
[3] Department of Mathematics, East Carolina University, 124 Austin Building, East Fifth Street, Greenville, NC 27858-4353, USA
[4] Clínica Diana Campos, Recife, PE 52020-030, Brazil.
[5] Research and Development in Electromagnetic Theory Applications at VDG Applications, 4700 Keele Street, Toronto, ON, M3J 1P3, Canada

*Corresponding author. E-mail: teresinha.goncalves@pq.cnpq.br
Tel: +55 31 81 2126 8347. Fax: +55 31 81 2126 8346.

Abstract: Hyperthermia, the procedure of raising the temperature of a part of or the whole body above normal for a defined period of time, is applied alone or as an adjunctive with various established cancer treatment modalities such as radiotherapy and chemotherapy. In this study used a method for inducing hyperthermia in solid tumors with a combination of gold macro rod (GR) and ultrasound, the feasibility of this technique was described only with computational models and in vitro. The Ehrlich tumor, derived from a *mouse* adenocarcinoma, has been used to investigate the bio-heat transfer and the effect of gold rods irradiated with ultrasound. The in vivo measurements demonstrated that the technique inhibited more 80% of the tumor growth in both experimental models tested. These results not only confirm the bio heat transfer to tissue as predicted by analytical calculation and in vitro measurements, but are also proved to be a potential alternative to kill cancer cells.

Keywords: Ultrasound; Gold Macro-Rods; Hyperthermia; Cancer.

---

1. Introduction

Hyperthermia (also called thermal therapy or thermotherapy) is a noninvasive anticancer approach in which biological tissues are exposed to temperatures higher than normal (up to 41°C) to promote selective destruction of abnormal cells. In the temperature range of 41-47º C tumors are selectively destroyed because of their reduced heat tolerance [1]. The elevation from the normal temperature for a certain time interval causes irreversible cell damage by denaturing proteins, which affects the structure of the cell membrane. Thus, hyperthermia for anticancer treatment could inhibit tumor cell proliferation by destroying cancer cells or making them more sensitive to the effects of conventional antitumor therapies, such as radiation or chemotherapy [2]. The use of heating sources conventionally employed for hyperthermia is limited because of the damage they cause to surrounding healthy tissues. Various heating sources ranging from radiofrequency to microwaves as well as ultrasound waves have been used to produce moderate heating in a specific target region [3, 4, 5]. The use of gold nanospheres, nanorods, nanoshells and nanocages in vitro assays, ex vivo and in vivo imaging, cancer therapy, and drug delivery, has been discussed by [6], despite of the great effort that has been put in the application of gold nanoparticles (GNPs) for cancer therapy related to thermal therapy, GNPs face some major inconveniences: improvement of delivery methods to induce accumulation of a larger number of particles to the tumor site [7]; vasculature is highly abnormal in tumor [8]. Therefore, it may not be expected that GNPs are homogeneous distributed inside the tumor; and the bio heat transfer from GNPs to the tissue is in order of a few nm, associated with bio distribution, the relatively short range of the bio-heat transferred from the GNPs to the surrounding tissue may result in heterogeneous high-thermal and cold regions in the tumor leading to failed treatments.

A method for inducing hyperthermia in solid tumors with a combination of gold macro rod (GR) and ultrasound has been described elsewhere [9-12]. The feasibility of this method has been demonstrated by means of analytical considerations about bio-heat transfer in tissue [9, 10], infrared pictures of GR exposed to ultrasound [12]. However, there are no data performed with such method based on in vivo tumor cells. Based on the analytical considerations about bio-heat transfer in tissue, the aim of this study was establish a Preclinical Model to confirm the viability of Hyperthermia Using Gold Macro-Rods and Ultrasound on Treatment of Cancer.

2. Materials and Methods

2.1. Animals

In this study, 96 BALB/c mice (male, 25-30 g), were obtained from the Laboratory of Immunopathology Keizo-Asami (LIKA) of the Federal University of Pernambuco (UFPE), Brazil. The animals were kept in cages with free access to food and water, under 12 h light-dark cycles. The animals were treated in accordance with the International Council for Laboratory Animal Science (ICLAS), and following the ethical principles of the Brazilian Society of Science in Laboratory Animals (SBCAL). All experiments were approved by the Ethics Committee for Animal Experimentation of the Biological Sciences Center of the Federal University of Pernambuco, Brazil, number 23076.013243/2012-04.l.

2.2. Solid Ehrlich Carcinoma (SEC) Tumor Model

Ehrlich ascites carcinoma (EAC) cells were derived from a spontaneous murine mammary adenocarcinoma. EAC cells were maintained in the undifferentiated form by passaging in syngeneic mice by transplanting $2{,}5 \times 10^6$ cells/mL (i.p.) each week. The ascitic fluid was removed by opening the belly and collecting all of the fluid with a sterile syringe. Ascitic tumor cell counts were carried out using the trypan blue dye exclusion method with a neubauer hemocytometer. Animals received 200 μL of a suspension containing 5×10^6 cells/mL (i.p.). Tumor volume was measured using a electronic caliper, assuming a fairly constant relationship of mass to volume, tumor development can be expressed in terms of volume increment. In order to determine tumor volume by external caliper, the greatest longitudinal diameter (length) and the greatest transverse diameter (width) were determined. Tumor volume based on caliper measurements were calculated by the modified ellipsoidal formula [13, 14]:

$$\textit{Tumor volume } (mm^3) = 1/2(\textit{length} \times \textit{width}^2)$$

The inhibition rate (%) was calculated as follows [15]:

$$\textit{Inhibition rate } (\%) = [(A - B)/ A] \times 100$$

where A is the average weight of the non treated group and B is the average tumor weight of the treated group.

2.3. Insertion of Gold Macro-Rods and Ultrasound Irradiation Setup

After 5 days of the transplanted tumor (Tumor volume approximately equal to 350mm^3), the mice were anesthetized with 0.1 to 0.1 mL/100 g of ketamine and xylazine (1:1), the hair around the tumor area was removed then the gold rod (0.155 cm diameter and 0.54 cm height) was inserted in the center of tumor by means of a trocar needle (Fig. 1). A layer of ultrasound transmission gel was spread on the shaved mice's skin as contact media gel and exposed for 15 or 30 minutes with a 1 cm transducer connected to a GS8 2E ultrasound under a nominal frequency of 1 MHz and about 75 W. The temperature increase was measured every minute in the central and peripheral region of the tumor with needle type thermistor connected to a thermometer FLUKE. Changes in body temperature were valued by rectal temperature.

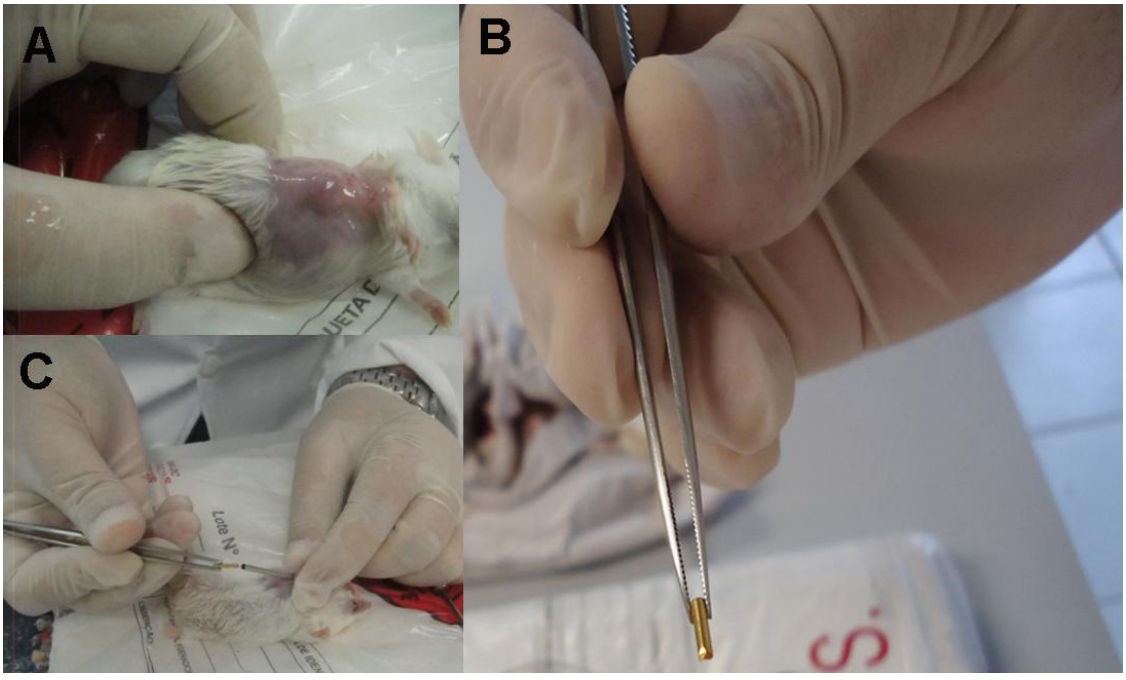

Figure 1. Insertion of gold macro-rods in the tumor.

2.4. Experimental Design

After five days of tumor implantation (Tumor volume= 300± 18mm^3), mice were randomly assigned into four groups (6 mice/group) as follows:

Group 1 (Control): untreated control
Group 2 (GR): gold macro-rods inserted on tumor not irradiated with ultrasound.
Group 3 (U): irradiated with ultrasound only.
Group 4 (GR+U): gold macro-rods inserted on tumor and irradiated with ultrasound.

2.4.1. Treatment model 1 (single dose)

Mice with gold macro-rods inserted on tumor were irradiated with ultrasound for 30 minutes. Three hour after the irradiation, the mices were sacrificed and the tumors were dissected, weighed and two fragments (central and peripheral region) were fixed in 10% formaldehyde for Histopathological analyzes.

2.4.2. Treatment model 2 (three doses)

Mice with gold macro-rods inserted on tumor were irradiated with ultrasound for 15 minutes every 5 days, totaling 3 irradiations. Tumor volume was measured from the 5th to the 16th day after implantation of SEC. 24 hours after the last irradiation, the mice were sacrificed and the tumors were dissected and weighed, additionally blood samples were collected from each group for evaluation of adverse effects.

2.5. Histopathological analyzes

After being fixed in formaldehyde, the tumors were put into paraffin. The blocks were cut using a microtome to a thickness of 4 μm, and the slides were stained with hematoxylin and eosin for morphological analysis. Histological analysis was performed by light microscopy and histological sections were photographed with an MC 80 DX camera coupled to a Zeiss Axiophot light microscope, and tumor/necrotic areas were quantified using Image ProPlus 5.1 software.

2.6. Hematological analysis

Hematological analysis was carried out using an automatic cell counter (ABX-MICROS-60 cell counter Horiba, Inc). The samples were evaluated for the following hematological parameters: number of erythrocytes, concentration of hemoglobin, number of

platelets and total count and differential of leukocytes.

2.7. Statistical Analysis

The results are presented as the mean ± standard deviation (SD). One-way ANOVA followed by the Newman-Keuls test was used to evaluate the differences among the treatments. P values < 0.05 were considered to be statistically significant.

3. Results

3.1. Treatment model 1 (single dose)

In this study was observed the enhancement in the temperature only in group 4. The temperature in the tumor was measured with the FLUKE thermistor in two regions defined in accordance with the proximity to the GR inserted. In central region, the heat rate produced increased about 0,81^{o}C/min from 36,6 to 60,9 ^{o}C and in peripheral region 0,38 ^{o}C/min from 36,3 to 48,8 ^{o}C (Fig. 2). Significatives changes in rectal temperature not were observed.

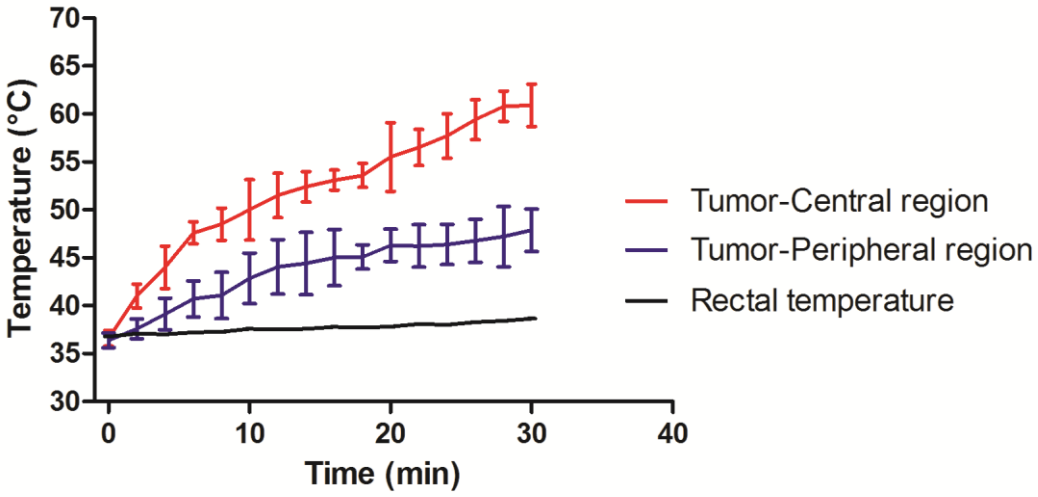

Figure 2. The heat enhancement on tumor during the irradiation of the gold rod with ultrasound.

The effect of gold macro-rods irradiated with ultrasound, against solid Ehrlich carcinoma is showed in Figure 3. The mass of the tumors not presented statistically significant differences between groups, however in the histopathology analysis, the GR+U group showed extensive areas of coagulating necrosis accounting for 81,9 ±7,2% of the total area (Fig. 4D). Histological sections from control, GR and U groups showed a typical pattern consisting of viable tumor with pleomorphic polygonal cells, hyperchromatic nucleus, some binucleated cells and cytoplasm limits (Fig. 5A, Fig. 5B, Fig. 5C). The degeneration characteristics of early stages of coagulative necrosis can be observed in Figure 5D.

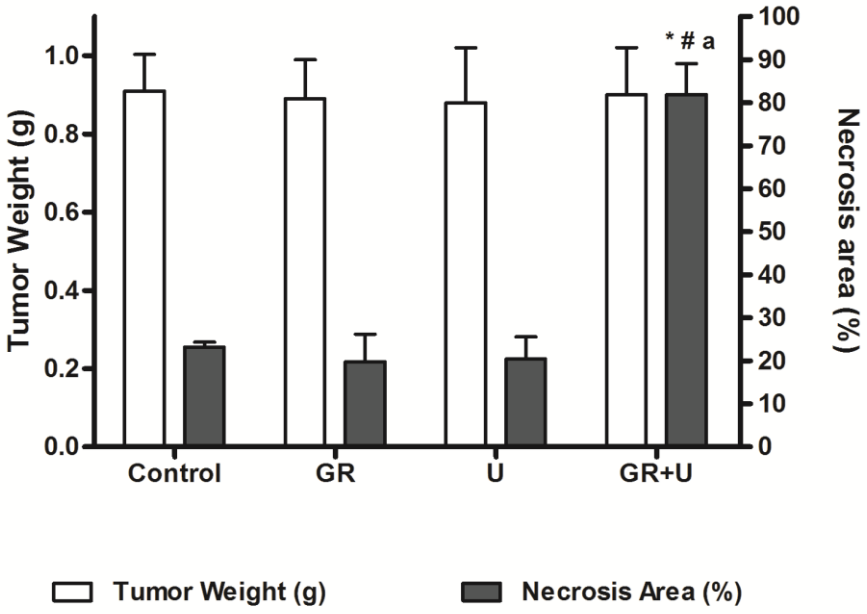

Figure 3. The effect of gold rods irradiated with single dose of ultrasound for 30 minutes, in mice transplanted with Ehrlich carcinoma. Data are presented as mean ± standard deviation. * $p<0.05$ compared to control by ANOVA followed by Newman-Keuls test. # $p<0.05$ compared to GR by ANOVA followed by Newman-Keuls test. a $p<0.05$ compared to U by ANOVA followed by Newman-Keuls test.

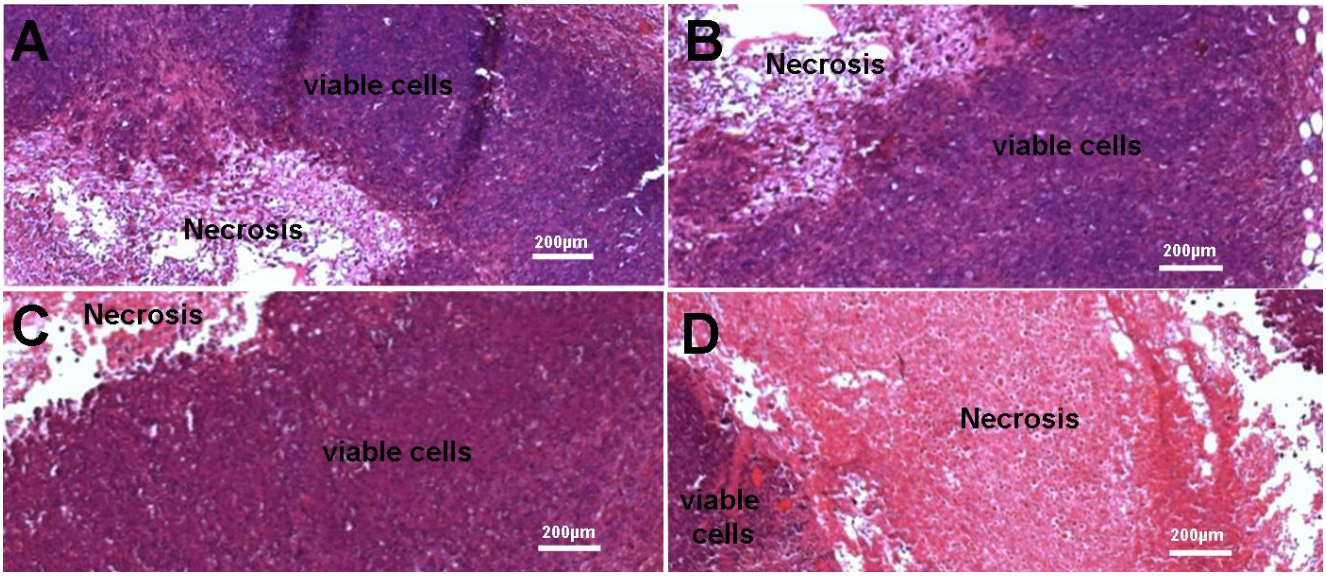

Figure 4. Ehrlich tumor histopathology after treatment using gold rods irradiated with single dose of ultrasound for 30 minutes. Sections refer to: (A) control, (B) GR, (C) U and (D) GR+U.

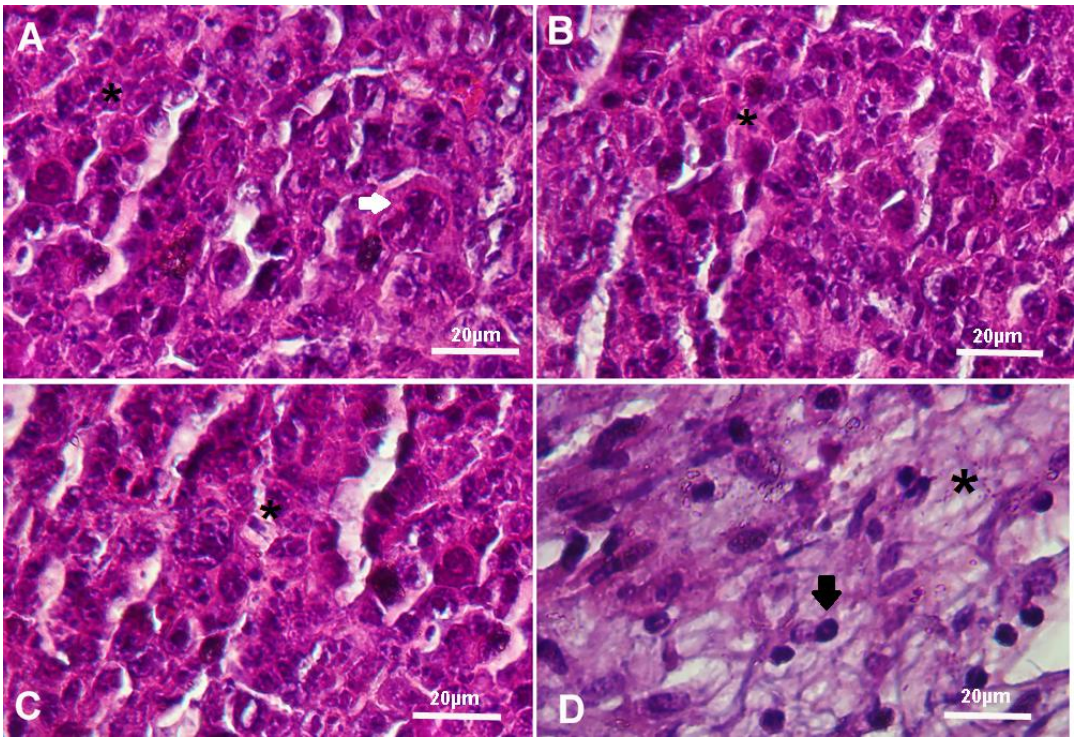

Figure 5. Photomicrograph showing the histopathology evaluation of the Ehrlich carcinoma from (A) animals control: normal cells morphology showing intact membrane and nucleus (black asterisk) and cell division (white arrow); (B) GR: intact cells (black asterisk); (C) U: intact cells (black asterisk) and (D) GR+ U: plasma membrane degeneration (black asterisk) and intense chromatin condensation (black arrow). Analyzed In light microscope.

3.1. Treatment model 2 (three doses)

In this treatment protocol, the GR + U group was irradiated three times for 15 min (5, 10 and 15 days after implantation of Erhlich carcinoma). The enhancement in the temperature in central region was from 37,2 to 53,4 ^{o}C the heat rate increased about 1,08 ^{o}C/min and in peripheral region 0,54 ^{o}C/min from 36,7 to 44,8 ^{o}C. As it is shown in Figure 6, Ehrlich tumors in GR+U group were significantly inhibited as compared with tumors of untreated mice ($P < 0.05$). Furthermore, there were no differences between control, GR and U groups.

The tumor reduction is described in Figure 7. The sequential irradiation, blocked tumor development over the trial period. In GR + U group, the inhibition rate was 84.7%. The control group, GR and U not were significantly different. In the Hemogram, the only significant differences induced for GR + U with respect to the other groups were concerning the increased Leukocytes (Table 1.)

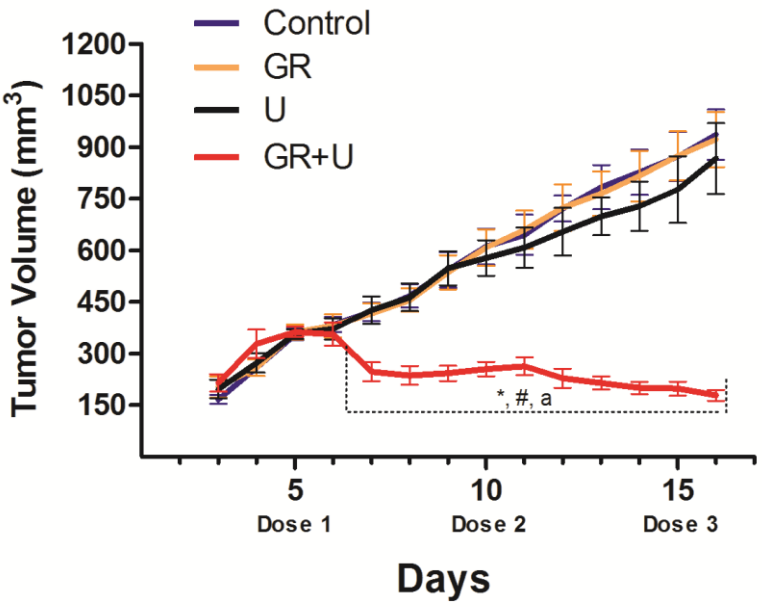

Figure 6. The effect of gold rods irradiated with three doses of ultrasound for 15 minutes on the growth curve of Ehrlich tumor. Data are presented as mean ± standard deviation. * $p<0.05$ compared to control by ANOVA followed by Newman-Keuls test. $^{\#}$ $p<0.05$ compared to GR by ANOVA followed by Newman-Keuls test. ^{a} $p<0.05$ compared to U by ANOVA followed by Newman-Keuls test.

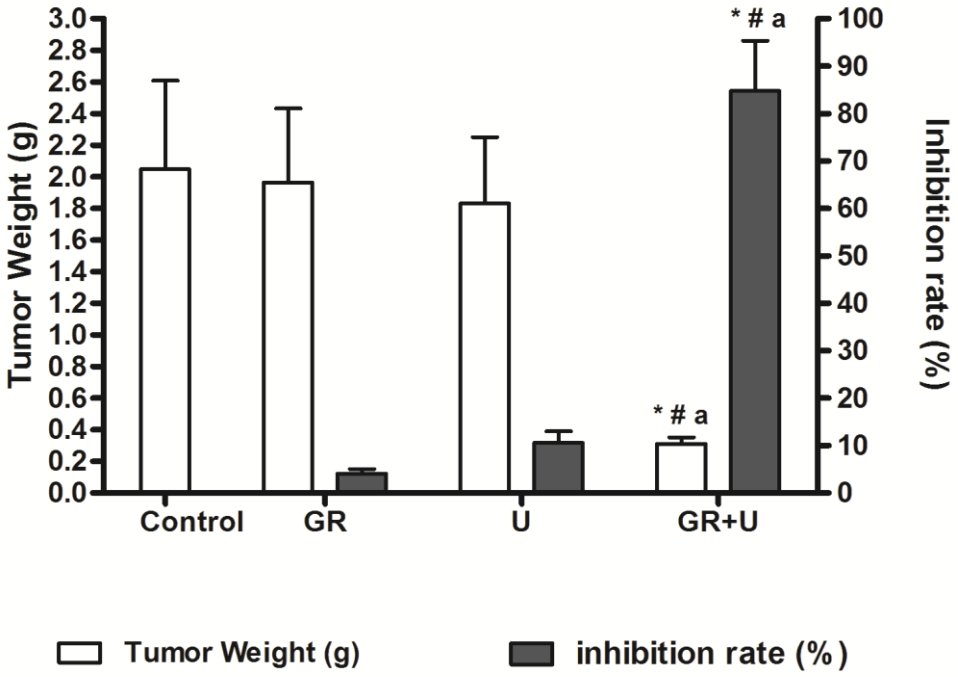

Figure 7. The effect of gold rods irradiated with three doses of ultrasound for 15 minutes in mice transplanted with SEC. Data are presented as mean ± standard deviation. * $p<0.05$ compared to control by ANOVA followed by Newman-Keuls test. # $p<0.05$ compared to GR by ANOVA followed by Newman-Keuls test. a $p<0.05$ compared to U by ANOVA followed by Newman-Keuls test.

Table I: Effect of gold rods irradiated with three doses of ultrasound for 15 minutes on hematological parameters of mice 16 days after implantation of Erhlich carcinoma.

Parameter	Control	GR	U	GR+U
Red blood cells (10^6/mm^3)	8.90 ±0.75	8.40±0,82	9.11 ±0,95	8.71 ±0.79
Leukocytes (10^3/mm^3)	7.98±0.55	8.06 ±0.72	8.12 ±0,68	14.4 ±1.03*
Platelets (10^3/mm^3)	436 ±39.3	457 ±61.3	463±69.0	461 ±49.6
Hemoglobin (g/dL)	14.6 ±0.93	14.9 ±1.02	14.0 ±0.91	14.7 ±0.95
Hematocrit (%)	41.0 ±1.6	42.1 ±1.81	41.7 ±1.32	40.8 ±1.72
VCM (μμg)	48.3 ±1.62	46.3 ±1.35	46.2 ±0.98	45.7 ±1.76
HCM (pg)	16.4 ±0.81	16.8 ±0.67	17.0 ±0.93	19.9 ±0.91
CHCM (%)	31.1 ±1.41	32.4 ±1.72	31.8 ±1.52	30.9 ±1.37

The values are presented as the average ± the standard deviation. * ($p < 0.05$) compared to the control and other groups by ANOVA followed by the Student Newman-Keuls post-test

4. Discussion

The experimental design of this study was based on analytical considerations and measurements in vitro as described by [9, 10, 11, 12] and our results confirm what was predicted mathematically by these authors where, the about 1-cm radial bio heat transferred to the tumor from the gold rod causing cell death.

Ehrlich carcinoma is an undifferentiated carcinoma that has high transplantable capability, no regression, rapid proliferation, 100% malignancy and also does not have tumor-specific transplantation antigen [16]. Following the inoculation the number of cells increases rapidly and after a given time, the host animal died due to the pressure exerted by the tumor volume and/or the damage that resulted from the tumor [17]. In this study the holders SEC animals were treated from the initial proliferative stage of tumor development.

In the tumors with gold rods irradiated for 30 minutes with ultrasound the temperature in the central region was greater than 42 °C for 28 minutes while that in the peripheral region for about 20 minutes. The heat transfer in irradiated tumors for 15 minutes induced temperatures above 42 °C showed by 13 and 5 min in the central and peripheral regions, respectively. Temperatures in the range of moderate hyperthermia can be non-lethal (39 to 42°C) or lethal (>42°C). Temperatures above 42°C were shown to kill cancer cells in a time and temperature-dependent manner that was measured by the clonogenic cell survival assay [18].

The rate of proliferation of cancer cells makes them more sensitive to the effects of hyperthermia where the intensity of cell death is dependent on the cell cycle phase. In general, high heat sensitivity can be observed during the S and M phases. Microscopic examinations of M-phase cells subjected to hyperthermia show damage of their mitotic apparatus leading to inefficient mitosis and consecutive polyploidy. S-phase cells are also sensitive to hyperthermia, where chromosomal damage is observed. Both S- and M-phase cells undergo a “slow mode of cell death” after hyperthermia, whereas those exposed to heat during G1-phase are relatively heat resistant and do not show any microscopic damage. Cells during G1-phase may follow a “rapid mode of death” immediately after hyperthermia. These variations existing between the different cell cycle phases indicate the possible diversity of molecular mechanisms of cell death following hyperthermia [19-21].

Gold rods irradiated with single dose of ultrasound for 30 minutes or three doses for 15 minutes demonstrated ability of tissue destruction in SEC. The histopathological analysis showed extensive areas of coagulative necrosis and progressive inhibition of tumor directly

related to heat transfer in tissue. Classical hyperthermia relies on a temperature of 42°C to 45°C for periods of 30 to 60 min to cause irreversible cellular damage [21-23]. The inactivation of vital enzymes is a key feature of tissue injury at these temperatures [24]. As the tissue temperature rises to 60°C, the time required to achieve irreversible cellular damage decreases exponentially. Protein denaturation occurs between 60°C and 140°C and leads to immediate cell death followed by coagulative necrosis [24]. Other cellular changes as membrane rupture, cell shrinkage, pyknosis, hyperchromasia are also observed at temperatures above 60°C.

The increase in leukocyte numbers shown in the GR + U group can be explained by the indirect effects of hyperthermia. In the area of coagulative necrosis, studies have reported inflammatory infiltrates that include neutrophils, macrophages, dendritic cells (DCs), natural killer (NK) cells, as well as B cells and T cells that are specific to the ablated tissue [25,26]. Pro-inflammatory cytokines that are released from the injuried tissue or tumour cells, as well as from the disruption of local extracellular matrix and tissue components such as fibrinogen, hyaluronic acid and endothelial cells trigger the release of additional cytokines, chemokines and vascular adhesion molecules. Levels of serum interleukin-1β (IL-1β), IL-6, IL-8 and tumour necrosis factor-α (TNFα) have all been shown to increase after thermal ablation or hyperthermia (on the timescale of hours to days) [27-31].

In summary, the experimental models tested in this study showed that gold macro rods irradiated with high-frequency ultrasound were effective in cancer cell destruction and furthermore confirmed the bio heat transferred to tissue as predicted by calculation and in vitro measurements.

Acknowledgements

The authors thank the Conselho Nacional de Desenvolvimento Científico e Tecnológico (CNPq) for financial support.

Conflicts of Interest

The authors declare no conflict of interest.

References

1. van der Zee J. Heating the patient: a promising approach? Ann Oncol. 2008;13:1173–1184.

2. Svaasand LO, Gomer CJ, Morinelli E. On the physical rationale of laser induced hyperthermia. Lasers Med Sci. 1990; 5:121–128.

3. Mirza AN, Fornage BD, Sneige N, et al. Radiofrequency ablation of solid tumors. Cancer J. 2001; 7:95–102.

4. Seki T, Wakabayashi M, Nakagawa N, et al. Percutaneous microwave coagulation therapy for patients with small hepatocellular carcinoma, comparison with percutaneous ethanol injection therapy. Cancer. 1999; 85:1694–1702.

5. Ahmed M and SN Goldberg. Basic science research in thermal ablation. Surg Oncol Clin N Am. 2011; 20(2): 237-58.

6. Cai W, Gao T, Hong H, et al. Applications of gold nanoparticles in cancer nanotechnology, Nanotechnology, Science and Applications. 2008; 1:17–32.

7. Kennedy LC, Bickford LR, Lewinski NA, et al. A New Era for Cancer Treatment: Gold-Nanoparticle-Mediated Thermal Therapies. Small. 2011; 7: 169-183.

8. Kennedy AS, Nutting C, Coldwell D, Gaiser J, Drachenberg C. Pathologic response and microdosimetry of Y-90 microspheres in man: Review of four explanted whole livers, International Journal of Radiation Oncology Biology Physics. 2004; 60:1552-1563.

9. Gkigkitzis I, Austerlitz C, Campos D. The Effect of the Shape and Size of Gold Seeds Irradiated with Ultrasound on the Bio-heat Transfer in Tissue. American Journal of Clinical Oncology-Cancer Clinical Trials. 2012; 35(2): 195-196.

10. Gkigkitzis I, Austerlitz C. East Carolina University, University Committee on Intellectual Property / Patents Review of Case # TT1212; Use of Gold Macro-Rods and Ultrasound as a

Hyperthermia Cancer Treatment. Office of Technology Transfer, Division of Research and Graduate Studies June 19, 2012.

11. Austerlitz C, Gkigkitzis I, Campos, D. Macro gold rod and ultrasound: a potential alternative to kill cancer cells, East Carolina University, University Committee on Intellectual Property / Patents Review of Case # TT1212; Use of Gold Macro-Rods and Ultrasound as a Hyperthermia Cancer Treatment. Office of Technology Transfer, Division of Research and Graduate Studies June 19, 2012.

12. Austerlitz C, Gkigkitzis I, Campos D. An Approach to Assess Bio-heat Transfer in Tissue with Infra-Red Camera, East Carolina University, University Committee on Intellectual Property / Patents Review of Case # TT1212; Use of Gold Macro-Rods and Ultrasound as a Hyperthermia Cancer Treatment. Office of Technology Transfer, Division of Research and Graduate Studies June 19, 2012.

13. Euhus DM, Hudd C, LaRegina MC, Johnson FE: Tumor measurement in the nude mouse. J Surg Oncol. 1986; 31:229-234.

14. Tomayko MM, Reynolds CP: Determination of subcutaneous tumor size in athymic (nude) mice, Cancer Chemother. Pharmacol. 1989; 24:148-154.

15. Bezerra DP, Castro FO, Alves APNN, et al. In vitro and in vivo antitumor effect of 5- FU combined with piplartine and piperine. J. Appl. Toxicol. 2008; 28:156–163

16. Kabel AM, Abdel-Rahman MN, El-Sisi Ael-D, Haleem MS, Ezzat NM, El Rashidy MA. Effect of atorvastatin and methotrexate on solid Ehrlich tumor. Eur J Pharmacol. 2013; 713(1-3):47-53.

17. Ozaslan M, Karagoz ID, Kilic IH, Guldur ME. Ehrlich ascites carcinoma. Afr J Biotechnol. 2011; 10(13): 2375-2378.

18. Dewey WC et al. Cellular responses to combinations of hyperthermia and radiation. Radiology. 1977; 123(2): 463-74.

19. Laszlo A. “The effects of hyperthermia on mammalian cell structure and function,” Cell Proliferation. 1992; 25: 59–87.

20. Kregel KC. Invited review: heat shock proteins: modifying factors in physiological stress responses and acquired thermotolerance. Journal of Applied Physiology. 2002; 92(5): 2177–2186.

21. Coss AR, Dewey WC, Bamburg JR. Effects of hyperthermia on dividing Chinese hamster ovary cells and on microtubules in vitro. Cancer Research. 1982; 42(3):1059-1071.

22. Thomsen S. Pathologic analysis of photothermal and photomechanical effects of laser-tissue interactions. Photochem. Photobiol. 1991; 53:825.

23. Hillegersberg R, de Witte MT, Kort WJ, Terpstra OT. Water-jet-cooled Nd:YAG laser coagulation of experimental liver metastases: correlation between ultrasonography and histology. Lasers Surg. Med. 1993; 13:332.

24. Haen SP, Pereira PL, Salih HR, et al.. More than just tumor destruction: immunomodulation by thermal ablation of cancer. Clin. Dev. Immunol. 2011; 1–19.

25. Dromi S A, et al. Radiofrequency ablation induces antigen-presenting cell infiltration and amplification of weak tumor-induced immunity. Radiology. 2009; 251: 58–66.

26. Wissniowski TT, et al. Activation of tumor-specific T lymphocytes by radio-frequency ablation of the VX2 hepatoma in rabbits. Cancer Res. 2003, 63:6496–6500.

27. Ali MY, et al. Activation of dendritic cells by local ablation of hepatocellular carcinoma. J. Hepatol. 2005; 43:817–822.

28. Fietta AM, et al. Systemic inflammatory response and downmodulation of peripheral CD25+Foxp3+ T-regulatory cells in patients undergoing radiofrequency thermal ablation for lung cancer. Hum. Immunol. 2009; 70:477–486.

29. den Brok MHMGM, et al. In situ tumor ablation creates an antigen source for the generation of antitumor immunity. Cancer Res. 2004; 64:4024–4029.

30. Sabel MS. Cryo-immunology: a review of the literature and proposed mechanisms for stimulatory versus suppressive immune responses. Cryobiology. 2009; 58:1–11.

31. Erinjeri JP, et al. Image-guided thermal ablation of tumors increases the plasma level of Interleukin-6 and Interleukin-10. J. Vasc. Interv. Radiol. 2013; 24:1105–1112.

6 ARTIGO CIENTÍFICO III

GOLD RODS IRRADIATED WITH ULTRASOUND FOR COMBINATION OF HYPERTHERMIA AND CANCER CHEMOTHERAPY

Artigo será submetido ao periódico: International Journal of Hyperthermia

GOLD RODS IRRADIATED WITH ULTRASOUND FOR COMBINATION OF HYPERTHERMIA AND CANCER CHEMOTHERAPY

Andre Barros[1], Carlos Austerlitz[2], Ioannis Gkigkitzis[3], Diana Campos[4], Jeyce Andrade[1], Christina Peixoto[5], Jaciana Aguiar[1], Silene Nascimento[1] and Teresinha G. Silva[1*]

[1] Bioassays Laboratory for Pharmaceutical Research, Antibiotics Department, Biological Sciences Center, Federal University of Pernambuco, Recife, Brazil.

[2] Department of Computer Science, Southern Illinois University, USA

[3] Department of Mathematics, East Carolina University, 124 Austin Building, East Fifth Street, Greenville, NC 27858-4353, USA

[4] Clínica Diana Campos, Recife, PE 52020-030, Brazil.

[5] Ultrastructure Laboratory, Aggeu Magalhães Research Center, Recife, Brazil.

*Corresponding author. E-mail: teresinha.goncalves@pq.cnpq.br

Tel: +55 31 81 2126 8347. Fax: +55 31 81 2126 8346.

Abstract

Purpose: The aim of this study was to analyze feasibility (*in vitro* and *in vivo*) the use of hyperthermia produced by gold rods irradiated with ultrasound and their combination with chemotherapy with doxorubicin. *Materials and Methods:* initially was determined the cell viability and Hsp70 levels after treatment by gold rods irradiated with ultrasound (GR+U) in cell culture. The pretreatment with GR+U combined with doxorubicin (DOX) was evaluated from IC_{50}, caspase-3 expression and mechanisms of cell death by electron microscopy. For evaluate the in vivo effects was used solid Ehrlich carcinoma (SEC) Tumor. The animals received three treatments with the combination of GR+U+DOX over 16 days. *Results:* The cell viability was completely inhibited after 40 min of treatment with GR+U and significant increases the expression of HSP70 was only observed after 10 minutes of treatment. GR+U+DOX presented significant reduction of IC_{50} representing 50,7%, 76,5% 45,2% and 46,6% for cell lines K562, NCI-H292, Hep-2 and MCF-7 respectively. GR+U+DOX presented significant reduction of IC_{50} representing 50,7%, 76,5% 45,2% and 46,6% for cell lines K562, NCI-H292, Hep-2 and MCF-7 respectively. The caspase-3 level and ultraestructural analysis showed that treatment with GR+U+DOX enhances induction of apoptosis. Pretreatment with GR + U combined with doxorubicin (1 mg) showed 87% inhibition against SEC. and no showed cardiotoxic effect. *Conclusions:* The combined treatment of GR+U and DOX exhibit synergistic characteristics observed by increasing the efficiency of doxorubicin.

Keywords: Cancer; Hyperthermia; Gold Rods; Ultrasound; Doxorubicin.

1. Introduction

Hyperthermia therapy can be defined as a treatment approach in which the temperature of a particular area of the body or the whole body is heated above normal temperatures to achieve therapeutic effects. An advantage of using hyperthermia to kill cancer cells is that usually normal tissues or cells are not as susceptible to high temperature as are cancerous tissues [1]. A variety of changes have been observed in cells after hyperthermia treatment including changes in cell membrane, metabolism, nuclear and cytoskeletal structures, macromolecular synthesis, expression of the heat shock genes and intracellular signal transduction. However, it is generally believed that protein denaturing and cell membrane damage is the most direct effect of hyperthermia toxicity [2–5].

Hyperthermia combination therapy refers to the simultaneous or continuous administration of thermal therapy with radiotherapy and/or chemotherapy for tumor treatment. Many preclinical and clinical trials for advanced and intractable tumor types, showed that thermal combination therapy can serve as an effective adjuvant to radiotherapy and/or chemotherapy as powerful enhancer[6–8].

Numerous studies have shown out that hyperthermia can increase tumor sensitivity to chemotherapeutic drugs and the uptake rates of drugs, and also increases drug accumulation in tumor tissues, which enhances the therapeutic effect of chemotherapy [9,10]. This synergism is observed as a continuous change with increasing temperatures of the rate at which cells are killed by the drug. The associated mechanisms to thermal enhancement include increased rate constants of alkylation, increased drug uptake and inhibition of repair of drug-induced lethal or sublethal damage [7,11].

The irradiation of gold macro rod (GR) with ultrasound is a method for inducing hyperthermia described by [12]. This method has been demonstrated by means of analytical

considerations about bio-heat transfer in tissue, infrared pictures of GR exposed to ultrasound and most recently the viability in Preclinical Model[13]. Based on the above, the aim of this study was to analyze the use of gold rods irradiated with ultrasound for combination of hyperthermia and chemotherapy with doxorubicin.

2. Materials and Methods

2.1. Cell culture conditions

The cell lines used to evaluate the effects of hyperthermia alone and combined with chemotherapy were K562 (human erythroleukemia), NCI-H292 (human lung mucoepidermoid carcinoma), HEp-2 (human laryngeal epidermoid carcinoma) and MCF-7 (human breast adenocarcinoma). The cells were grown in DMEM supplemented with 10% fetal bovine serum, 2 mM L-glutamine, 100 μg/ml Strep and 100 U/ml Pen, and incubated at 37°C in a 5% CO2 atmosphere. Human cells were obtained from the Adolfo Lutz Institute, São Paulo, Brazil.

2.2. Animals

In this study, 48 BALB/c mice (male, 25-30 g), were obtained from the Laboratory of Immunopathology Keizo-Asami (LIKA) of the Federal University of Pernambuco (UFPE), Brazil. The animals were kept in cages with free access to food and water, under 12 h light-dark cycles. The animals were treated in accordance with the International Council for Laboratory Animal Science (ICLAS), and following the ethical principles of the Brazilian Society of Science in Laboratory Animals (SBCAL). All experiments were approved by the Ethics Committee for Animal Experimentation of the Biological Sciences Center of the Federal University of Pernambuco, Brazil, number 23076.013243/2012-04.

2.3. Cell viability after Heat treatment by gold rods irradiated with ultrasound

The cells were seeded in 24-well plates (10^5 cells/ml for adherent cells or 3×10^5 cells/ml for leukemias). After 24 hours were performed four different experimental models as follows:

Control: untreated cells

GR: gold macro-rods inserted on plate not irradiated with ultrasound.

U: plates irradiated with ultrasound only.

GR+U: gold macro-rods inserted on plate and irradiated with ultrasound.

In GR+U model, gold rods(24 K, 0.155 cm diameter and 0.54 cm height) were plated in the wells and stimulated by ultrasound generated by a 4 cm diameter transducer oscillating with a nominal frequency of 1 MHz and power of about 75 W. increasing the temperature in each well was measured using a Precision Infrared Thermometer (Fluke®). All experimental models were tested at 10, 20, 30 and 40min. Six hours after treatments, the cell survival was quantified by the mitochondrial oxidation of 3-(4,5-dimethyl-2-thiazolyl)-2,5-diphenyl-2H-tetrazolium bromide (MTT assay)[14,15]. Was added 25 μL of MTT (5 mg/mL), 3 h later, the MTT formazan product was dissolved in 100 μL of DMSO, and absorbance was measured at 450 nm in plate spectrophotometer.

2.4. Quantification of HSP70

To the quantification of HSP70 from GR+U-treated cancer cells a commercially available kit HSP70 ELISA (Sigma) was used. The supernatants of GR+U-treated were collected at different post-GR+U times for ELISA analysis by adding to the microtiter wells coated with human anti-HSP70 monoclonal antibody. The captured HSP70 was detected with a HSP70-specific biotinylated rabbit polyclonal antibody that was subsequently bound by an horseradish peroxidase conjugate. The color development was stopped with acid stop solution

which converts the endpoint color to yellow. The intensity of the color was measured in a microplate reader at 450 nm.

2.5. Effect of pretreatment with GR+U on cytotoxic activity of doxorubicin

For these experiments, the cells were plated in 24-well plates (10^5 cells/mL for adherent cells or 3×10^5 cells/mL for leukemias) and incubated for 24h. The dose-response curve of doxorubicin (alone and pre-treated with GR+U 10min) was obtained by the dissolution in culture medium to final concentrations of 0–50 µM, incubated for 24 h. After 72 h, the cytotoxicity was quantified by MTT assay (as described in section 2.3). The IC_{50} values and their 95% confidence intervals for three different experiments were obtained by nonlinear regression using Graphpad Prism version 6.0 for Windows (GraphPad Software, San Diego, California USA).

2.6. Caspase-3 assay

The effect of doxorubicin alone and combined with hyperthermia on caspase-3 activity was determined using a commercially available caspase-3 (active) ELISA kit (Invitrogen Corporation, Camarillo, CA). The cells was treated with DMSO (control), GR+U (10min), DOX (1µM) and GR+U (10min) + DOX (0,5µM) and incubated for 24h. Later 24h, the cells were collected and lysed in cell extraction buffer and 100 µl of cell lysates were incubated in the microplate wells provided in the kit and incubated at room temperature for 2h. The samples were aspirated and washed 4 times with washing buffer and incubated with 100 µl of detection antibody (caspase-3) for 1h at room temperature. After removal of the antibody solution, the wells were washed again and incubated with 100 µl of HRP anti-rabbit antibody for 30 min at room temperature. After the aspiration of the anti-rabbit antibody, blue color was developed by adding 100 µl of stabilized chromogen solution for 15–20 min at room

temperature. The reaction was stopped adding 100µl of stopping solution and the yellow color developed was read using a microplate reader at 450 nm. The results were expressed as ng of caspase per mg of total proteins of the treated cells relative to control.

2.7.Electron microscopy analysis of cell death

For morphological assessment of cell death, transmission electron microscopy was used for K562, NCI-H292, HEp-2 and MCF-7 cells. The cells was treated with DMSO (control), GR+U (10min), DOX (1µM) and GR+U (10min) + DOX (0,5µM) and incubated for 24h, after this period, were fixed with 2.5% glutaraldehyde (Sigma) and 4% paraformaldehyde (Sigma) in 0.1 M cacodylate (Sigma) buffer. After fixation, the samples were washed twice in the same buffer and post-fixed in 0.1 M cacodylate buffer (pH 7.2) containing 1% osmium tetroxide (Sigma), 2 mM calcium chloride and 0.8% potassium ferricyanide. Next, cells were dehydrated using acetone and embedded in SPIN-PON resin (Embed 812). Polymerization was performed at 60°C for three days. Ultrathin sections were collected on nickel 300-mesh grids, counterstained with 5% uranyl acetate and lead citrate and examined with an FEI Morgani 268D transmission electron microscope. A minimum of 100 cells per sample were observed from three independent experiments to evaluate any cellular morphological alterations[16].

2.8. Solid Ehrlich Carcinoma (SEC) Tumor Model

Ehrlich ascites carcinoma (EAC) cells were derived from a spontaneous murine mammary adenocarcinoma. EAC cells were maintained in the undifferentiated form by passaging in syngeneic mice by transplanting $2{,}5 \times 10^6$ cells/mL (i.p.) each week. The ascitic fluid was removed by opening the belly and collecting all of the fluid with a sterile syringe. Ascitic tumor cell counts were carried out using the trypan blue dye exclusion method with a

neubauer hemocytometer. Animals received 200 μL of a suspension containing 5×10^6 cells/mL (i.p.). Tumor volume was measured using a electronic caliper, assuming a fairly constant relationship of mass to volume, tumor development can be expressed in terms of volume increment. In order to determine tumor volume by external caliper, the greatest longitudinal diameter (length) and the greatest transverse diameter (width) were determined.

Tumor volume based on caliper measurements were calculated by the modified ellipsoidal formula[17,18]:

$$Tumor\ volume\ (mm^3) = 1/2(length \times width^2)$$

The inhibition rate (%) was calculated as follows[19]:

$$Inhibition\ rate\ (\%) = [(A - B)/ A] \times 100$$

where A is the average weight of the non treated group and B is the average tumor weight of the treated group.

2.9. In vivo antitumor activity

After five days of tumor implantation (Tumor volume= 300± 18mm^3), mice were randomly assigned into four groups (6 mice/group). In this experiment were evaluated the treatments with NaCl 0,9% (control), GR+U (10min), DOX (3mg/kg) and GR+U (10min) + DOX (1mg/kg). The treatment with GR+U was carried out by insertion of the gold rod (0.155 cm diameter and 0.54 cm height) in the center of tumor using of a trocar needle. A layer of ultrasound transmission gel was spread on the shaved mice's skin as contact media gel and exposed for 10 minutes with a 1 cm transducer connected to a GS8 2E ultrasound under a nominal frequency of 1 MHz and about 75 W. The temperature increase was measured every minute in the central and peripheral region of the tumor with needle type thermistor connected to a thermometer FLUKE. Changes in body temperature were valued by rectal temperature.

The experiment lasted 16 days, during this period the groups were treated 3 times (5th, 10th and 15th day). Tumor volume was measured from the 5th to the 16th day after implantation of SEC. On 16th day, the mice were sacrificed and the tumors were dissected and weighed, additionally blood samples were collected from each group for evaluation of adverse effects.

2.10. Hematological and Biochemical analysis

Hematological analysis was carried out using an automatic cell counter (ABX-MICROS-60 cell counter Horiba, Inc). The samples were evaluated for the following hematological parameters: number of erythrocytes, concentration of hemoglobin, number of platelets and total count and differential of leukocytes. Part of the collected blood was poured into heparinized tubes for analysis of blood levels of alanine aminotransferase (ALT), aspartate aminotransferase (AST), lactate dehydrogenase (LDH), and creatine phosphokinase (CPK).

2.11. Statistical Analysis

The results are presented as the mean ± standard deviation (SD) or confidence intervals. One-way ANOVA followed by the Newman-Keuls test was used to evaluate the differences among the treatments. P values < 0.05 were considered to be statistically significant.

3. Results

3.1. Cell viability after Heat treatment by gold rods irradiated with ultrasound

In this assay was observed the heat generated by the gold rods irradiated with ultrasound in each well of the plate. increasing the temperature as a function of time can be seen in figure 1, the heat rate produced increased about 0,72°C/min from 37 to 66°C during of assessment 40min.

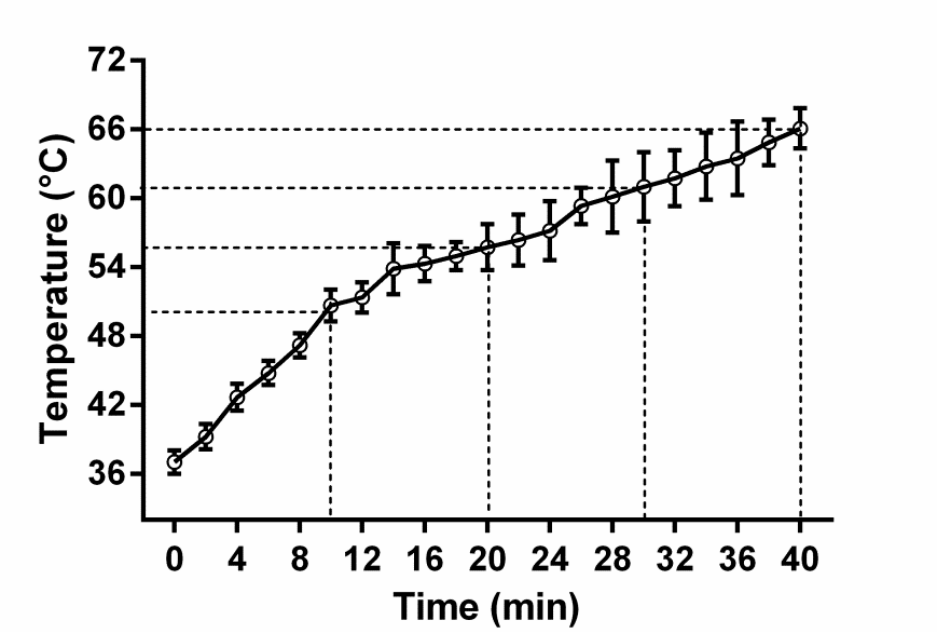

Figure 1. The heat enhancement on cell culture during the irradiation of the gold rod with ultrasound.

The effect of the temperature elevation induced by GR+U varied according to the tested cell lines (Fig 2). The cell viability, in all cell lines, was completely inhibited after 40 min of treatment with GR+U.

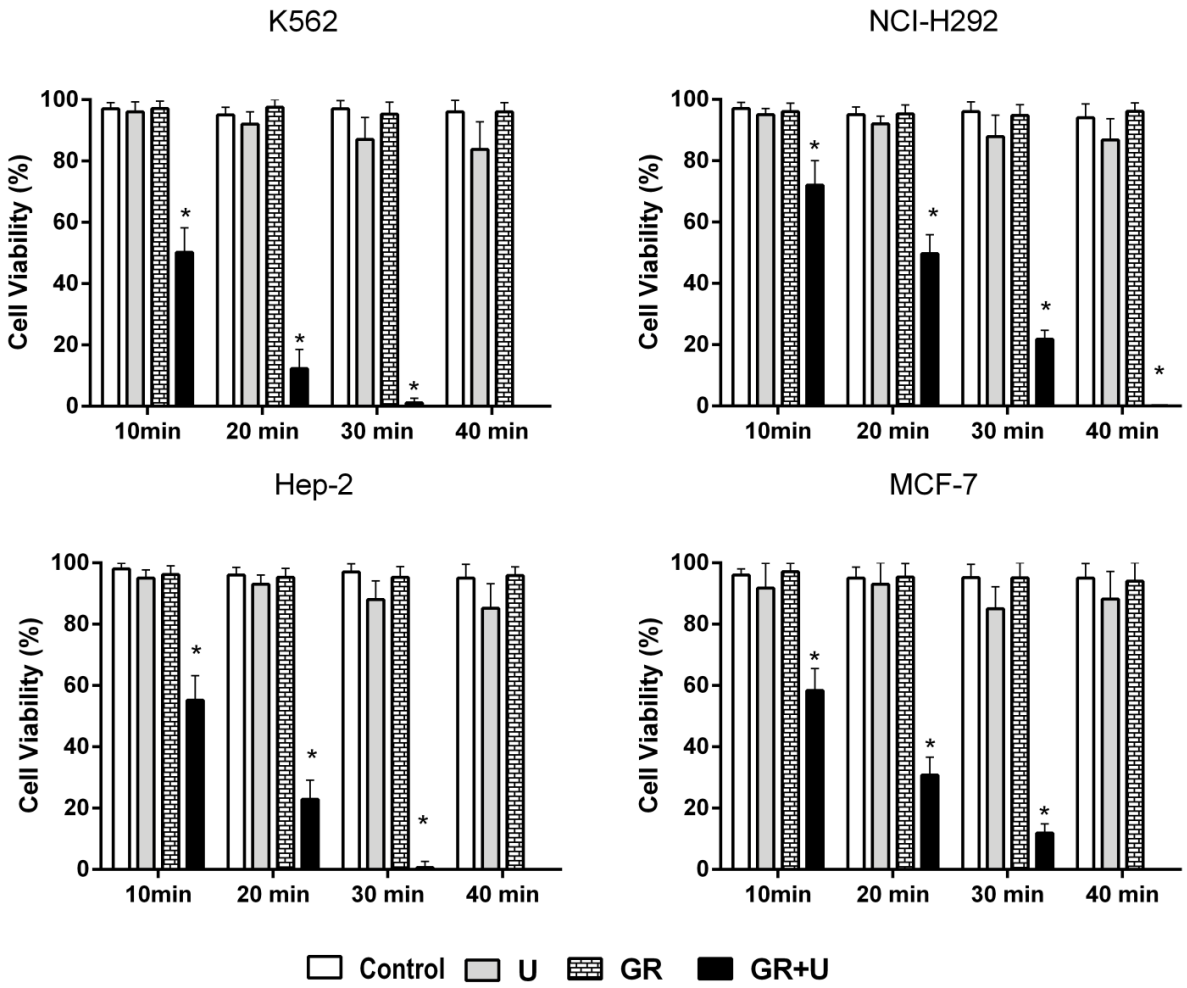

Figure 2. The effect of gold rods irradiated with ultrasound for 10, 20, 30 and 40 minutes, in K562, NCI-H292, Hep-2 and MCF-7 cell lines. Results represent mean ± standard deviation of two experiments. * $p<0.05$ compared to control by ANOVA followed by Newman-Keuls test.

3.2. The effect of GR+U in HSP70 levels on cell culture

HSP70 levels were assessed into culture supernatants after treatment with GR + U by 10, 20 and 30 min (Fig. 3). The GR+U treatment by 10 min don't showed alterations compared with control in any tested cells types, however, in the treatments of 20 and 30 minutes there was significant increases the expression of HSP70.

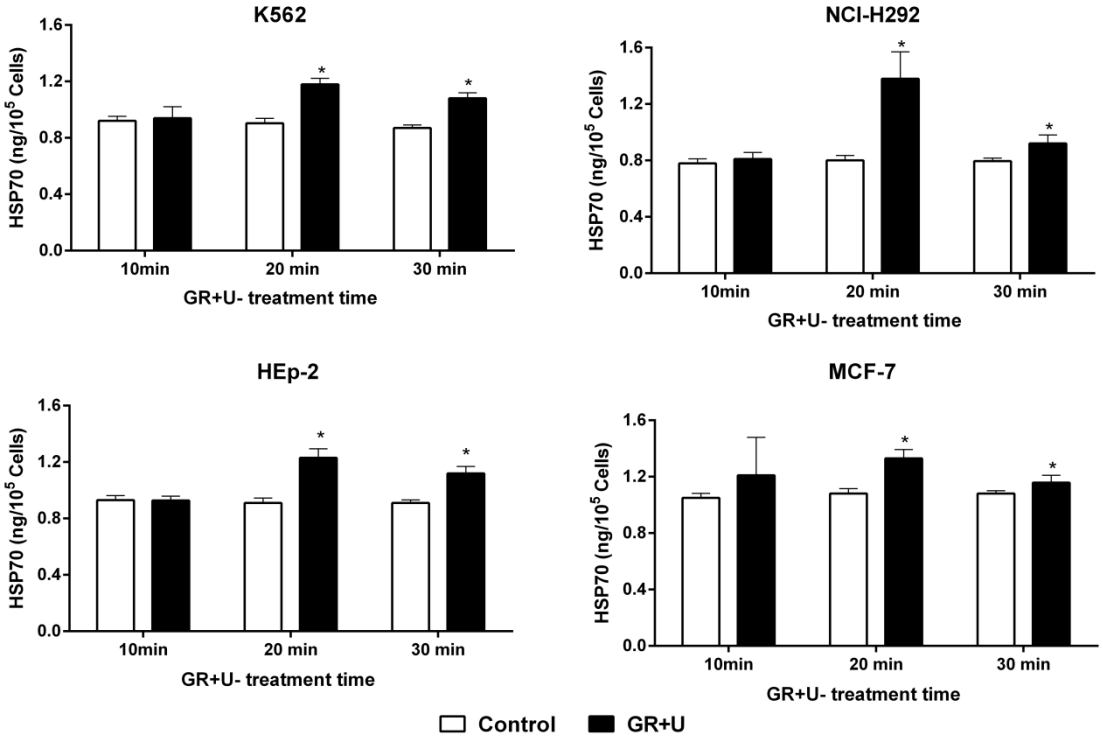

Figure 3. HSP70 level into culture supernatants from K562, NCI-H292, Hep-2 and MCF-7 cells treated by gold rods irradiated with ultrasound for 10, 20 and 30 minutes. Results represent mean ± standard deviation of two experiments. * $p<0.05$ compared to control by ANOVA followed by bonferroni post-hoc correction.

3.3. Effect of pretreatment with GR+U on cytotoxic activity of doxorubicin

The cytotoxic activity of doxorubicin alone and combined with GR+U pretreatment on the human tumor cell lines were evaluated after 24 h using MTT, and the results are presented in figure 4. Pretreatment with GR+U increased the cytotoxic effect of doxorubicin in all tested cell lines. Was observed significant reduction of IC_{50} representing 50,7%, 76,5% 45,2% and 46,6% for cell lines K562, NCI-H292, Hep-2 and MCF-7 respectively.

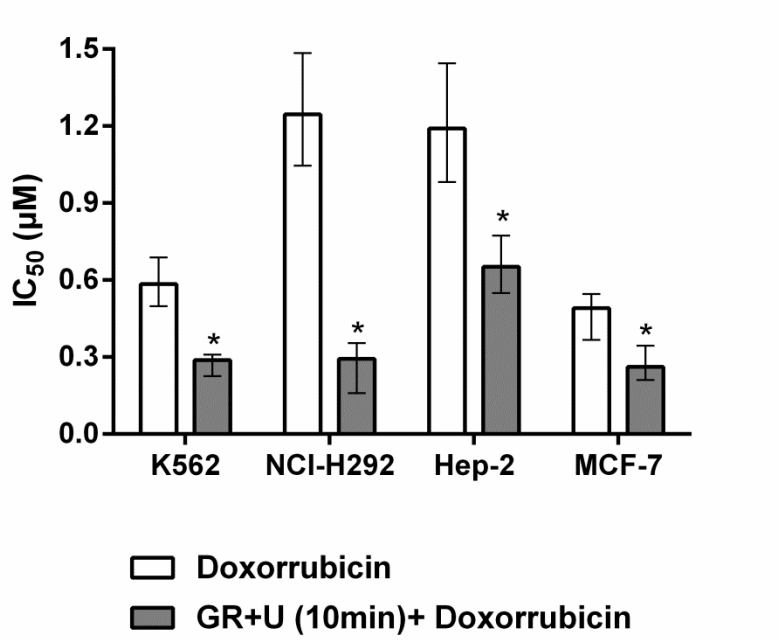

Figure 4. Effect of pretreatment with GR+U on cytotoxic activity of doxorubicin. Results represent IC_{50} values and confidence intervals of three different experiments obtained by nonlinear regression. * $p<0.05$ compared to DOX alone treatment by ANOVA followed by Newman-Keuls test.

3.4. Effect of GR+U combined with doxorubicin treatment on caspase-3 activation

The effect of treatment with DMSO (control), GR+U (10min), DOX (1µM) and GR+U (10min) + DOX (0,5µM) in caspase-3 activity is showed in Figure 5. There were no statistically significant differences between treatment with DOX (1µM) and GR+U (10min) + DOX (0,5µM) in K562, Hep-2 and MCF-7 cell lines. The caspase-3 activity in NCI-H292 cells was 42% higher in treatment with GR+U (10min) + DOX (0,5µM) compared to cells treated with DOX (1µM). These results may indicate that pretreatment with GR+U enhances the efficacy of doxorubicin.

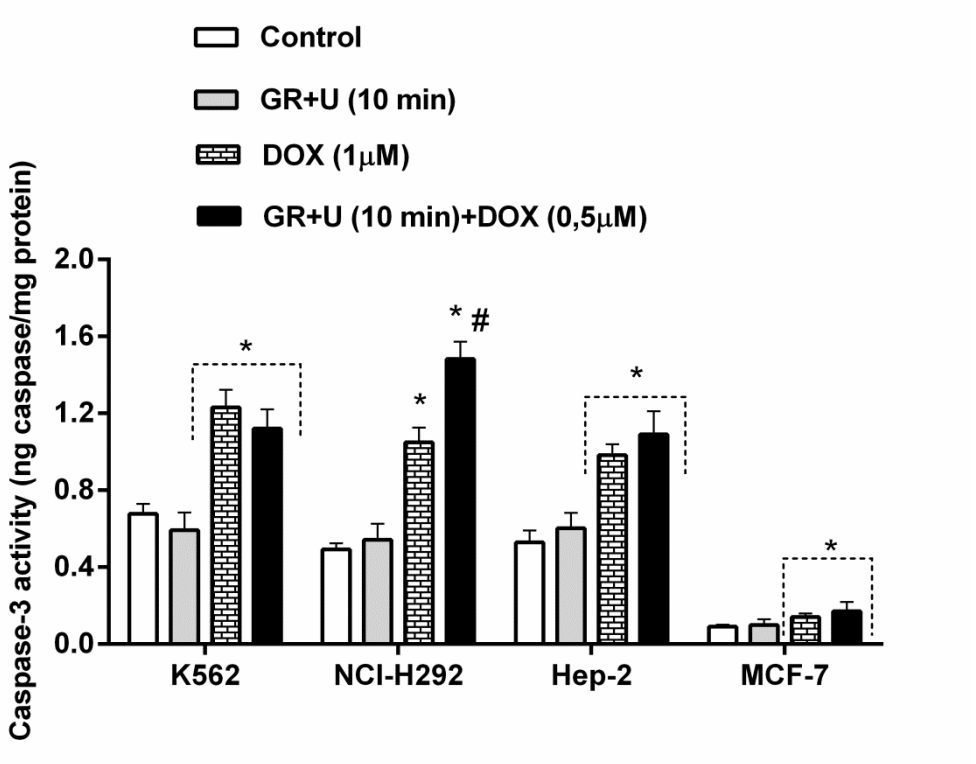

Figure 5. Effects of GR+U combined with doxorubicin treatment on caspase-3 activity after 24h incubation. Data are presented as mean ± standard deviation of two independently performed experiments. * $p<0.05$ compared to DMSO-treated and # $p<0.05$ compared to all treatments by ANOVA followed by Newman-Keuls post-test.

3.5. Cell death analysis by electron microscopy

The specific morphological parameters used to classify apoptosis were: chromatin condensation, nuclear fragmentation, cell shrinkage, cell retraction, nuclear blebbing and presence of apoptotic bodies. For the identification of necrosis morphological parameters used were: cell swelling, lack of an intact cell membrane and disintegration or ruptures of the intracellular organelles. The ultrastructural analyses of the cell lines treated with DMSO (control), GR+U (10min), DOX (1μM) and GR+U (10min) + DOX (0,5μM) can be observed in figure 6. The treatment with GR+U (10min) + DOX (0,5μM) produced the same effects of 1 μM doxorubicin in K562, Hep-2 and MCF-7 cells. The combination of GR + U and

doxorubicin increased the number of apoptotic cells (64,5%) compared to treatment with doxorubicin alone (53%) in NCI-H292 cell line. Cell morphology of NCI-H292 on transmission electron microscopy after aforementioned treatments is shown in figure 7.

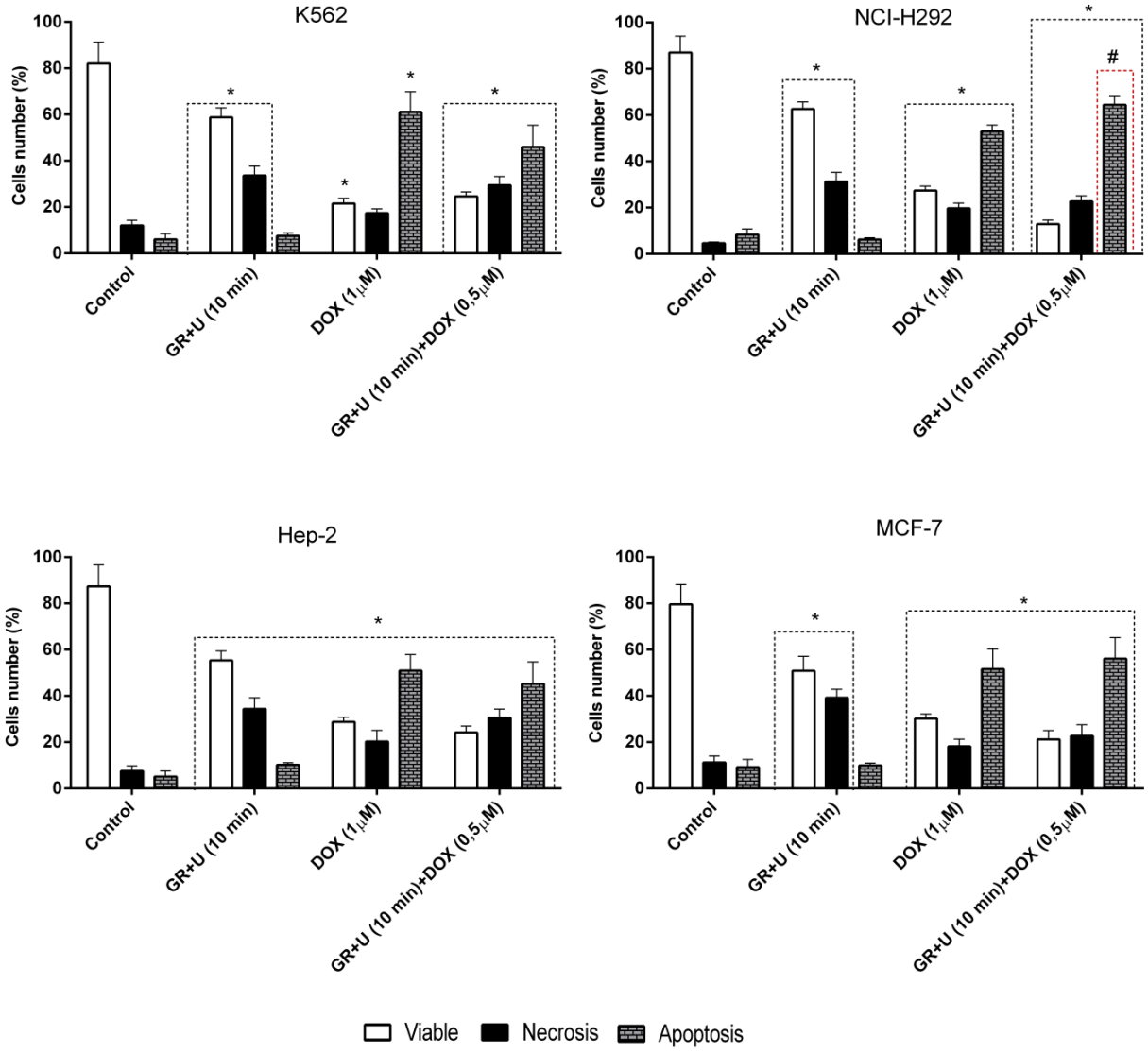

Figure 6. Ultrastructural analyses of cell death after treatment with DMSO (control), GR+U (10min), DOX (1μM) and GR+U (10min) + DOX (0,5μM). Results represent mean ± standard deviation of three experiments for each cell line tested. * $p<0.05$ compared to DMSO-treated and # $p<0.05$ compared to all treatments by ANOVA followed by Newman-Keuls post-test.

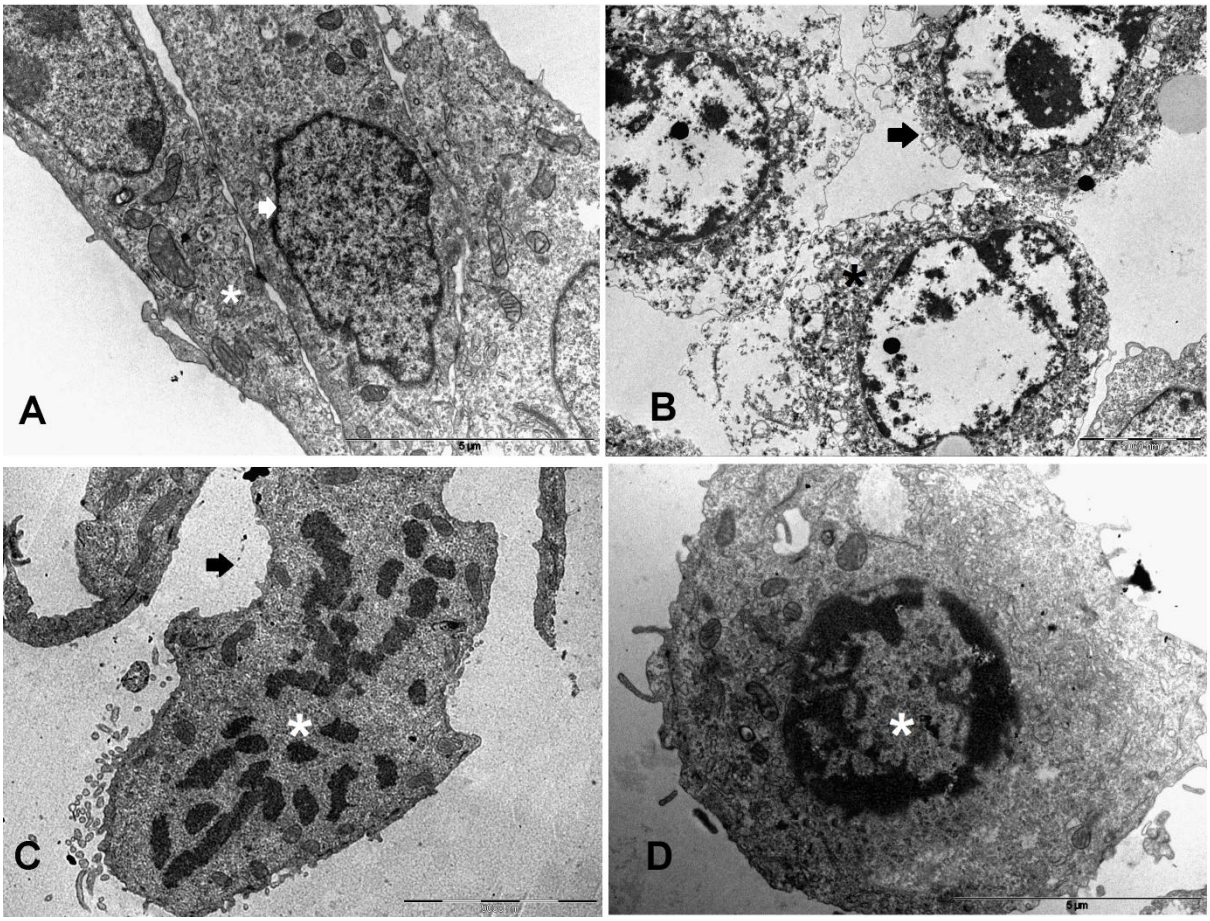

Figure 7. Electron micrograph of NCI-H292 cells. (A) DMSO control: normal cells morphology showing intact nuclear membrane (white arrow) and cytoplasmic organelles preserved (white asterisk); (B) GR+U (10min): Necrotic cells showing plasmatic membrane disintegration (black arrow) and ruptures of the intracellular organelles (black asterisk); (C) DOX (1µM): apoptotic cell with fragmentation of the nucleus and chromatin condensation (white asterisk) and cell retraction (black arrow); (D) GR+U (10min) + DOX (0,5µM): apoptotic cell with perinuclear condensation of chromatin (white asterisk). All images are shown at the same magnification (3500x).

3.6. *In vivo* antitumor activity

In this study was observed the influence of pretreatment with gold rods irradiated with ultrasound on the efficacy of doxorubicin. The effect of GR+U (10min), DOX

(3mg/kg) and GR+U (10min) + DOX (1mg/kg) against solid Ehrlich carcinoma is showed in Figure 8. Tumor volumes were evaluated for 16 days, in this period, treatment with the combination of GR + U and doxorubicin induced significant reductions in developing SEC as of the 11th day. The tumor volume of the group GR + U (10min) + DOX (1mg / kg) observed at the final of assessment was 178mm^3, whereas the groups treated with GR + U and DOX alone showed 486 and 388mm^3 respectively.

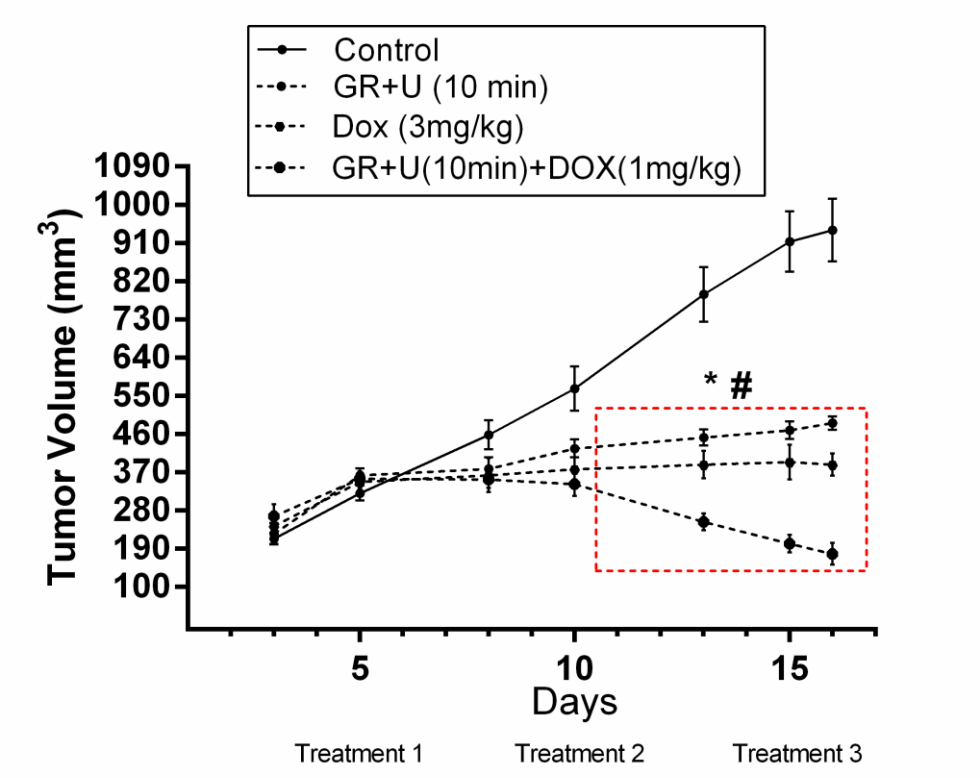

Figure 8. The effect of treatment with GR+U (10min), DOX (3mg/kg) and GR+U (10min) + DOX (1mg/kg) on the growth of Ehrlich tumor. Data are presented as mean ± standard deviation. * $p<0.05$ compared to control by ANOVA followed by Newman-Keuls test. # $p<0.05$ compared to all treatments by ANOVA followed by Newman-Keuls post-test.

The temperature in the tumor was measured with the FLUKE thermistor in two regions defined in accordance with the proximity to the GR inserted. In central region, the

heat rate produced increased about 1,5°C/min from 36 to 51°C and in peripheral region 0,78°C/min from 36,4 to 44,2 °C (Fig. 9). Significatives changes in rectal temperature not were observed.

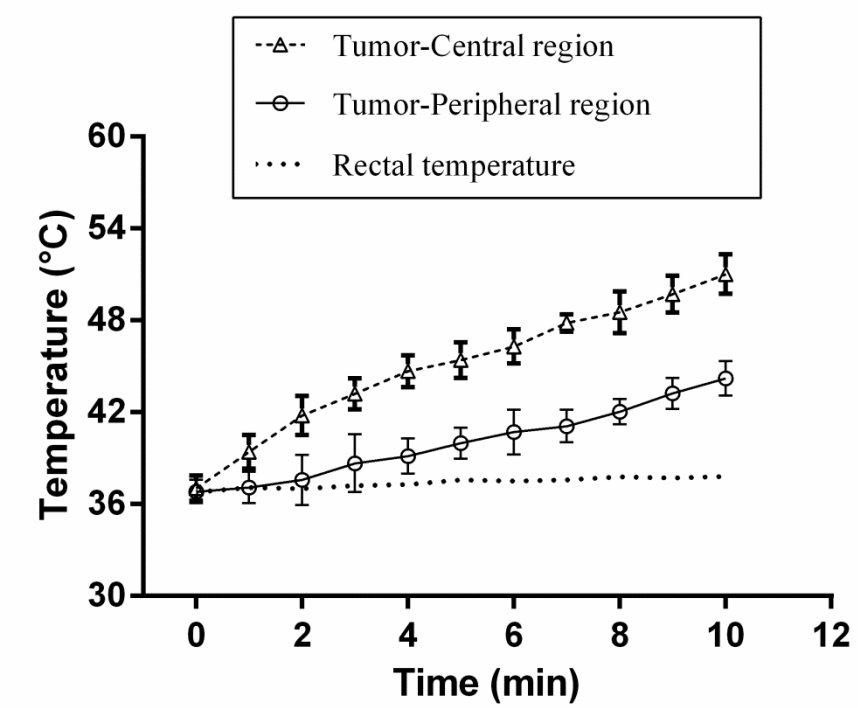

Figure 9. The heat enhancement on tumor during the irradiation of the gold rod with ultrasound for 10 minutes.

The antitumor activity of treatments with GR + U, DOX alone and the combination GR+U+DOX is described in Figure 10. The three treatments tested inhibited the tumor development over the trial period, however, the GR+U+DOX group had higher rate of inhibition (87%) in relation to other treatments.

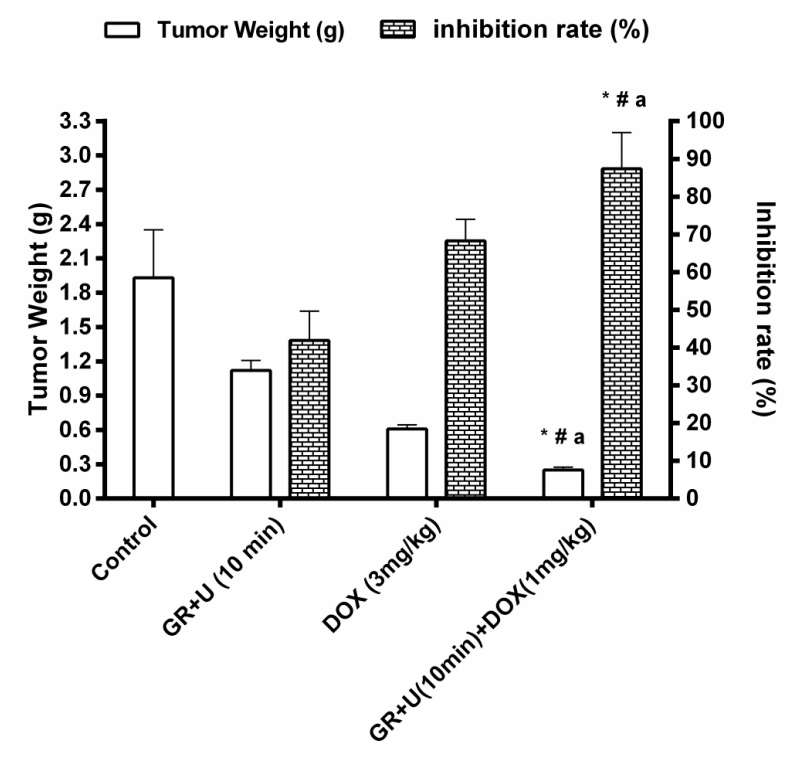

Figure 10. Antitumor activity of treatment with GR+U (10min), DOX (3mg/kg) and GR+U (10min) + DOX (1mg/kg) in mice transplanted with SEC. Results are presented as mean ± standard deviation. * $p<0.05$ compared to control by ANOVA followed by Newman-Keuls test. # $p<0.05$ compared to GR+U (10min) by ANOVA followed by Newman-Keuls test. a $p<0.05$ compared to DOX (3mg/kg) by ANOVA followed by Newman-Keuls test.

3.7. Toxicological analysis

In animals treated with the combination GR+U+DOX, the doxorubicin dose used was approximately 33% of the dose received by animals treated with doxorubicin only. The use of a lower dose reduced the toxic effects of doxorubicin on hematological parameters as shown in Table 1. Furthermore, it was also observed significant inhibition of the cardiotoxic and hepatotoxic effects of doxorubicin, measured by reduction in levels of alanine aminotransferase, aspartate aminotransferase, lactate dehydrogenase and creatine phosphokinase (Fig. 11).

Table I: Effect of treatment with three doses of GR + U (10min) + DOX (1mg / kg) on hematological parameters of mice 16 days after implantation of Erhlich carcinoma.

Parameter	Control	GR+U	DOX	GR+U+DOX
Leukocytes (10^3/mm^3)	8.73±0.68	9.67 ±0.88	3.22 ±0,47	5.3 ±1,03$^{*\#}$
Neutrophil (%)	9.4	11.7	13.7	17.6
Monocyte (%)	15.5	24.5	12.4	13.6
Lymphocyte (%)	73.6	62.2	61.2	67.8
Red blood cells (10^6/mm^3)	9.13 ±0.94	10.2±1.12	4.03 ±0.65	8.82 ±0.99$^{\#}$
Platelets (10^3/mm^3)	483 ±37.5	437 ±64.8	223±57.8	419 ±69,8$^{\#}$

The values are presented as the average ± the standard deviation. * ($p < 0.05$) compared to the control and $^{\#}$ ($p<0.05$) compared to DOX (3mg/kg) treatment by ANOVA followed by Newman-Keuls post-test.

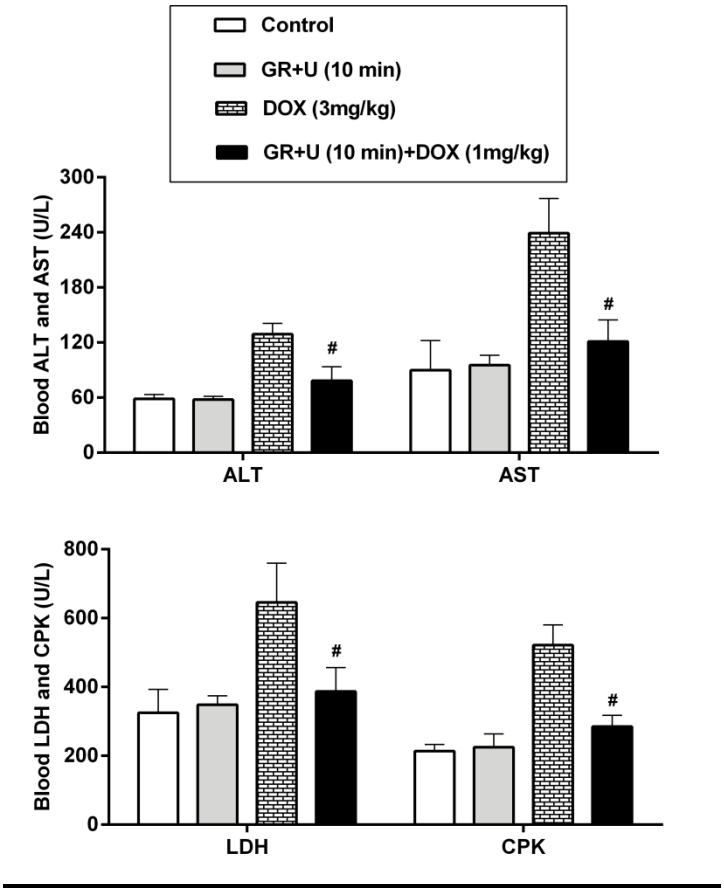

Figure 11. Effect of treatment with three doses of GR + U (10min) + DOX (1mg / kg) on biochemical parameters parameters of mice 16 days after implantation of Erhlich carcinoma. ALT, alanine aminotransferase; AST, aspartate aminotransferase; LDH, lactate dehydrogenase; CPK, creatine phosphokinase. # ($p<0.05$) compared to DOX (3mg/kg) treatment by ANOVA followed by Newman-Keuls post-test.

4. Discussion

The cancer treatment by hyperthermia using macro of gold rods irradiated with ultrasound was described initially by [12]. The dimensions of the gold rod and the thermal energy produced under irradiation with ultrasound was described from theoretical observations and computer simulations by [13] and all the experimental setup involving hyperthermia by GR+U as well as the development of surgical technique for insertion of gold rods in tumors and the application of the technique, were based on these results.

In this study, the temperature increase produced by the gold rods irradiated with ultrasound induced decrease in cell viability in direct proportion to the irradiation time. After 40 minutes nearly all the cells died. The Hyperthermia has cytotoxic effects on tumor cells via several mechanisms. The first phase of direct killing is characterized by linear growth arrest, which is typified by decreased RNA (brief) and DNA (prolonged) synthesis specifically at the S phase but also by a slowed M phase of the cell cycle [11]. Deficiencies in DNA repair mechanisms become evident as early as 40∘C and above 43∘C, occurs cell membrane disruption, transmembrane proteins denaturation, cellular architectural distortion, and ultimately, necrotic and apoptotic pathway activation [20,21].

To combine hyperthermia produced by GR+U with a conventional chemotherapeutic agent was considered the interference of heat shock proteins in apoptosis mechanisms. Heat-shock proteins (HSPs) are expressed constitutively and are further induced under stress conditions, including temperature increase. Hsp70 blocks several steps of the apoptotic cascade: upstream from mitochondria, release of cytochrome C and apoptosis-inducing factor (AIF), nuclear import of AIF, activation of procaspases-9 and -3, and even downstream of active caspase-3[22–27]. In vitro results presented in our work showed that cells treated with GR + U for 10 minutes don't showed significant changes in hsp70 level. For this reason, was used this irradiation time in the combined treatment of GR+U+DOX.

The advantages of combined hyperthermia and chemotherapy have been explained in clinical trial reports[28,29]. In this study, pretreatment with GR + U (10min) increased the cytotoxicity of doxorubicin about 65% compared to treatment with DOX alone. Increased efficiency of drug on combination therapy with hyperthermia can be correlated to the plasma membrane fluidity changes at hyperthermic range of temperature[30].

The anthracyclin drug doxorubicin is one of the most effective antineoplastic agents, and widely used to treat a number of malignancies, despite extensive clinical utilization, the mechanisms of action of anthracyclines in cancer cells remain a matter of controversy. The main mechanisms considered are: 1) intercalation into DNA, leading to inhibited synthesis of macromolecules; 2) generation of free radicals, leading to DNA damage or lipid peroxidation; 3) DNA binding and alkylation; 4) DNA cross-linking; 5) interference with DNA unwinding or DNA strand separation and helicase activity; 6) direct membrane effects; 7) initiation of DNA damage via inhibition of topoisomerase II [31–33]. For this reason, in order to quantify apoptosis, was used in this study the levels of caspase-3.

Caspase-3, an executioner caspase, can be activated by mitochondrial or intrinsic pathway involving caspase-9 or a death receptor/extrinsic pathway involving caspase-8[34]. Activation of caspase-3 is thought to be a fundamental biochemical event marking the induction of apoptosis, followed by the cell death in a systematic fashion in such a manner that surrounding cells and tissues are unaffected[35]. Caspase-3 levels induced by pretreatment with GR + U (10min) + DOX (0,5uM) were statistically equivalent to treatment with DOX (1uM) in K562, Hep-2 and MCF-7. In NCI-H292 cell line, the amount of caspase-3 in the combined treatment was 36% higher compared to DOX alone. The increase of caspase-3 in NCI-H292 was confirmed by ultrastructural analysis.

The increase in the number of apoptotic cells shown by treatment with GR+U+DOX against the NCI-H292 line cells can be explained by the activation stress-activated protein

kinases (SAPKs). Under stress, activation of SAPKs appears to be important in promoting apoptosis in many cell types, including NCI-H292 cells in culture. SAPKs, and especially the JNK pathway, contribute is important in the activation of the mitochondria-dependent apoptotic pathway (also known as the intrinsic pathway) but dispensable for apoptosis induced by the activation of death receptors (the extrinsic pathway) [36]. JNK- and p38-mediated phosphorylation of p53, which augments the p53 response, may also play a role in their pro-apoptotic actions [37,38].

In the current study we investigated the effect of pretreatment with GR + U (10min) on the cytotoxic activity of DOX against the growth of solid Ehrlich carcinoma in mice. SEC is an undifferentiated carcinoma that has high transplantable capability and rapid proliferation. After the inoculation the number of cells increases rapidly and the host animal died due to the pressure exerted by the tumor volume and/or the damage that resulted from the tumor[39,40].

According to the analysis of tumor growth per 16 days, the difference between the antitumor effects by the treatment with GR+U(10min)+DOX(1mg/kg) compared to treatment with doxorubicin(3 mg/kg) was observed only from 10th day. The tumor inhibition, at the end of the experiment was 20% more in GR+U+DOX compared with DOX only. Our results showed that pretreatment with hyperthermia increased the efficiency of doxorubicin enabling the use of smaller doses without compromising the effect of the drug.

Doxorubicin is highly effective in treating of leukemias and many solid tumors [41]. However, this drug presents dose-dependent adverse effects on bone marrow, heart and other organs. Like other members of the anthracycline class, its usage is greatly limited especially by the risk of severe cardiotoxicity leading to potentially lethal congestive heart failure[42,43]. Due to the great importance of DOX in chemotherapy for the treatment of many types of cancer, researchers have exerted great efforts to attenuate their side effects. In

this study, the pretreatment GR + U combined with low doses of doxorubicin reduced toxic effects in bone marrow. Furthermore, animals treated with DOX + GR + U not show cardiotoxic effects in accordance with the observed biochemical parameters.

5. Conclusion

Significant effects are observed by use of gold rods irradiated with ultrasound and doxorubicin. Combined treatment of hyperthermia and DOX exhibit synergistic characteristics observed by increasing the efficiency of doxorubicin. The combined treatment accelerated the DOX passive permeation and therefore increasing intracellular DOX concentration and cytotoxicity. In the evaluation of antitumor effects in vivo, the pretreatment with GR+U showed similar results to those observed on in vitro tests. However from the observations in vivo, our study showed that in combination with hyperthermia the toxic effects of doxorubicin were minimized.

Acknowledgements

The authors thank the Conselho Nacional de Desenvolvimento Científico e Tecnológico (CNPq) for financial support.

Conflicts of Interest

The authors declare no conflict of interest.

References

1. Van der Zee J. Heating the patient: A promising approach? Annals of Oncology. 2002. p. 1173–84.

2. Hokland SL, Pedersen M, Salomir R, Quesson B, Stødkilde-Jørgensen H, Moonen CTW. MRI-guided focused ultrasound: Methodology and applications. IEEE Trans Med Imaging. 2006;25:723–31.

3. Hegyi G, Szigeti GP, Szász A. Hyperthermia versus oncothermia: Cellular effects in complementary cancer therapy. Evidence-based Complementary and Alternative Medicine. 2013.

4. Vertree RA, Leeth A, Girouard M, Roach JD, Zwischenberger JB. Whole-body hyperthermia: a review of theory, design and application. Perfusion. 2002;17:279–90.

5. Day ES, Morton JG, West JL. Nanoparticles for thermal cancer therapy. J Biomech Eng. 2009;131:074001.

6. Horsman MR, Overgaard J. Hyperthermia: a potent enhancer of radiotherapy. Clin Oncol (R Coll Radiol) [Internet]. 2007 Aug [cited 2014 Nov 30];19(6):418–26. Available from: http://www.ncbi.nlm.nih.gov/pubmed/17493790

7. Issels RD. Hyperthermia adds to chemotherapy. Eur J Cancer. 2008;44:2546–54.

8. Wust P, Hildebrandt B, Sreenivasa G, Rau B, Gellermann J, Riess H, et al. Hyperthermia in combined treatment of cancer. Lancet Oncol. 2002;3:487–97.

9. Bergs JWJ, Franken NAP, Haveman J, Geijsen ED, Crezee J, van Bree C. Hyperthermia, cisplatin and radiation trimodality treatment: a promising cancer treatment? A review from preclinical studies to clinical application. Int J Hyperthermia. 2007;23:329–41.

10. Oyama T, Kawamura M, Abiko T, Izumi Y, Watanabe M, Kumazawa E, et al. Hyperthermia-enhanced tumor accumulation and antitumor efficacy of a doxorubicin-conjugate with a novel macromolecular carrier system in mice with non-small cell lung cancer. Oncol Rep. 2007;17:653–9.

11. Hildebrandt B, Wust P, Ahlers O, Dieing A, Sreenivasa G, Kerner T, et al. The cellular and molecular basis of hyperthermia. Critical Reviews in Oncology/Hematology. 2002. p. 33–56.

12. Gkigkitzis I, Campos D, Haranas I. An experimental study on the heat enhancement and the bio-heat transfer using gold macro rod and ultrasound : a potential alternative to kill cancer cells. Phys Int. 2014;5(2):132–5.

13. Gkigkitzis I, Austerlitz C, Haranas I, Campos D. The Effect of the Shape and Size of Gold Seeds Irradiated with Ultrasound on the Bio-Heat Transfer in Tissue. Adv Exp Med Biol Vol. 2015;820:103–24.

14. Mosmann T. Rapid colorimetric assay for cellular growth and survival: application to proliferation and cytotoxicity assays. J Immunol Methods. 1983;65:55–63.

15. Alley MC, Scudiero DA, Monks A, Hursey Czerwinski MLMJ, Fine DL, Abbott BJ, et al. Feasibility of drug screening with panels of human tumor cell lines using a microculture tetrazolium assay. Cancer Res. 1988;48:589–601.

16. Krysko D V., Vanden Berghe T, D'Herde K, Vandenabeele P. Apoptosis and necrosis: Detection, discrimination and phagocytosis. Methods. 2008;44:205–21.

17. Euhus DM, Hudd C, LaRegina MC, Johnson FE. Tumor measurement in the nude mouse. J Surg Oncol. 1986;31:229–34.

18. Tomayko MM, Reynolds CP. Determination of subcutaneous tumor size in athymic (nude) mice. Cancer Chemother Pharmacol. 1989;24:148–54.

19. Bezerra DP, De Castro FO, Alves APNN, Pessoa C, De Moraes MO, Silveira ER, et al. In vitro and in vivo antitumor effect of 5-FU combined with piplartine and piperine. J Appl Toxicol. 2008;28:156–63.

20. Eppink B, Krawczyk PM, Stap J, Kanaar R. Hyperthermia-induced DNA repair deficiency suggests novel therapeutic anti-cancer strategies. International Journal of Hyperthermia. 2012. p. 509–17.

21. Purschke M, Laubach H-J, Anderson RR, Manstein D. Thermal injury causes DNA damage and lethality in unheated surrounding cells: active thermal bystander effect. J Invest Dermatol. 2010;130:86–92.

22. Yenari MA, Liu J, Zheng Z, Vexler ZS, Lee JE, Giffard RG. Antiapoptotic and anti-inflammatory mechanisms of heat-shock protein protection. Annals of the New York Academy of Sciences. 2005. p. 74–83.

23. Guo F, Sigua C, Bali P, George P, Fiskus W, Scuto A, et al. Mechanistic role of heat shock protein 70 in Bcr-Abl-mediated resistance to apoptosis in human acute leukemia cells. Blood. 2005;105:1246–55.

24. Mosser DD, Caron AW, Bourget L, Denis-Larose C, Massie B. Role of the human heat shock protein hsp70 in protection against stress-induced apoptosis. Mol Cell Biol [Internet]. 1997;17:5317–27. Available from: http://www.pubmedcentral.nih.gov/articlerender.fcgi?artid=232382&tool=pmcentrez&rendertype=abstract

25. Lui JCK, Kong SK. Heat shock protein 70 inhibits the nuclear import of apoptosis-inducing factor to avoid DNA fragmentation in TF-1 cells during erythropoiesis. FEBS Lett. 2007;581:109–17.

26. Beere HM, Wolf BB, Cain K, Mosser DD, Mahboubi A, Kuwana T, et al. Heat-shock protein 70 inhibits apoptosis by preventing recruitment of procaspase-9 to the Apaf-1 apoptosome. Nat Cell Biol. 2000;2:469–75.

27. Jäättelä M, Wissing D, Kokholm K, Kallunki T, Egeblad M. Hsp7O exerts its anti-apoptotic function downstream of caspase-3-like proteases. EMBO J. 1998;17:6124–34.

28. Li TJ, Huang CC, Ruan PW, Chuang KY, Huang KJ, Shieh D Bin, et al. In vivo anti-cancer efficacy of magnetite nanocrystal - based system using locoregional hyperthermia combined with 5-fluorouracil chemotherapy. Biomaterials [Internet]. Elsevier Ltd; 2013;34(32):7873–83. Available from: http://dx.doi.org/10.1016/j.biomaterials.2013.07.012

29. Roviello F, Caruso S, Marrelli D, Pedrazzani C, Neri A, De Stefano A, et al. Treatment of peritoneal carcinomatosis with cytoreductive surgery and hyperthermic intraperitoneal chemotherapy: State of the art and future developments. Surgical Oncology. 2011.

30. Preetha A, Banerjee R, Huilgol N. Effect of temperature on surface properties of cervical tissue homogenate and organic phase monolayers. Colloids Surfaces B Biointerfaces. 2007;60:12–8.

31. Gewirtz DA. A critical evaluation of the mechanisms of action proposed for the antitumor effects of the anthracycline antibiotics adriamycin and daunorubicin. Biochemical Pharmacology. 1999. p. 727–41.

32. Thorn CF, Oshiro C, Marsh S, Hernandez-Boussard T, McLeod H, Klein TE, et al. Doxorubicin pathways: pharmacodynamics and adverse effects. Pharmacogenet Genomics. 2011;21:440–6.

33. Tacar O, Sriamornsak P, Dass CR. Doxorubicin: An update on anticancer molecular action, toxicity and novel drug delivery systems. Journal of Pharmacy and Pharmacology. 2013. p. 157–70.

34. Rupinder SK, Gurpreet AK, Manjeet S. Cell suicide and caspases. Vascular Pharmacology. 2007. p. 383–93.

35. Fan TJ, Han LH, Cong RS, Liang J. Caspase family proteases and apoptosis. Acta Biochim Biophys Sin (Shanghai). 2005;37:719–27.

36. Tournier C, Hess P, Yang DD, Xu J, Turner TK, Nimnual A, et al. Requirement of JNK for stress-induced activation of the cytochrome c-mediated death pathway. Science. 2000;288:870–4.

37. Duch A, De Nadal E, Posas F. The p38 and Hog1 SAPKs control cell cycle progression in response to environmental stresses. FEBS Letters. 2012. p. 2925–31.

38. Sauter KAD, Magun EA, Iordanov MS, Magun BE. ZAK is required for doxorubicin, a novel ribotoxic stressor, to induce SAPK activation and apoptosis in HaCaT cells. Cancer Biol Ther. 2010;10:258–66.

39. Kabel AM, Abdel-Rahman MN, El-Sisi AEDE, Haleem MS, Ezzat NM, El Rashidy MA. Effect of atorvastatin and methotrexate on solid Ehrlich tumor. Eur J Pharmacol. 2013;713:47–53.

40. Vendramini-Costa DB, Castro IBD De, Ruiz ALTG, Marquissolo C, Pilli RA, Carvalho JE De. Effect of goniothalamin on the development of Ehrlich solid tumor in mice. Bioorganic Med Chem. 2010;18:6742–7.

41. Lüpertz R, Wätjen W, Kahl R, Chovolou Y. Dose- and time-dependent effects of doxorubicin on cytotoxicity, cell cycle and apoptotic cell death in human colon cancer cells. Toxicology. 2010;271:115–21.

42. Chatterjee K, Zhang J, Honbo N, Karliner JS. Doxorubicin cardiomyopathy. Cardiology. 2010. p. 155–62.

43. Zhang S, Liu X, Bawa-Khalfe T, Lu L-S, Lyu YL, Liu LF, et al. Identification of the molecular basis of doxorubicin-induced cardiotoxicity. Nature Medicine. 2012.

7. Conclusões

•Sementes de ouro irradiadas com ultrassom produzem calor suficiente para promover dano celular.

•As avaliações em modelos computacionais mostraram que a produção de calor pelas sementes de ouro depende da sua dimensão.

•A análise computacional demonstrou que a irradiação nas frequências de 1- 1,5Mhz induzem a produção de calor pelas sementes de ouro acima de 43 °C.

•As sementes de ouro com diâmetro de 0,155cm e 0,54 cm comprimento foram menos invasivas para inserção nos tumores.

•Na avaliação pré-clínica, A utilização das sementes de ouro irradiadas com ultrassom por 30 minutos provocou necrose em 81% da área total dos tumores.

•O Tratamento com três doses de 15 minutos inibiu 84,7% do desenvolvimento do tumor ao longo dos 16 dias.

•O uso de sementes de ouro irradiadas com ultrassom em cultura de células durante 40 minutos inibiu completamente a viabilidade celular.

•O tratamento com sementes de ouro e ultrassom durante 10 minutos não induziu a expressão de proteínas de choque térmico.

•A combinação entre os tratamentos com sementes de ouro irradiadas com ultrassom e quimioterapia com doxorrubicina potencializou os efeitos da doxorrubicina in vitro e in vivo.

•A combinação do pré-tratamento com sementes de ouro e ultrassom provocou morte celular predominantemente por apoptose.

•O pré-tratamento com sementes de ouro e ultrassom permite a utilização de doses mais baixas de doxorrubicina reduzindo os seus efeitos adversos.

ANEXOS

ANEXO A: Patentes de procedimentos depositadas

1

Use of Gold Macro-Rods and Ultrasound as a Hyperthermia Cancer Treatment Patents Review of Case # TT1212

From:

Ioannis Gkigkitzis, Department of Mathematics, ECU
Carlos Austerlitz, 21st Century Oncology
André Luiz de Souza Barros Universidade Federal de Pernambuco
Teresinha Gonçalves- Universidade Federal de Pernambuco

To:

University Committee on Intellectual Property
Division of Research and Graduate Studies
Office of Technology Transfer, ECU

2

A model between cell thermal enhancement and cell death by hyperthermia

I. Gkigkitzis[1], C. Austerlitz[2], Andre Luiz de Souza Barros[3], and D. Campos[4]

[1]Department of Biomedical Physics, East Carolina University, Greenville NC, USA, gkigkitzisi@ecu.edu
[2]Physics Quality Control Section, 21st Century, Sarasota, FL, USA, carlosausterlitz@gmail.com
[3]Department of Antibiotics, Federal Universy of Pernambuco, PE, Brazil, alsb5@yahoo.com.br
[4]Clínica Diana Campos, Recife, PE, BR, dmtcampos@ig.com.br

Submitted to

East Carolina University, University Committee on Intellectual Property / Patents Review of Case # TT1213; Use of Gold Macro-Rods and Ultrasound as a Hyperthermia Cancer Treatment. Office of Technology Transfer, Division of Research and Graduate Studies

September 13, 2012.

ANEXO B- Esquema do setup de irradiação das placas de cultura de células.

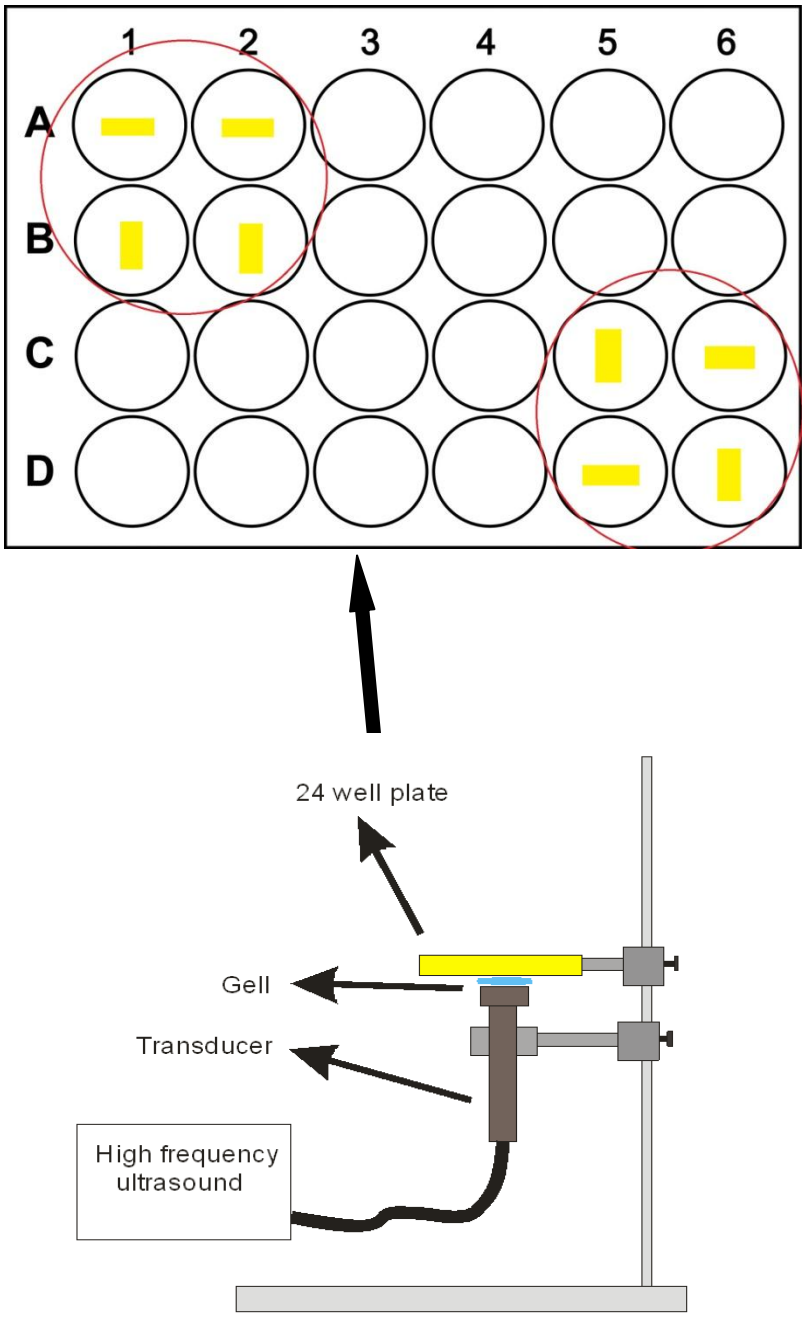

ANEXO C: Detalhes da inserção e irradiação das GRs.